VOL. 363 NO. 1 AUGUST 8, 1986

1st Int. Symp. on Preparative and Up-scale LC
Paris, January 15–17, 1986

OF CHROMATOGRAPHY

TIONAL JOURNAL ON CHROMATOGRAPHY, ELECTROPHORESIS AND RELATED METHODS

ELSEVIER

Scope. The *Journal of Chromatography* publishes papers on all aspects of chromatography, electrophoresis and related methods. Contributions consist mainly of research papers dealing with chromatographic theory, instrumental development and their applications. The section *Biomedical Applications,* which is under separate editorship, deals with the following aspects: developments in and applications of chromatographic and electrophoretic techniques related to clinical diagnosis (including the publication of normal values); screening and profiling procedures with special reference to metabolic disorders; results from basic medical research with direct consequences in clinical practice; combinations of chromatographic and electrophoretic methods with other physicochemical techniques such as mass spectrometry. In *Chromatographic Reviews,* reviews on all aspects of chromatography, electrophoresis and related methods are published.

Submission of Papers. Papers in English, French and German may be submitted, in three copies. Manuscripts should be submitted to: The Editor of *Journal of Chromatography,* P.O. Box 681, 1000 AR Amsterdam, The Netherlands, or to: The Editor of *Journal of Chromatography, Biomedical Applications,* P.O. Box 681, 1000 AR Amsterdam, The Netherlands. Review articles are invited or proposed by letter to the Editors and will appear in *Chromatographic Reviews* or *Biomedical Applications.* An outline of the proposed review should first be forwarded to the Editors for preliminary discussion prior to preparation. Submission of an article is understood to imply that the article is original and unpublished and is not being considered for publication elsewhere. For copyright regulations, see below.

Subscription Orders. Subscription orders should be sent to: Elsevier Science Publishers B.V., P.O. Box 211, 1000 AE Amsterdam, The Netherlands. The *Journal of Chromatography* and the *Biomedical Applications* section can be subscribed to separately.

Publication. The *Journal of Chromatography* (incl. *Biomedical Applications, Chromatographic Reviews* and *Cumulative Author and Subject Indexes, Vols. 326–350*) has 38 volumes in 1986. The subscription prices for 1986 are:

J. Chromatogr. (incl. *Chromatogr. Rev.* and *Cum. Indexes, Vols. 326–350*) + *Biomed. Appl.* (Vols. 346–383): Dfl. 6080.00 plus Dfl. 912.00 (postage) (total *ca.* US$ 2742.00)

J. Chromatogr. (incl. *Chromatogr. Rev.* and *Cum. Indexes, Vols. 326–350*) only (Vols. 346–373): Dfl. 5040.00 plus Dfl. 672.00 (postage) (total *ca.* US$ 2240.00)

Biomed. Appl. only (Vols. 374–383): Dfl. 1850.00 plus Dfl. 240.00 (postage) (total *ca.* US$ 819.50).

Journals are automatically sent by airmail at no extra costs to Argentina, Australia, Brasil, Canada, China, Hong Kong, India, Israel, Japan, Malaysia, Mexico, New Zealand, Pakistan, Singapore, South Africa, South Korea, Taiwan, Thailand and the U.S.A. Back volumes of the *Journal of Chromatography* (Vols. 1 through 345) are available at Dfl. 219.00 (plus postage). Claims for issues not received should be made within three months of publication of the issue. If not, they cannot be honoured free of charge. Customers in the U.S.A. and Canada wishing information on this and other Elsevier journals, please contact Journal Information Center, Elsevier Science Publishing Co. Inc., 52 Vanderbilt Avenue, New York, NY 10017. Tel. (212) 916-1250.

Abstracts/Contents Lists published in Analytical Abstracts, ASCA, Biochemical Abstracts, Biological Abstracts, Chemical Abstracts, Chemical Titles, Current Contents/Physical, Chemical & Earth Sciences, Current Contents/Life Sciences, Deep-Sea Research/Part B: Oceanographic Literature Review, Excerpta Medica, Index Medicus, Mass Spectrometry Bulletin, PASCAL-CNRS, Referativnyi Zhurnal and Science Citation Index.

See page 3 of cover for Publication Schedule, Information for Authors and information on Advertisements.

0021-9673/86/$03.50

Printed in The Netherlands

For contents see p. VI

Gilson Fraction Collectors

any quantity ● any vessel ● any mode

France : B.P. 45, F-95400 Villiers-le-Bel. Tél. : (1) 39.90.54.41. Télex : 696 682 F.
USA : Box 27, 3000 W. Beltline, Middleton, Wisc. 53562. Tel : (608) 836 1551. Telex : 26.5478 MTWI.

THE WORLD IS AT YOUR FINGERTIP

If chemical analysis is your world, explore it in ways never before possible with th BAS 200 PROBLEM SOLVER™. One finger on our System Director™ will take you places you've never been. Built-in methods files help you down the road. Direct changes in a multi-electrode electrochemical detector of 4-channel variable wavelength UV/VIS detector up to 8 times during a single run. Let your column, c and valve bask in controlled temperatures up to 80°C. Discover the advantages o the first complete LC deoxygenation system. Cruise through ternary gradient analysis with a solvent delivery system so smooth that it requires NO pulse dampin

Take the BAS 200 for a test drive and let us expand your horizons.

BAS

2701 Kent Ave
West Lafayette
Indiana 47906

Telex 276141
(317) 463-4527

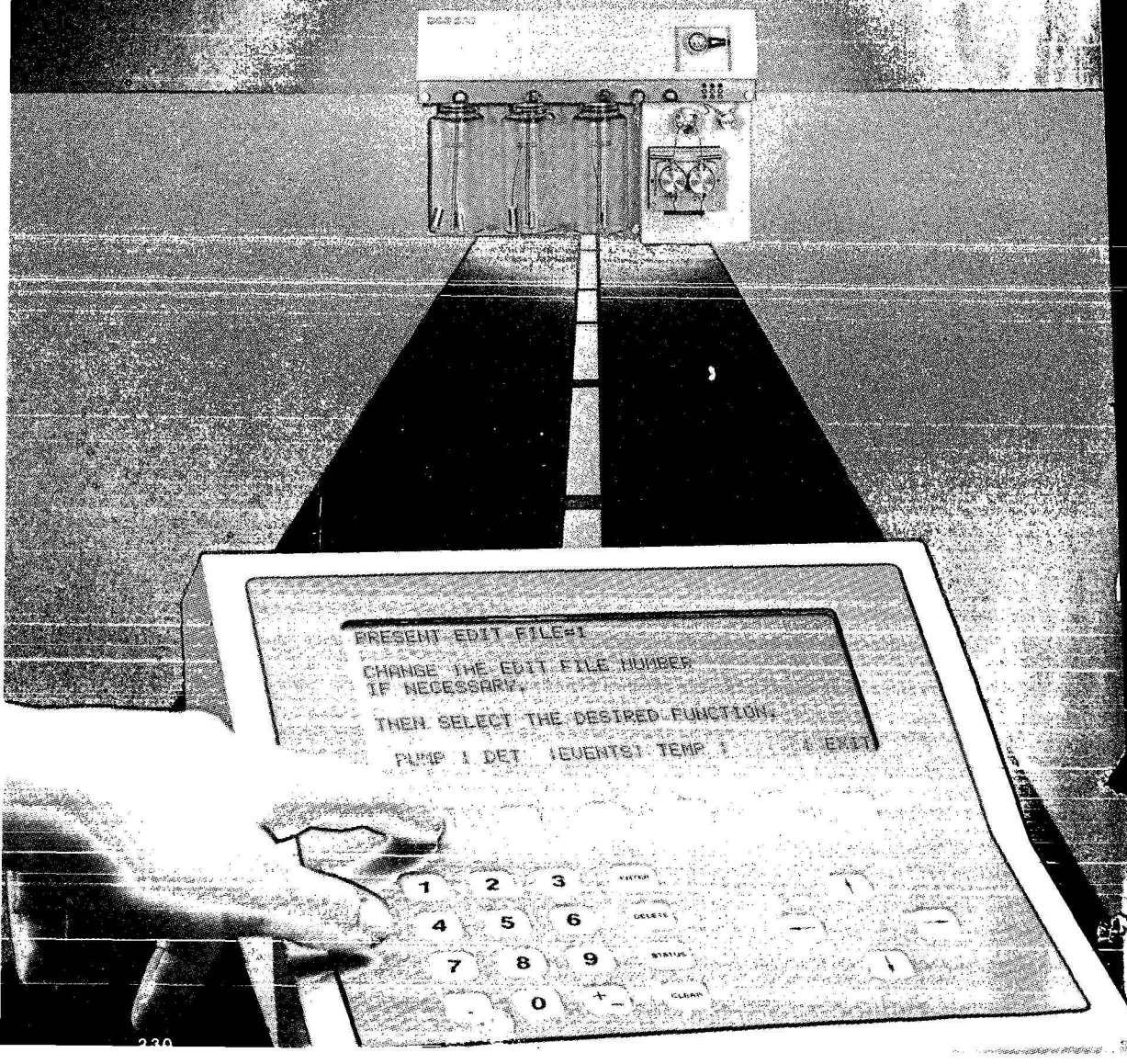

SCALE-UP TO
PILOT PLANT/PROCESS HPLC :

SepTech

ST/Process 2000

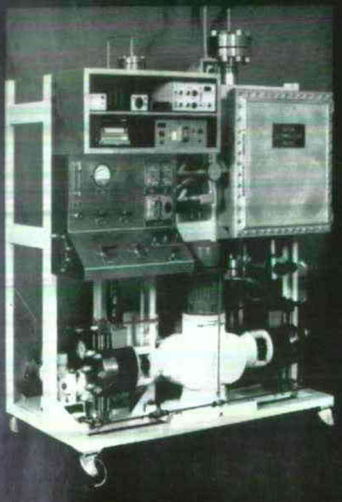

- Multi-Kilogram Sample Loads
- Continuous Gradient Formation
- Completely Explosion Proof
- 2000 p.s.i. Capability
- 8.5 Liters per Minute
- Double Diaphragm Pumps for Sample Protection
- 4, 6, 8, 10-inch or Larger I.D. MEGABORE Columns
- A.S.M.E. Code Rated Columns
- Automation Module Available

SepTech

SEPARATIONS TECHNOLOGY

Your Prep/Process HPLC Company

P.O. Box 63, 2 Columbia Street
Wakefield, R.I. 02879

(401) 789-5660

629

The all Purpose Modular System

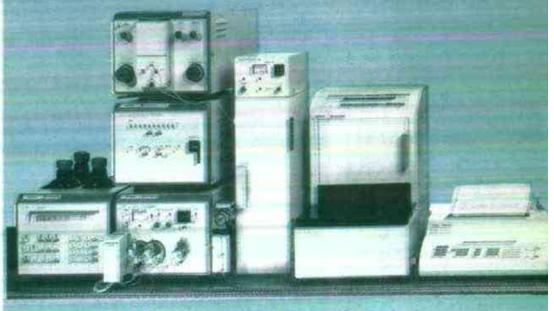

Solvent Delivery:

- Isocratic system
- Low pressure gradient
- High pressure gradient

Injection:

- Flexible autosampler for 108 vials, variable injection volume
- Manual injection

Detection:

- Variable wavelength UV-detector
- Photo diode aray-detector for UV and VIS
- Fluorescence detector
- Reaction detector

Integrator:

- Data processor with printer/plotter
- Convenient programming via LC-display
- 160 KByte RAM memory for raw data
- Reintegration and replot of up to 250 chromatograms
- Individual report format

Column Oven:

- Contact oven for two columns, 30° - 100° C

Communication:

- Interactive system interface (PAN)
- RS 232 C interfaces, BCD, relays etc.

**...more than perfect –
MERCK/Hitachi
HPLC-Instruments**

E. Merck, Frankfurter Straße 250,
D-6100 Darmstadt 1,
Telefon (0 61 51) 72 35 33
E 2900

515

514A Switzerland: MACHEREY-NAGEL AG · P.O.Box 46 · CH-4702 Oensingen

MinoRPC

UN-PARALLELED SELECTIVITY.

MinoRPC IS PART OF THE FPLC SYSTEM, TODAY'S MOST VERSATILE AND BIOCOMPATIBLE CHROMATOGRAPHY PROGRAM FOR THE FAST SEPARATION OF BIOMOLECULES.

MinoRPC™ is the new high performance medium for reversed phase chromatography. It improves your separation capabilities for a wide range of small biomolecules, including peptides, amino acids and nucleotides.

No other medium combines such high selectivity with such versatility. MinoRPC is unparalleled. It is optimised to give you fast, high resolution results.

To ensure high reproducibility, we have developed a special synthesis. You can always rely on MinoRPC to be the same every time we make it; every time you use it. And for that extra efficiency and reproducibility, you can work at elevated temperatures, carefully controlled by the Pharmacia high performance Column Heater.

MinoRPC reflects the high standard you've come to expect from Pharmacia. Our contribution to high performance liquid chromatography has already brought success to thousands of chromatographers.

Share the success. Contact your local Pharmacia representative for more information on columns prepacked with MinoRPC.

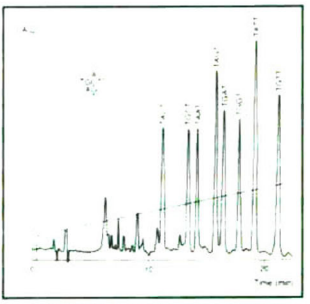

SEPARATION OF OLIGONUCLEOTIDE "WOBBLE SEQUENCES."

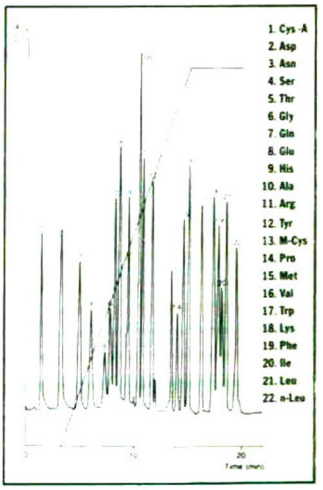

ANALYSIS OF PTH-DERIVATIZED AMINO ACIDS.

Pharmacia

Laboratory Separation Division
S-751 82 Uppsala, Sweden

Two new gradient HPLC systems

Here's what makes them irresistible.

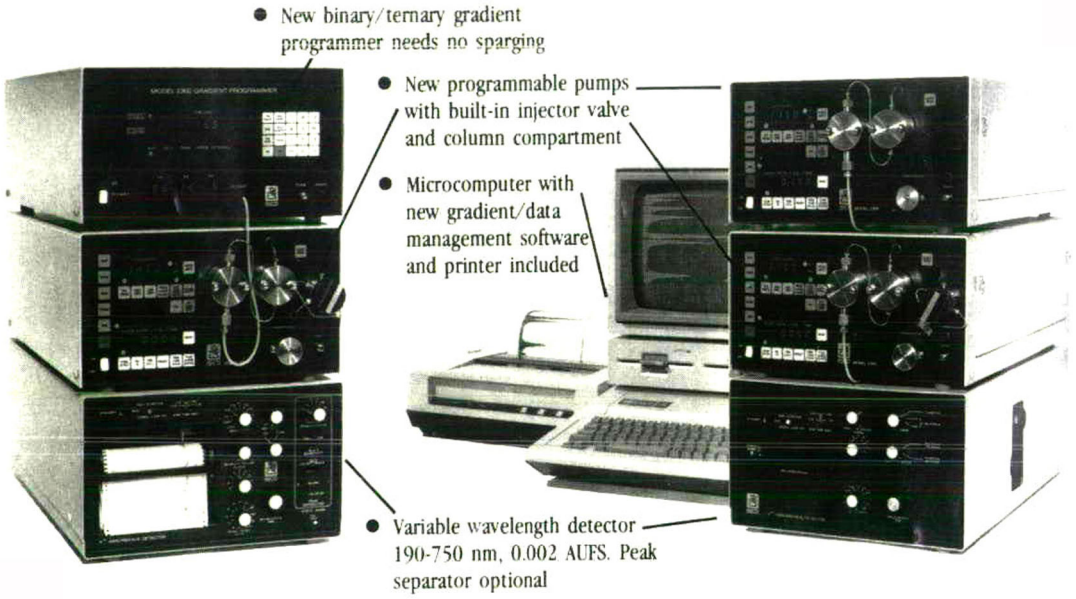

Isco's two new gradient chromatographs offer you an irresistible combination of attractive features and economical price. You get a programmable pump that changes flow rate based on either time or volume delivered, and a sensitive, variable wavelength detector with an 8,000 hour lamp life and flow cells for any application from microbore to industrial prep LC.

Choose either a single pump binary/ternary gradient programmer or a two pump gradient system with data management controlled by an Apple IIc or IBM-PC. Both chromatographs are complete with all extras including column, valve, fittings, and recorder or printer. Isco, Inc., P.O. Box 5347, Lincoln, NE 68505, USA. In USA, phone toll free (800)228-4250.

ISCO

ref no 497

JOURNAL OF CHROMATOGRAPHY

VOL. 363 (1986)


RESPECT COPYRIGHT
BERNE
CONVENTION
100 YEARS
1886-1986
ENCOURAGE CREATIVITY

JOURNAL *of* CHROMATOGRAPHY

INTERNATIONAL JOURNAL ON CHROMATOGRAPHY,
ELECTROPHORESIS AND RELATED METHODS

ELSEVIER
AMSTERDAM — OXFORD — NEW YORK — TOKYO

J. Chromatogr., Vol. 363 (1986)

Dôme des Invalides, Paris, ca. 1875

0021-9673/86/$03.50

Printed in The Netherlands

SYMPOSIUM ISSUE

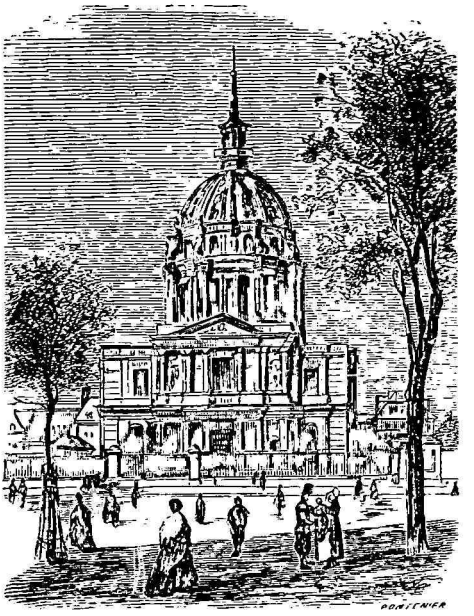

FIRST INTERNATIONAL SYMPOSIUM ON PREPARATIVE AND UP-SCALE LIQUID CHROMATOGRAPHY

Paris (France), January 15–17, 1986

CONTENTS

FIRST INTERNATIONAL SYMPOSIUM ON PREPARATIVE AND UP-SCALE LIQUID CHROMATOGRAPHY, PARIS, JANUARY 15–17, 1986

Journal of Chromatography, 363 (1986) 1–30
Elsevier Science Publishers B.V., Amsterdam — Printed in The Netherlands

CHROM. 18 649

FRAMEWORK FOR MAXIMIZING THROUGHPUT IN PREPARATIVE LIQUID CHROMATOGRAPHY

JOHN H. KNOX*
Department of Chemistry, University of Edinburgh, West Mains Road, Edinburgh, EH9 3JJ (U.K.)
and
HAZEL M. PYPER
Huntingdon Research Centre, Huntingdon, Cambridgeshire (U.K.)

SUMMARY

This paper addresses the questions: (a) Should one use volume or concentration overloading or both to achieve maximum throughput in preparative liquid chromatography? (b) Is the plate height concept valid for overloaded columns? (c) What are the main factors limiting throughput? (d) What column lengths, L, and particle diameters, d_p, provide maximum throughput?

We conclude (a) that concentration overloading will always provide the greatest throughput but that the injected sample volume may be a substantial fraction of the volume of the eluted peak, (b) that peak widths increase as the square root of the distance migrated under concentration overload and that the plate height concept can be used in optimisation calculations, (c) that the major restriction on throughput is the minimum number of theoretical plates, N^*, required to achieve adequate resolution of solutes being isolated, (d) that maximum throughput is achieved for a specific ratio d_p^2/L determined by N^* and other operating parameters.

In practice for N^* values between 2000 and 50 we are likely to use columns 200–2000 mm long packed with 10–60 μm diameter particles giving throughputs between 0.1 and 20 g/h per cm^2 of column cross section at a capacity ratio of 4.

INTRODUCTION

Preparative liquid chromatography (PLC) is distinguished from high-performance liquid chromatography (HPLC) not so much by its scale as by its purpose. PLC may be defined as LC carried out for the purpose of isolating purified chemical substances, whereas analytical LC or HPLC is carried out for the purpose of identifying and quantifying the components of mixtures. The scale of PLC is normally larger than that of HPLC but per run may nonetheless range from micrograms to grams. Production liquid chromatography, for which we shall also use the acronym PLC, can be defined as LC carried out for the purpose of commercial production and differs from preparative LC in that the cost element now becomes all-important. Its scale will normally be within the range of milligrams to kilograms per run.

0021-9673/86/$03.50

In nearly all practical cases PLC will also be associated with column overloading since a maximum throughput within stated limits of purity and yield is always desired. It is with PLC in this form that the present paper is primarily concerned.

A column is said to be overloaded when the sample injected is so large that the eluted peak is significantly wider than that resulting from the injection of an infinitesimal or analytical sample. "Significantly wider" in this context might mean 10–20% wider, indicating an increase of 20–50% in the height equivalent to a theoretical plate (HETP).

Optimisation of performance in analytical LC implies seeking conditions which combine maximum plate efficiency and minimum elution time, under the restriction of a limited pressure drop. The theory of such optimisation has been widely discussed[1–6] and leads to the specification of the optimum column dimensions, in particular optimum particle size, d_p, and column length, L, for a specified plate number, N.

Optimisation of performance in preparative LC implies seeking conditions which provide the maximum injection rate or collection rate (throughput) of material with specified purity and at specified yield, but again under the restriction of a limited pressure drop across the length of the column. Any theory of optimisation must lead to the prediction of the combinations of column length and particle diameter which lead to maximum throughput.

In what follows we shall assume that the throughput for any type of column (given length and particle size) will be proportional to its cross sectional area. Accordingly our task is to optimise the throughput per unit cross sectional area of column. We note that Hupe and Lauer[7] have considered in detail the trade-off between increasing the column length and cross section for solutes which are just resolved. We shall in general consider only the case where there is already sufficient resolution at the analytical level to allow some degree of column overloading before adequate resolution is lost.

Optimisation of performance in production LC implies minimizing the cost of production per unit volume of product with specified purity. Pressure drop and yield are no longer restrictions but can be chosen to minimize cost. This optimisation exercise is much more complex than for preparative LC as it has to include considerations of capital cost of equipment, cost of solvents and packings, cost of recycling solvents etc. Such matters will only be considered in passing.

Before embarking on the theory of optimisation of PLC, we take it as self evident that the initial step in developing any practical preparative separation will be to find the elution conditions which, under analytical loading, give the best possible α values (relative values of retention ratios) for the solutes of interest. As in optimisation of HPLC, the larger the relevant α values, the faster can a separation with given resolution be achieved, and so the greater the throughput.

PEAK MIGRATION AND RESOLUTION UNDER CONDITIONS OF OVERLOAD

There are two ways in which a column may be technically "overloaded". First, the volume of the injected sample may be so large that eluted peaks are significantly wider than those from analytical samples, although the solute concentration is low

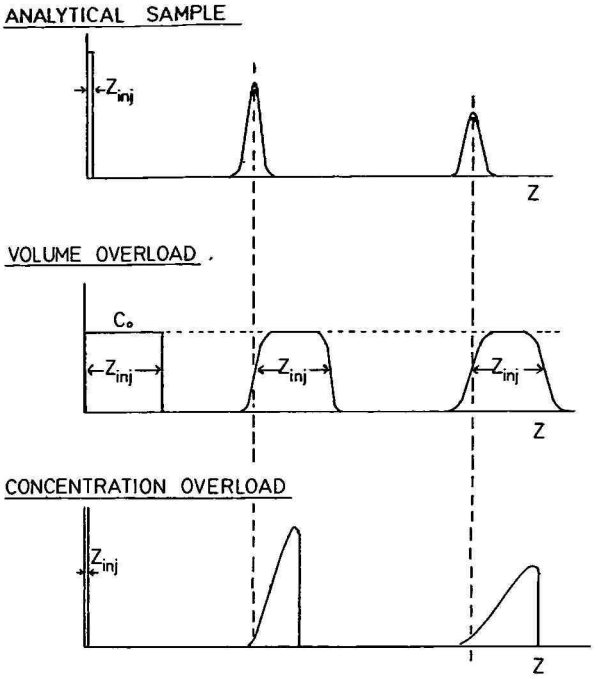

Fig. 1. Development of peak profiles during migration along a column for analytical and overload samples.

and still remains within the range of the linear part of the partition isotherm. We term such overloading "pure volume overloading".

Second, the concentration or quantity of solute injected may be so large that, even with a very small injection volume, the resulting peak is wider than that from an analytical sample. In this case the solute concentration no longer falls within the range of the linear part of the partition isotherm. Such overloading is termed "concentration overloading". Volume and concentration overloading may, of course, be combined. In such a case the width of the eluted peak may be reduced either by reducing the injected volume or by reducing the injected quantity.

Under conditions of pure volume overloading, when the injected volume is sufficiently large, eluted peaks will be flat topped, but symmetrical. Under conditions of concentration overloading peaks will generally be asymmetric, normally showing sharp fronts and extended tails.

The way in which the peak of a single solute migrates along a column under analytical and overload conditions is shown schematically in Fig. 1 which plots solute concentration against distance from the injection point at different stages in elution.

The peak concentration–distance profile for an analytical injection follows the well known Gaussian equation

$$C = \frac{Q}{\sqrt{2\pi H_0 z}} \exp\left[-\Delta z^2/2H_0 z\right] \tag{1}$$

where C is the total concentration of solute within the column at a distance z from

the column inlet measured as quantity per unit volume of the packed bed, Q the quantity of solute injected per unit area of column, H_0 the plate height for an infinitesimal sample, z the distance migrated by peak maximum and Δz the distance measured from peak maximum.

When a similar low concentration of solute is injected but the injection volume is large, the peak profile is represented by[8-11]

$$C = \frac{Q}{2\,z_{inj}} \left\{ \mathrm{erf}\left[\frac{\Delta z}{\sqrt{2H_0 z}}\right] - \mathrm{erf}\left[\frac{\Delta z - z_{inj}}{\sqrt{2H_0 z}}\right] \right\} \tag{2}$$

where z_{inj} is the width of solute band within the column (assumed rectangular in profile) immediately following its injection. The error function is defined as

$$\mathrm{erf}\left[\frac{X}{\sqrt{2}}\right] = \sqrt{\frac{2}{\pi}} \int_0^X \exp\left[-\frac{x^2}{2}\right] \mathrm{d}x \tag{3}$$

z_{inj} is related to the volume of sample injected, V_{inj}, by

$$z_{inj} = V_{inj}/A_m\,(1 + k) \tag{4}$$

where A_m is the cross section of eluent phase within the column bed and k the column capacity ratio of solute (note: k will be used in place of k' in order to simplify the writing of equations). The total concentration within the column immediately after injection, C_0, is given by

$$C_0 = Q/z_{inj} \tag{5}$$

When $z_{inj} \to 0$ eqn. 2 reduces to eqn. 1.

With an analytical sample the maximum solute concentration in the band is $C_{max} = Q/\sqrt{2\pi Hz}$ and falls in proportion to $1/\sqrt{z}$ as the band migrates whereas in the volume overload situation if z_{inj} is sufficiently large, say greater than eight standard deviations (*i.e.* $8/\sqrt{Hz}$), the peak is flat-topped and the maximum concentration remains at C_0.

Under conditions of concentration overload the situation is much more complex due to the combined effects of kinetic and thermodynamic dispersion[12]. However, when kinetic dispersion is negligible a straightforward result is obtained[13-15]. When the partition isotherm is concave to the C_m axis (C_m is the concentration in eluent) the peak has a sharp front and extended tail. The column capacity ratio corresponding to the migration of an element with a specified mobile phase concentration C_m in the tail of the peak is given by

$$k_{C_m} = \frac{\mathrm{d}C_s}{\mathrm{d}C_m} \tag{6}$$

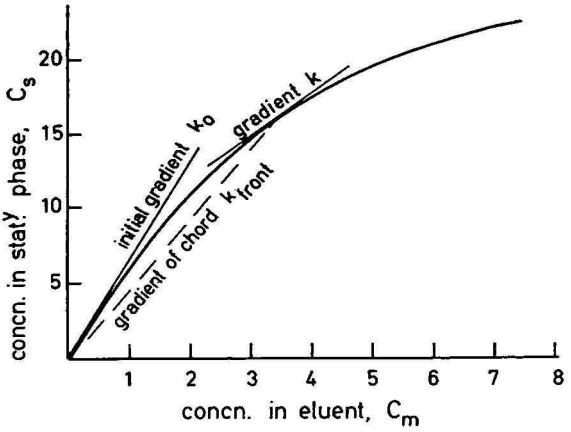

Fig. 2. Relationship between various capacity factors and the partition isotherm. k_0 = Capacity ratio of solute at $C = 0$; k = capacity ratio for a particular concentration C_m in eluent; k_{front} = capacity ratio for a front with concentration C_m.

where C_s and C_m are the concentrations per unit volume of the column bed for solute in the stationary and mobile phases respectively, so that the total concentration within the column bed, C, is given by

$$C = C_m + C_s \tag{7}$$

The column capacity ratio for the front on the other hand follows the equation

$$k_{front} = C_s/C_m \tag{8}$$

These equations are illustrated in Fig. 2.

The very complex situation which arises when band dispersion arises from both kinetic and thermodynamic effects (*i.e.* those due to non-linearity of isotherm) has been examined by Haarhoff and Van der Linde[12]. They were able to obtain an explicit mathematical expression only for the case where the partition isotherm could be written in the simple form

$$C_s = k_0 C_m (1 - \alpha C_m) \tag{9}$$

As shown later this approximates to the Langmuir isotherm at low C_m values. Their closed solution has been tested experimentally by Cretier and Rocca[16] and using computer simulation by Poppe and Kraak[17].

While the equations of Haarhoff and Van der Linde[12] are undoubtedly realistic they are somewhat complex and do not readily give guidance to the general practitioner who wishes to derive optimised conditions for a particular PLC separation. Nevertheless an important conclusion arises from their work, which has also been used by De Jong *et al.*[18], namely that if the apparent HETP is defined as the second moment of the peak divided by the column length, it is possible to a good approximation to separate the total HETP into two contributions:

$$H_{total} = H_0 + H_{th} \tag{10}$$

H_0 is the kinetic contribution to the plate height for an infinitesimal sample and H_{th} is the thermodynamic contribution arising from the non-linearity of the isotherm.

Fig. 3 illustrates the problem of peak resolution under analytical and overload conditions, and re-emphasises the importance, when optimising PLC, of initially obtaining the highest possible resolution of solutes on the analytical scale. Under pure volume overload, adequate resolution of the two solutes 1 and 2 will be maintained until the peak first eluted occupies the entire space between the two peaks. The maximum volume which can be injected before significant overlap occurs is given approximately by

$$V_{inj} = (V_{R2} - V_{R1}) - \sqrt{2\pi}\,(\sigma_1 + \sigma_2) \tag{11}$$

where V_{R2} and V_{R1} are the retention volumes of solutes 1 and 2, and σ_1 and σ_2 are the standard deviations of peaks for analytical injection of solutes 1 and 2.

If sample cutting is employed overlap may be allowed and the optimum overlap for specified restrictive conditions of purity and yield may be obtained[9,19].

With increasing concentration overload while using small injected volumes, the fronts of the overloaded peaks elute progressively earlier until the front of peak

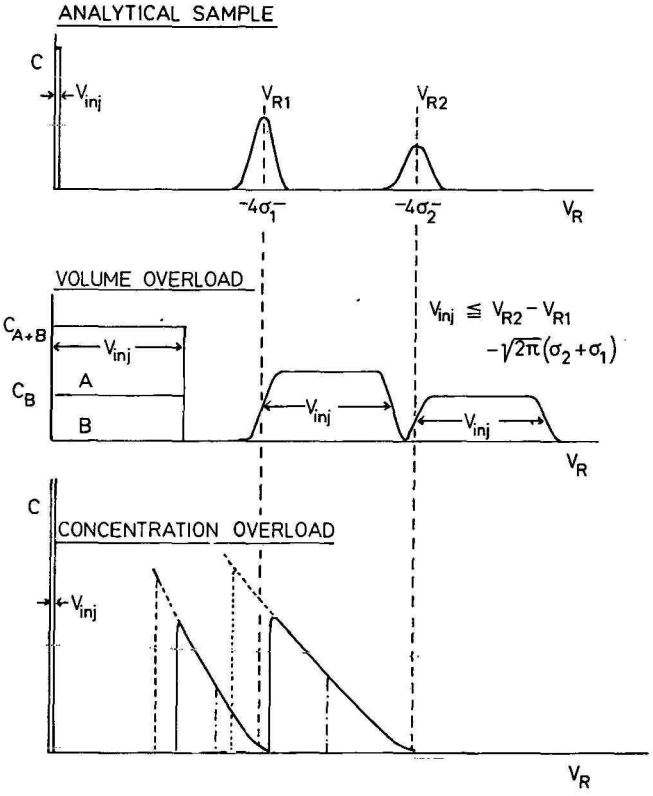

Fig. 3. Resolution of solutes 1 and 2 under analytical and overload conditions.

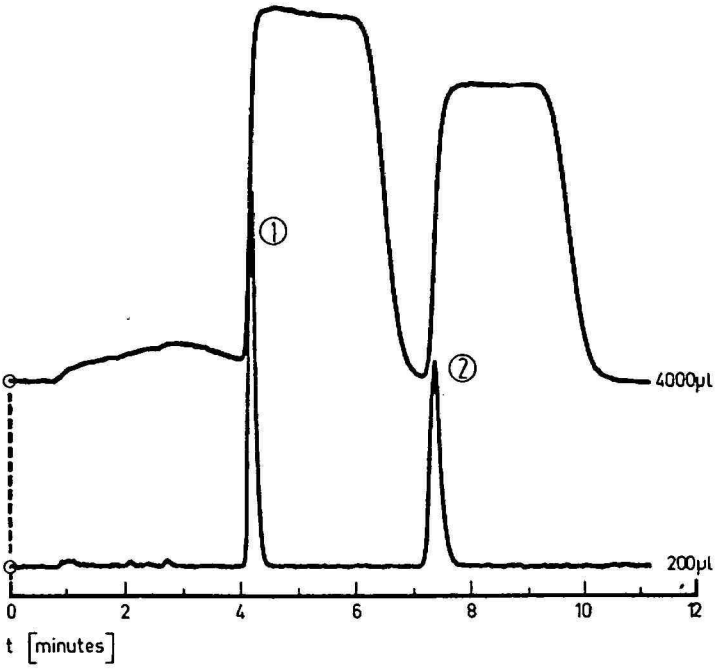

Fig. 4. Practical illustration of volume overload from Eisenbeiss et al.[20]. Solutes, pentylbenzene (1) and octylbenzene (2); injection, 200 µl containing 2.5 µg each solute (lower), 4000 µl containing 50 µg each solute (upper); column, 250 × 4 mm I.D.; packing, 7 µm LiChrosorb RP-8; eluent, acetonitrile–water (75:25, v/v); flow-rate, 1.5 ml min^{-1}; detector, UV, 254 nm, 0.04 a.u.f.s. (Reproduced by permission of the authors and of *Chromatographia.*)

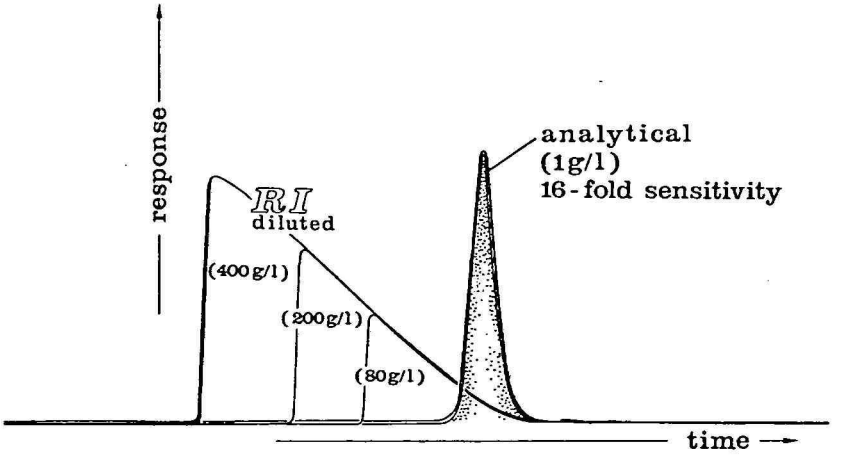

Fig. 5. Practical illustration of concentration overload from Eisenbeiss *et al.*[20]. Solute, diethylphthalate; injections, 30 µl of solutions containing 1, 80, 200 and 400 g/l; column, 250 × 4 mm I.D.; packing, 5 µm LiChrosorb SI60; eluent, heptane–ethylacetate (90:10, v/v); flow-rate, 3 ml min^{-1}; detector, refractive index with scavenging flow for overload samples. (Reproduced by permission of the authors and of *Chromatographia.*)

2 elutes at the tail of peak 1. Thereafter overlap occurs and resolution deteriorates. The optimisation of the overload when peak cutting is used can again in principle be carried out. Experimental justification of the above conclusions is provided by Eisenbeiss *et al.*[20] and is illustrated by Figs. 4 and 5 taken from their publication.

The simple picture presented in Fig. 3 shows that a higher load can always be resolved under concentration overload conditions than under pure volume overload conditions. However, the question arises as to whether a judicious combination of volume and concentration overload might not produce higher loading and throughput than concentration overload alone.

Fig. 6 addresses this question. To simplify the analysis we assume that kinetic dispersion is small and can be neglected to a first approximation. Accordingly a low concentration injection of a finite volume (pure volume overload conditions) will migrate down the column with an unchanging rectangular concentration–distance profile. A small volume injection of high-concentration solution (concentration overload situation) will migrate along the column as a tailing peak having a sharp front. For convenience we take the peak shape to be triangular as indicated by the

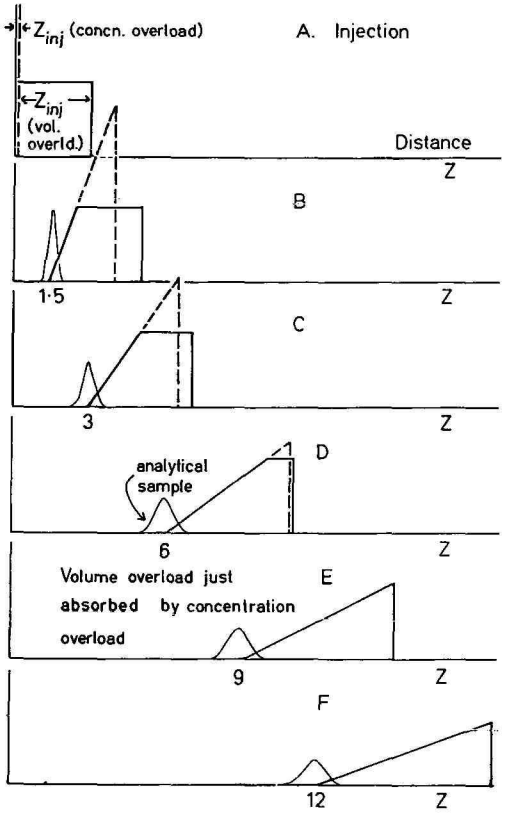

Fig. 6. Development of peak profiles for concentration overload when peak profile is triangular, and for combined volume–concentration overload showing that volume overload can be absorbed by concentration overload.

broken lines in Fig. 3. The peak shape reflects the partition isotherm as given by eqn. 6.

Since the element of eluate containing a given concentration C_m will migrate at the uniform rate given by eqn. 6, the peak shape remains constant during migration except in so far as it becomes wider in proportion to the distance migrated and at the same time is truncated on the high concentration side so that the peak area remains constant. In the case of the triangular peak shown in Fig. 6, dC_m/dz is proportional to $1/z$.

Consider now the migration of an initially rectangular concentration plug where maximum concentration lies in the overload region. Such a plug will maintain a sharp front but will develop a sloping tail as shown by the full lines in Fig. 6. This tail will coincide with the lower part of the tail of the concentration-overloaded peak containing the same quantity of solute. As the plug migrates the length of the plateau region declines. This is clearly necessary if the peak area is to remain constant but is also required by eqns. 6 and 7 and Fig. 2. They show that the migration rate of the front must be slower than the migration rate of the element in the tail having the same concentration where the isotherm is concave to the C_m axis. Eventually, as shown in Fig. 6E, the plateau disappears and the peak arising from the plug-injection has exactly the same profile as the peak arising from the small volume injection. This result is not restricted to a triangular peak as has been demonstrated by Smit *et al.*[21]. However, with a triangular peak, whose validity is justified later, the peak width at stage E is exactly twice that of the initial injection. At this stage the volume overload may be said to be absorbed into the concentration overload.

From this elementary analysis of the situation the following conclusions may be reached.

(1) The final eluted peak profile under concentration overload conditions for a given quantity of solute is independent of the sample volume up to a critical volume V^*.

(2) V^* is approximately half of the volume of the peak arising from a small volume injection, the exact proportion depends upon the shape of the isotherm.

(3) In PLC the injected volume V_{inj} may be any volume up to V^* without affecting the peak width.

(4) In determining the maximum quantity which can be injected in practice, volumes of around V^* of progressively more concentrated solutions should be injected until resolution deteriorates to the minimum acceptable value.

(5) Combination of concentration and volume overload does not increase the load which can be placed upon a column. For injection volumes up to V^* the load for a stated resolution will be independent of the injected volume. For larger injection volumes it will be less.

The main conclusion that injection volumes up to V^* have no effect on peak shape or peak width raises the question of whether one should inject small concentrated samples ($V_{inj} \rightarrow 0$) or a larger more dilute sample ($V_{inj} \rightarrow V^*$). There seem to us to be several arguments in favour of using relatively large volumes close to V^*.

(1) The key to optimising sample injection in PLC is the uniform distribution of sample over the column cross section. In this way, particularly under concentration overload conditions, the overload is uniform over the column section and the migrating band therefore has the same profile along any line parallel to the axis of the

column. A number of studies of how this can best be achieved have been published[9,22,23].

(2) Often large samples will contain minor contaminants which are permanently adsorbed at the inlet end of the column. If these are not uniformly distributed over the column section variations in the retentive power and possibly flow resistance over the top layers of the column will develop leading to deterioration in column performance with use.

(3) In general with current injection devices, uniform distribution of sample will be achieved most reliably with the largest permissible sample volume.

(4) The viscosity of a concentrated solution will normally differ significantly from that of eluent. If the viscosity of the injected sample exceeds that of the eluent and if the sample is not uniformly distributed it will form a viscous plug at the head of the column which will only slowly be absorbed into the main eluent stream. This will lead to a severely tailed elution peak. On the other hand if the injected sample is less viscous than eluent, fingering will occur again leading to peak distortion and unnecessary broadening.

We have examined the effects of volume and concentration overloading using a specially designed PLC injector and column system as described elsewhere[24]. The results confirm the above conclusions.

DISTRIBUTION ISOTHERMS AND PEAK SHAPES

In developing guidelines for optimising throughput in PLC it is particularly helpful if peaks can be approximated by triangles. In practice this is often the case when columns are overloaded[17,20,25] and a good illustration is shown by Fig. 5. It is, however, important to establish that partition isotherms which correspond to triangular peaks are in fact realistic.

The simplest isotherm which takes account of concentration overloading is the Langmuir isotherm which was originally conceived to handle adsorption on to energetically homogeneous surfaces from a liquid or gas. In chromatography, and particularly in liquid chromatography, great stress is laid on the achievement of energetically homogeneous adsorbents since such adsorbents exhibit a substantial range of concentration over which the isotherm is linear. Accordingly they give symmetrical elution peaks up to a relatively high sample loading. Since the absolute concentration of retained solute in the stationary phase is nearly always much greater than that in the mobile phase (since $V_s \ll V_m$ and k normally exceeds unity) molecular overcrowding as solute concentration increases, first occurs in the stationary phase. The Langmuir isotherm must therefore describe the *most favourable* situation which can arise in practice under overload conditions. In many cases the isotherm curvature and the change in curvature will be more severe.

Our first task is then to state the form of the Langmuir isotherm and the forms of the two idealized peaks; these are the triangular R_F peak in which the plot of concentration C_m against distance migrated is a straight line and the triangular k peak where the plot of concentration against retention time is a straight line. We use the symbols L, $R\Delta$, and $k\Delta$ to refer to these three cases. They are shown diagramatically in Fig. 7 and are represented by eqns. 12–14.

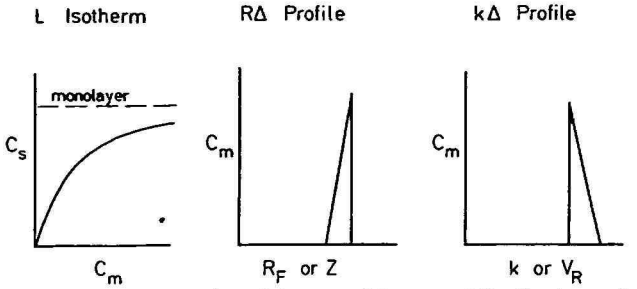

Fig. 7. Formal illustration of three possible types of distribution under overload conditions. The Langmuir distribution isotherm, the triangular R_F peak profile and the triangular k peak profile.

L Isotherm

$$C_s = \frac{k_0 C_m}{1 + \alpha C_m} \tag{12}$$

RΔ Peak

$$R_F = R_{F_0}\left\{1 + 2\left(\frac{k_0}{1 + k_0}\right)\alpha C_m\right\} \tag{13}$$

kΔ Peak

$$k = k_0(1 - 2\alpha C_m) \tag{14}$$

Isotherms corresponding to the *RΔ* and *kΔ* peak shapes are obtained using eqn. 15 which is the integral form of eqn. 6 along with eqn. 16 as required.

$$C_s = \int_0^{C_m} k \, dC_m \tag{15}$$

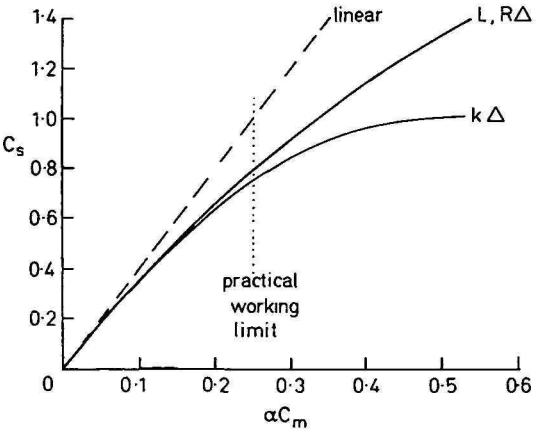

Fig. 8. Isotherms corresponding to the three cases illustrated in Fig. 7, when $k_0 = 4$ and $\alpha = 1$.

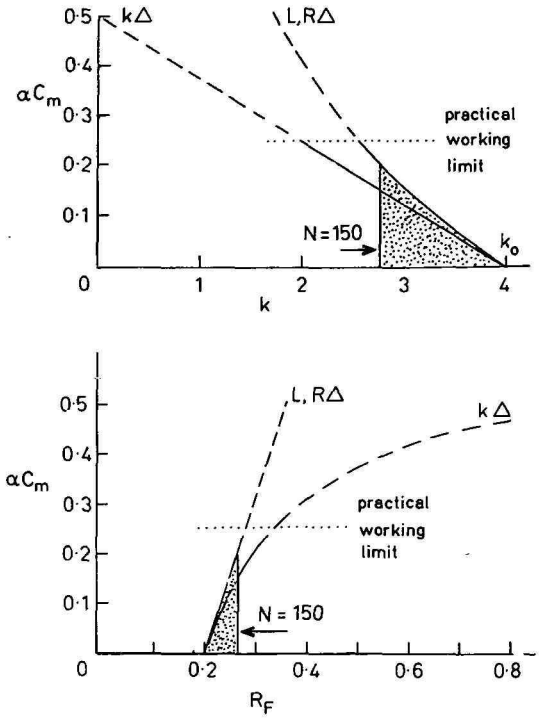

Fig. 9. Peak profiles corresponding to the three cases illustrated in Figs. 7 and 8. Plate numbers calculated on basis of eqn. 28.

$$k = \frac{1}{R_F} - 1 \qquad \text{or} \qquad R_F = \frac{1}{1 + k} \tag{16}$$

The peak shape corresponding to the Langmuir isotherm is obtained by eqn. 6 coupled with eqn. 16 as required. The mathematical manipulations are straightforward and the final results are most usefully expressed in the form of power series which enable direct comparisons to be made. The equations for the three isotherms, peak profiles on an R_F basis, and peak profiles on a k basis are given by eqns. 17–25 and illustrated in Figs. 8 and 9.

Isotherms

$$\text{L:} \quad C_s = k_0 C_m \{1 - (\alpha C_m) + (\alpha C_m)^2 - (\alpha C_m)^3 + \ldots .\} \tag{17}$$

$$R\Delta\text{:} \quad C_s = k_0 C_m \left\{1 - (\alpha C_m) + \frac{4}{3}\psi(\alpha C_m)^2 - 2\psi^2(\alpha C_m)^3 + \ldots .\right\} \tag{18}$$

$$k\Delta\text{:} \quad C_s = k_0 C_m \{1 - (\alpha C_m)\} \qquad \text{(exact)} \tag{19}$$

Peak shapes on k basis

$$\text{L:} \quad k = k_0 \{1 - 2(\alpha C_m) + 3(\alpha C_m)^2 - 4(\alpha C_m)^3 + \ldots .\} \tag{20}$$

$$R\Delta\text{: } k = k_0\{1 - 2(\alpha C_m) + 4\psi(\alpha C_m)^2 - 8\psi^2(\alpha C_m)^3 + \ldots.\} \quad (21)$$

$$k\Delta\text{: } k = k_0\{1 - 2(\alpha C_m)\} \quad \text{(exact)} \quad (22)$$

Peak shapes on R_F basis

$$\text{L: } R_F = R_{F_0}\left\{1 + 2(\psi\alpha C_m) + \left(\frac{k_0 - 3}{k_0}\right)(\psi\alpha C_m)^2 + \left(\frac{k_0 - 1}{k_0}\right)(\psi\alpha C_m)^3 + \ldots.\right\} \quad (23)$$

$$R\Delta\text{: } R_F = R_{F_0}\{1 + 2(\psi\alpha C_m)\} \quad \text{(exact)} \quad (24)$$

$$k\Delta\text{: } R_F = R_{F_0}\{1 + 2(\psi\alpha C_m) + 4(\psi\alpha C_m)^2 + 8(\psi\alpha C_m)^3 + \ldots.\} \quad (25)$$

where $\psi = k_0/(1 + k_0)$ and $R_{F_0} = 1/(1 + k_0)$.

It may be noted that all three isotherms (Fig. 8) show the same initial gradient, k_0, and initial curvature α. They differ only in the third and later terms in the bracketted polynomials. It is noteworthy that the L and $R\Delta$ isotherms have identical third terms when $k_0 = 3$ and that, for all practical LC purposes, they are identical. The $k\Delta$ isotherm deviates significantly from the other two at values of αC_m above 0.2. Similar conclusions, of course, apply to the various peak shapes (Fig. 9). Those for L and $R\Delta$ are almost indistinguishable while those for $k\Delta$ deviate significantly as αC_m increases.

It is important to note that marked deviation from the ideal peak shape is observed for quite low values of αC_m and relatively small deviations of the isotherm from linearity. Unless we are prepared to see peaks excessively widened by isotherm non-linearity, αC_m values at the column outlet must not exceed about 0.2 which corresponds, roughly speaking, to peaks spread over about one third of their elution time and so to N values of around 150. Greater peak asymmetry will, of course, occur at the start of the column. It must be noted that the maximum values of αC_m for the $R\Delta$ and $k\Delta$ peak profiles are limited since R_F cannot exceed unity and k cannot become negative. For the L isotherm αC_m may have any value since when $\alpha C_m = \infty$, $R_F = 1$ and $k = 0$. Such extreme values of αC_m are not, of course, realistic in practice and the unrealistic features of the proposed expressions need not be of concern.

RELEVANCE OF THE PLATE CONCEPT FOR OVERLOADED COLUMNS

It is often suggested that the plate concept cannot apply when eluted peaks are asymmetric or if they are broadened either by volume or concentration overload. This is incorrect. It is always possible to state that a particular column is "equivalent to a certain number, N, of theoretical plates", and we can define this number by

$$N = \left\{\frac{L}{\sigma_z}\right\}^2 \quad (26)$$

where L is the column length and σ_z^2 the second moment of peak measured in distance units within the column taken about the mean. In the same way it is possible to define the HETP by

$$H_{\text{total}} = \sigma_z^2/L \tag{27}$$

What is not legitimate is to interpret H in terms of purely kinetic phenomena. However, if the dispersions arising from both kinetic and thermodynamic effects are independent eqn. 10 can be applied. For this approach to be useful in optimisation it is desirable that both H_0 and H_{th} are more or less independent of column length. Only then can optimum column parameters be readily derived.

We must therefore examine how the peak variance or second moment arising from isotherm non-linearity develops as a peak migrates along a column.

A simplified approach is illustrated in Fig. 10 where a triangular peak ($R\Delta$ peak profile) migrates along a column. The quantity of solute in the mobile phase is taken as proportional to the peak area. Since the quantity in any peak as it migrates along the column is constant the area must remain constant while the peak broadens and becomes lower. The range of the isotherm which is embraced by the peak thus decreases as it migrates so the relative peak width declines. It is readily seen from the geometry of the figure that the width increases as the square root of the distance, z_0, migrated by the low concentration edge of the peak. Thus if N is measured as

$$N = q(z_0/w_z)^2 \tag{28}$$

N will increase linearly with z_0. When the distance migrated, z, is taken as other elution distances (*e.g.* that of the centre of mass of the peak or its maximum, z_{cm} or z_{max}) the plots of N *versus* z deviate slightly from the straight line plot of N *versus* z_0 as illustrated in Fig. 10.

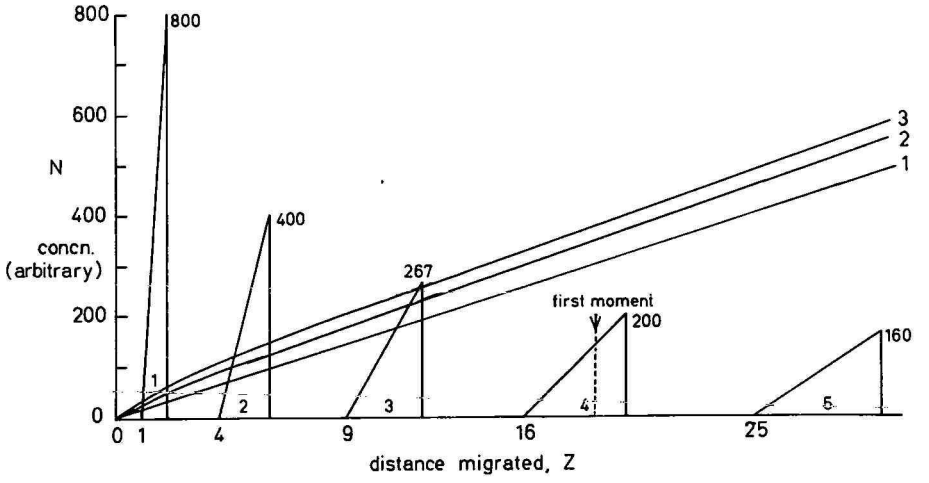

Fig. 10. Peak development with distance migrated for $R\Delta$ profile. Peak maximum concentrations shown on each peak. Lines are plots of N *versus* distance migrated calculated according to the formulae $16(z_0/w_z)^2$, line 1; $16(z_{\text{cm}}/w_z)^2$, line 2; $16(z_{\text{max}}/w_z)$, line 3, where w_z = base width. Note that line 1 is straight.

This analysis unfortunately ignores the content of solute in the stationary phase. Since the isotherm is non-linear the quantity of solute in the stationary phase is not exactly proportional to that in the mobile phase. Accordingly the peak width does not increase exactly in proportion to $\sqrt{z_0}$.

The total quantity of solute in the $R\Delta$ peak is obtained as follows: eqn. 17 is first recast as

$$C_s = \frac{C_m}{R_{F_0}} \left\{ \psi - (\beta C_m) + \frac{4}{3}(\beta C_m)^2 - 2(\beta C_m)^3 \ldots . \right\} \tag{29}$$

where $\beta = \psi\alpha$. The total concentration within the peak at any cross section is

$$C = C_m + C_s \tag{30}$$

and the quantity within the peak is

$$Q = \int C \, dz \tag{31}$$

The distance z is given by

$$z = z^{\ominus} R_F = z^{\ominus} R_{F_0} (1 + 2\beta C_m) = z_0(1 + 2\beta C_m) \tag{32}$$

Where $z^{\ominus}$is the distance moved by the unretained solute or solvent front. Insertion of eqn. 32 into eqn. 31 gives

$$Q = 2 \int_0^{C_m^*} (C_m + C_s) \, z^{\ominus} R_{F_0} \beta \, dC_m \tag{33}$$

where C_m^* is the maximum concentration in the mobile phase at the front of the peak. Insertion of eqn. 29 for C_s followed by integration yields

$$Q = \frac{z^{\ominus}}{\beta} (\beta C_m^*)^2 \left\{ 1 - \frac{2}{3}(\beta C_m^*) + \frac{2}{3}(\beta C_m^*)^2 - \frac{4}{5}(\beta C_m^*)^3 + \ldots . \right\} \tag{34}$$

As $z^{\ominus}$increases the peak migrates along the column and z_0, the distance moved by the low concentration tail, increases in proportion.

Since Q is constant C_m^* decreases as $z^{\ominus}$increases and can be found from eqn. 34 by iteration as a function of $z^{\ominus}$or z_0. The peak width from eqn. 32 is $2\beta C_m^* z_0$. N is then obtained finally as

$$N = q \left(\frac{z}{2\beta C_m^* z_0} \right)^2 \tag{35}$$

Again z in eqn. 35 may be chosen as z_0, the position of the low concentration tail, z_{cm}, the position of the centre of mass of the peak, or z_{max} the position of the peak maximum. For a Gaussian peak the multiplier q is 16, for a triangle q is close to 18.

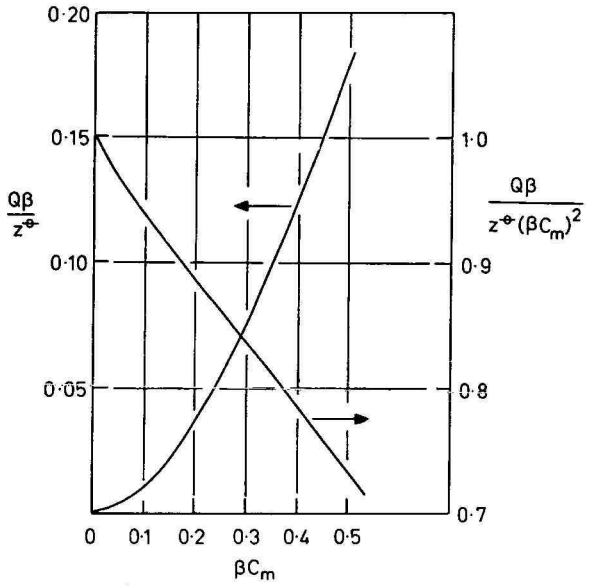

Fig. 11. Relevant parameters from eqn. 34 as a function of βC_m.

In reality peaks will show broadening partly from kinetic effects and partly from thermodynamic effects and we shall therefore use the approximation $q = 16$ throughout.

Fig. 11 shows plots relevant to eqn. 34. Fig. 12 revises Fig. 10 to accommodate the solute in the stationary phase. Fig. 12 shows that the initial curvatures of the upper lines of Fig. 10 are now reduced and that the plot of N *versus* z_{cm} has become an almost perfect straight line.

It may therefore be concluded that for peaks with an $R\Delta$ profile the plate count

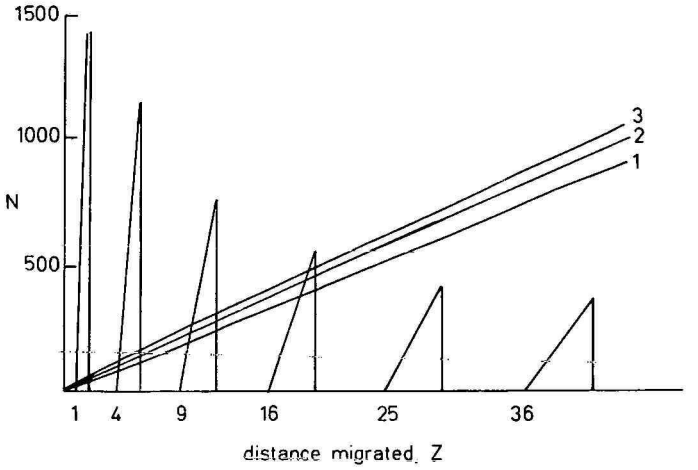

Fig. 12. As for Fig. 10 except that quantity of solute in stationary phase taken into account assuming $k_0 = 4$ and $\alpha = 1$. Note that line 2 is now straight.

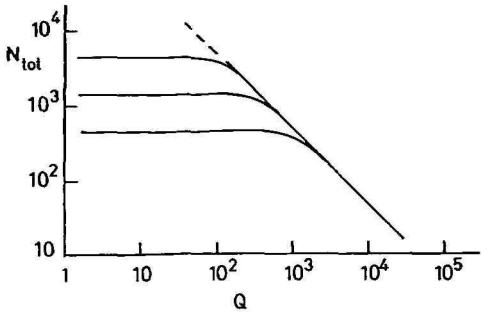

Fig. 13. Effect of load Q (arbitrary units) on number of theoretical plates to which column is equivalent.

for thermodynamic broadening is proportional to column length and that the HETP for this kind of dispersion is a constant independent of the column length.

EFFECT OF QUANTITY INJECTED ON THE NUMBER OF THEORETICAL PLATES FOR *RΔ* PEAK PROFILES

At the column outlet, if reasonable resolution of a solute peak is maintained, βC_m^* at the outlet will not exceed 0.2. For $\beta C_m^* = 0.2$, the polynomial within the brackets in eqn. 34 has the value of 0.89 (see Fig. 11). Accordingly, within this limit, the peak width $2\beta C_m^* z_0$ is proportional to $Q^{\frac{1}{2}}$ with a maximum error of $5\frac{1}{2}\%$. The contribution to H from sample load according to eqn. 26 is thus proportional to Q being given using the approximate form of eqn. 34 by

$$H_{th} = \frac{1}{16}\frac{(2\beta C_m^* z_0)^2}{z} = \frac{1}{16}\frac{(2z_0)^2}{z}\left\{\frac{\beta R_{F_0}}{z_0}\right\}Q$$
$$= \frac{1}{4}(\beta R_{F_0})Q \quad \text{(making the approximation } z = z_0\text{)} \tag{36}$$

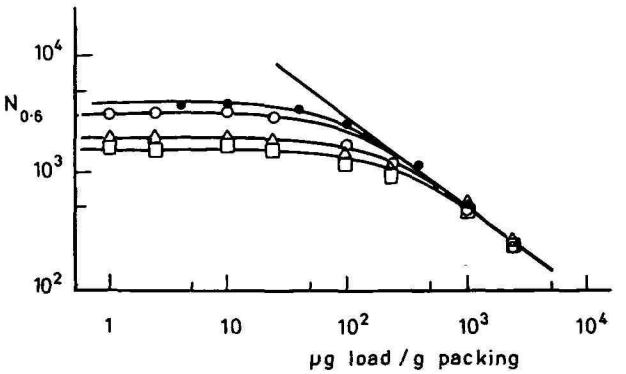

Fig. 14. Practical illustration of effect of load on plate number after de Jong *et al.*[14]. Solute, 2,4-dimethylphenol ($k_0 = 3$). Columns and linear velocities: ●, 100 × 10.8 mm I.D., 5.8 μm, 2.1 mm/s; ○, △, □, 1000 × 10 mm I.D., 20–25 μm, 1.8, 5.5 and 8.4 mm/s respectively. Packing, LiChrosorb SI60; eluent, dichloromethane. Plate height measured using width at 60% of peak height.

The thermodynamic plate height is then determined only by the isotherm curvature parameter α or β, which amounts to the same thing, the retention ratio of the zero concentration sample, R_{F_0}, and the sample quantity Q.

The plate number is then given by

$$N = \frac{L}{H_{\text{total}}} = \frac{L}{\left\{H_0 + \left(\frac{\beta R_{F_0}}{4}\right) Q\right\}} \tag{37}$$

Illustrative plots of log N against log Q are shown in Fig. 13. These plots may be compared with those obtained experimentally by de Jong *et al.*[14,22], an example of which is shown in Fig. 14. The striking similarity of the plots in the two figures gives encouraging support to the theory proposed here.

MAXIMISATION OF THROUGHPUT FOR PEAKS WITH $R\Delta$ PROFILE UNDER PRESSURE LIMITED OPERATION: OPTIMUM COLUMN CONFIGURATIONS

The first practical step in any optimisation procedure is to achieve maximum resolution at the analytical level for those solutes which one requires to isolate. It is then possible to calculate the minimum number of theoretical plates required to provide adequate resolution at the preparative level when the spaces between such solutes are fully closed by overload (see Fig. 3). We denote this number by N^*.

We now assume that preparative packings are available with a range of particle sizes having the same retentive characteristics as the packing used for the test analytical separation. The concept of the isochronic column set is now introduced (see ref. 26). Isochronic columns possess the same reduced length $\lambda = L/d_p$ and give the same elution times, t_m, for an unretained solute when using the same pressure drop, Δp, the same eluent (viscosity, η) and the same packing density (described by the column resistance factor φ). This elution time, t_m, is

$$t_m = \frac{\varphi \eta}{\Delta p} \lambda^2 \tag{38}$$

We define the throughput of any column as

$$T = Q/t_m \tag{39}$$

The practical throughput is defined as

$$PT = Q/t_{\text{cycle}} \tag{40}$$

where t_{cycle} is the cycle time for repeated injections. Often t_{cycle} will be expressed as

$$t_{\text{cycle}} = t_m (1 + k_f) \tag{41}$$

where k_f is the capacity factor for the termination of the cycle. Since the cycle time will normally have to be decided by separate considerations we consider first optimisation of T.

For convenience we express the kinetic plate height as

$$H_0 = d_p\, h(v) \tag{42}$$

where $h(v)$ is the reduced plate height at a reduced velocity v. The reduced velocity is defined as

$$v = \frac{L}{t_m}\frac{d_p}{D_m} \tag{43}$$

where D_m is the diffusion coefficient of solute in eluent and $L/t_m = u$, the linear eluent velocity. Replacing t_m by its value from eqn. 38 gives

$$v = \frac{\Delta P\, d_p^2}{D_m\, \varphi\eta\lambda} \tag{44}$$

We simplify eqn. 36 to

$$H_{th} = \gamma Q; \qquad \gamma = \frac{\beta R_{F_0}}{4} \tag{45}$$

Giving from eqn. 10

$$H_{total} = d_p\, h(v) + \gamma Q \tag{46}$$

whence using eqn. 39 and $H_{total} = L/N^*$

$$\gamma T = \left\{\frac{\lambda}{N^*} - h(v)\right\}\frac{d_p}{t_m} \tag{47}$$

elimination of t_m between eqns. 47 and 38 gives

$$\gamma T = \left\{\frac{\lambda}{N^*} - h(v)\right\}\frac{d_p \Delta p}{\lambda^2 \varphi\eta} \tag{48}$$

Eqn. 48 shows, in broad terms, that if kinetic dispersion can be ignored, the larger d_p the greater the throughput when λ is kept constant. However, as d_p is increased at constant λ the linear elution velocity increases as d_p and the reduced velocity as d_p^2. Since $h(v)$ depends upon v according to the widely accepted eqn. 49 (ref. 27)

$$h = \frac{B}{v} + Av^{1/3} + Cv \tag{49}$$

(where typical values for A, B and C are 1, 2 and 0.1 respectively) h will increase strongly for the isochronic set as d_p increases. A stage must then be reached when the $h(v)$ term in eqn. 48 begins to dominate the throughput and eventually reduces it as d_p is increased. This will normally occur when v is large and we can approximate $h(v)$ by

$$h = Cv \qquad \text{with } C \cong 0.1 \tag{50}$$

Inserting eqns. 44 and 50 into eqn. 48 gives

$$\gamma T = \left\{\frac{1}{N^*} - \frac{C\,\Delta p\,{d_p}^2}{D_m\,\varphi\eta\,\lambda^2}\right\}\frac{\Delta p}{\varphi\eta}\frac{d_p}{\lambda} \tag{51}$$

Differentiating γT with respect to (d_p/λ) and setting the differential to zero gives the value of d_p/λ for maximum throughput

$$\left(\frac{d_p}{\lambda}\right)_{opt} = \left(\frac{{d_p}^2}{L}\right)_{opt} = \left\{\frac{D_m\,\varphi\eta}{3N^*C\Delta p}\right\}^{\frac{1}{2}} \tag{52}$$

Insertion of this value for d_p/λ into eqn. 51 gives

$$\gamma T_{opt} = \frac{2}{3N^*}\left\{\frac{\Delta p\,D_m}{3\,\varphi\eta\,N^*C}\right\}^{\frac{1}{2}} \tag{53}$$

Under these conditions it is readily shown that the kinetic dispersion is one half of the thermodynamic dispersion.

The reduced velocity at which the optimum throughput is obtained is found by substituting eqn. 52 into eqn. 44 to eliminate d_p giving

$$\nu_{opt} = \frac{1}{3}\left(\frac{\lambda}{N^*C}\right) \tag{54}$$

Under typical conditions λ might be 20000 and N^* between 50 and 2000; taking $C = 0.1$, ν_{opt} will then lie between 33 and 1333. We can now check on the validity of approximation 50 by first expressing the reduced plate height given by eqn. 49 in the alternative forms

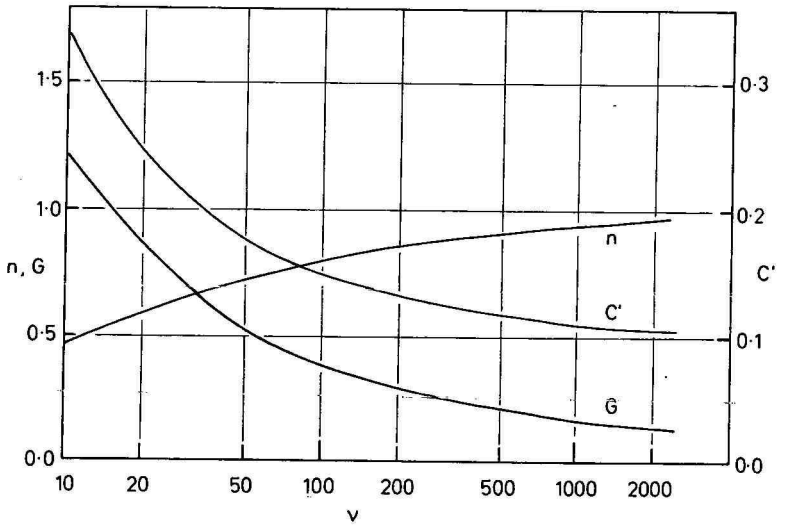

Fig. 15. Dependence of C', n and G (eqns. 55 and 56) upon reduced velocity, ν.

$$h = C'v \tag{55}$$

$$h = Gv^n \tag{56}$$

where C', G and n are now weak functions of v. Values of C', G and n as functions of v are shown in Fig. 15. Typical values of C' are 0.20 at $v = 33$ and 0.108 at $v = 1333$. It is thus clear that the approximation $C = 0.1$, eqn. 50, is poor at low values of v. The use of eqn. 55 with the correct value of C' provides a much closer approximation to the true optimum conditions but C' can only be found by successive approximation using eqns. 52 and 54 for specified values of λ and N^*. Iteration is initiated by taking $C = 0.1$ as the first value. Alternatively the better approximation (eqn. 56) can be used but eqns. 52–54 must now be replaced by

$$\frac{d_p}{\lambda} = \left\{\frac{\lambda}{(2n+1)N^*}\right\}^{\frac{1}{2n}} \left\{\frac{D_m\varphi\eta}{G\Delta p\lambda}\right\}^{\frac{1}{n}} \tag{57}$$

$$\gamma T_{opt} = \left\{\frac{2n}{(2n+1)N^*}\right\} \left\{\frac{\lambda}{(2n+1)N^*}\right\}^{\frac{1}{2n}} \left\{\frac{\Delta p D_m}{G\varphi\eta\lambda}\right\}^{\frac{1}{n}} \tag{58}$$

$$v_{opt} = \frac{1}{G}\left\{\frac{\lambda}{(2n+1)N^*}\right\}^{\frac{1}{n}} \tag{59}$$

Again iteration is required starting with initial values of $G = 0.1$ and $n = 1$ corresponding to approximation 50.

The three methods of estimating optimum conditions are compared in Figs. 16 and 17 for columns with a fixed reduced length $\lambda = 20000$.

Method a is based upon eqns. 52–54 with $C = 0.1$; method b is based upon eqns. 52–54 using values of C' found by iteration and method c is based upon eqns. 57–59 using values of G and n found by iteration.

The other operating parameters are assumed to have the values: $\Delta p = 2 \cdot 10^7$ N m^{-2} (200 bar), $D_m = 1.0 \cdot 10^{-9}$ m^2 s^{-1}, $\varphi = 1.0 \cdot 10^3$ and $\eta = 1.0 \cdot 10^{-3}$ N s m^{-2}. Plate height eqn. 49 with $B = 2$, $A = 1$ and $C = 0.1$, values of C', G and n as shown in Fig. 14.

Figs. 16 and 17 confirm that there is good agreement between the calculations for methods b and c but show that even method a gives reasonable approximations to d_p and T_{opt}.

An important feature of eqn. 53 is that the optimum throughput does not apparently depend upon either λ or d_p. These parameters only enter into the optimal conditions through eqn. 52 which specifies the ratio d_p/λ for optimum throughput. It thus appears that the optimum throughput can be achieved with a wide range of geometrical configurations. This conclusion is slightly modified when we recognise that C is not a true constant and ought to be replaced by C', or alternatively that the more precise eqn. 58 should be used. In this equation T is seen to be proportional to $\lambda^{(1+n)/2n}$. Since n is close to unity, T depends rather weakly upon λ in the sense that larger λ gives higher T until λ is so large that in the limit n becomes unity. Thus λ does have to have a large enough value for near maximum T to be obtained.

TABLE I

VARIOUS OPTIMUM CONDITIONS FOR PLC

Assumed parameters: Δp = 200 bar = $2 \cdot 10^7$ N m^{-2}; $D_m = 1.0 \cdot 10^{-9}$ m^2 s^{-1}; $\eta = 1 \cdot 10^{-3}$ N s m^{-2}; $\theta = 1000$, $h = 2/v + v^{1/3} + 0.1v$; $h = C'v = Gv^n$

N^*	$\lambda = 20000$					$L = 500$ mm					$d_p = 20$ μm				
	d_p (μm)	L (mm)	C'	v	γT (m s^{-1})	d_p (μm)	$\lambda/1000$	C'	v	γT (m s^{-1})	L (mm)	$\lambda/1000$	C'	v	γT (m s^{-1})
50	35	700	0.108	1240	$4.6 \cdot 10^{-4}$	30	17	0.109	1040	$4.7 \cdot 10^{-4}$	240	12	0.113	690	$4.6 \cdot 10^{-4}$
100	24	480	0.114	580	$1.6 \cdot 10^{-4}$	25	20	0.114	600	$1.6 \cdot 10^{-4}$	340	17	0.116	480	$1.6 \cdot 10^{-4}$
200	16	320	0.124	270	$5.5 \cdot 10^{-5}$	20	25	0.122	350	$5.5 \cdot 10^{-5}$	480	24	0.121	333	$5.5 \cdot 10^{-5}$
500	9.5	190	0.150	90	$1.3 \cdot 10^{-5}$	16	32	0.135	160	$1.3 \cdot 10^{-5}$	680	39	0.129	205	$1.3 \cdot 10^{-5}$
1000	6.8	140	0.196	35	$3.9 \cdot 10^{-6}$	13	39	0.151	90	$4.4 \cdot 10^{-6}$	980	49	0.138	140	$4.7 \cdot 10^{-6}$
2000	3.2	65	0.330	10	$1.0 \cdot 10^{-6}$	10	48	0.178	50	$1.4 \cdot 10^{-6}$	1400	69	0.150	100	$1.6 \cdot 10^{-6}$

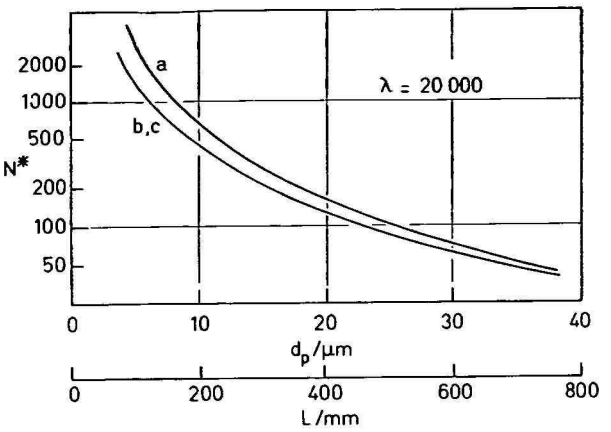

Fig. 16. Dependence of particle diameter, d_p, and column length, L, upon N^* for cases a, b and c (see text), with $\lambda = 20000$.

Nevertheless there is still wide flexibility in the choice of optimum conditions for PLC. Thus if λ is fixed, d_p will have optimum values for different N^*; if column length L is fixed, d_p will have a different set of optimum values, and if d_p is fixed, λ or L will take optimum values. The values of T and of other parameters for the restrictions $\lambda = 20000$, $L = 500$ mm and $d_p = 20$ μm are compared in Table I. The values are calculated using C' values in place of C in eqns. 52–54. It is clear that the throughput is relatively insensitive to the nature of the restriction imposed and depends primarily upon N^*. The throughput is given in the three cases to a good approximation by

$$\log_{10}\left\{\frac{\gamma\, T_{opt}}{\text{m s}^{-1}}\right\} = -1.58 \log_{10} N^* - 0.64 \tag{62}$$

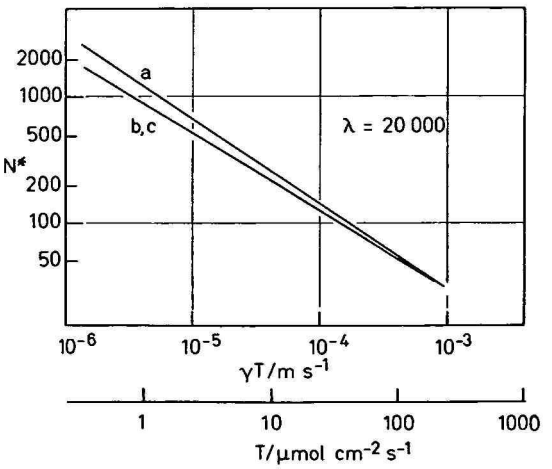

Fig. 17. Dependence of throughput, T, upon N^* for methods a, b and c (see text) with $\lambda = 20000$.

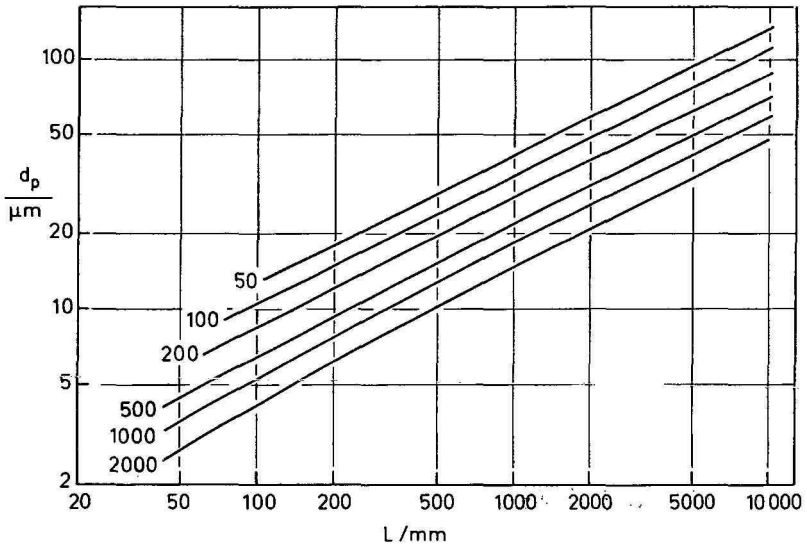

Fig. 18. Optimum combinations of particle size, d_p, and column length, L, for different values of N^* given on lines. Operating parameters as given in Table I.

The slope -1.58 is slightly steeper than the value of -1.5 predicted using constant C (eqn. 54).

Eqns. 53 and 58 for optimised throughput confirm that, as in analytical HPLC, performance can always be improved by (a) increasing pressure drop, Δp; (b) increasing diffusion rate of solute in eluent, D_m; (c) decreasing eluent viscosity, η, and (d) decreasing the column flow resistance factor, φ.

In practice it will be desirable to have available a range of both column lengths and particle diameters so that appropriate optimal combination can be selected for particular preparative applications.

The range of choice of L, λ and d_p for optimum conditions with different N^* requirements is summarised in Fig. 18. The calculations use method b with values of C' found by iteration for particular λ and N^* values. For each N^* the appropriate T is given to a good approximation by eqn. 62. Since there is little dependence of throughput upon any parameter other than N^* one is free to choose the most appropriate combination of L and d_p consistent with the desired N^* value. The choice may well be determined by a desire to avoid columns which are short and wide and will present problems of distribution of sample to the column cross section. Other considerations in practice may be the relative costs of say 5- and 20-μm materials or the available lengths of preparative scale columns. It is also likely that as the scale of the preparation increases there will be a tendency to use altogether larger systems, that is wider and longer columns packed with larger particles but keeping the d_p/λ ratio at the appropriate value for maximum throughput.

NUMERICAL ESTIMATION OF OPTIMUM PRACTICAL THROUGHPUT

In order to estimate the throughput (see eqns. 39 and 40) which might be

achieved in practice it is necessary first to evaluate $\gamma = \beta R_{F_0}/4$ which occurs as the multiple of throughput in eqns. 54 and 59. Rewriting in terms of k_0 we obtain

$$\gamma = \frac{1}{4}\left\{\frac{k_0}{(1+k_0)^2}\right\}\alpha \tag{63}$$

We now require to estimate α, the curvature of the isotherm. Assuming that a Langmuir isotherm applies, elementary adsorption theory given for the fractional coverage of an adsorbent surface, θ,

$$\theta = \frac{KC_m}{1+KC_m} \tag{64}$$

where K is the ratio of the adsorption to desorption rate constants. θ may be expressed as C_s/C_s^∞ where C_s^∞ is the saturation monolayer coverage of the adsorbent. Thus

$$C_s = \frac{KC_s^\infty\, C_m}{1+KC_m} \tag{65}$$

Identifying with the Langmuir isotherm as expressed by eqn. 12 we obtain

$$k_0 = KC_s^\infty, \qquad \alpha = K \qquad \text{and} \qquad k_0/\alpha = C_s^\infty \tag{66}$$

whence

$$\alpha = k_0/C_s^\infty \tag{67}$$

Substituting for α into eqn. 63 then gives

$$\gamma = \frac{1}{4}\left\{\frac{k_0}{1+k_0}\right\}^2 \frac{1}{C_s^\infty} \tag{68}$$

The final requirement is to estimate C_s^∞. Most HPLC bonded materials show coverages of bonded phase in the region of *ca.* 3 μmol m^{-2} and a typical silica gel will have a specific surface area of around 200 m^2 g^{-1} with a packed bed density of about 0.7 g cm^{-3}. The content of bonded phase is thus around 400 μmol cm^{-3}. It would not be unreasonable to take a value of this order for C_s^∞. Taking $k_0 = 4$ and $C_s^\infty = 400$ μmol cm^{-3} gives $\gamma = 4 \cdot 10^{-4}$ μmol^{-1} cm^3 $= 4 \cdot 10^{-4}$ mol^{-1} m^3.

Eqn. 62 with appropriate change of units then takes the form:

$$\log_{10}\left\{\frac{T_{opt}}{\mu\text{mol cm}^{-2}\text{ min}^{-1}}\right\} = 6.54 - 1.58 \log N^* \tag{69}$$

Supposing finally that the solute has molecular weight of 200 g mol^{-1}, the practical throughput, PT (eqn. 40) taking $k_f = k_0 + 1$, is then given by

TABLE II

SAMPLE DILUTION AT COLUMN OUTLET IN PLC

Conditions as specified for Table I, $k_f = 5$.

N^*	PT ($g\ cm^{-2}\ h^{-1}$)	$\lambda = 20000$			$L = 500$ mm			$d_p = 20\ \mu m$		
		d_p (μm)	Cycles (h^{-1})	Mean conc.* (g/l)	d_p (μm)	Cycles (h^{-1})	Mean conc.* (g/l)	L (mm)	Cycles (h^{-1})	Mean conc.* (g/l)
50	14	35	30	3.0	30	41	3.0	240	90	2.6
100	4.8	24	30	2.0	25	30	2.0	340	43	2.0
200	1.6	16	30	1.5	20	19	1.5	480	21	1.4
500	0.38	9.5	30	0.9	16	12	0.9	800	8	0.9
1000	0.13	6.8	30	0.6	13	8	0.6	1000	5	0.5
2000	0.042	3.2	30	0.5	10	5	0.5	1400	2.5	0.35

* Mean concentration is amount collected divided by base peak volume.

$$\log_{10}\left\{\frac{PT_{opt}}{\text{g cm}^{-2}\text{ h}^{-1}}\right\} = 3.84 - 1.58 \log N^* \quad (70)$$

Typical values of PT are then 0.13 g cm^{-2} h^{-1} at $N^* = 1000$ and 14 g cm^{-2} h^{-1} at $N^* = 50$.

Eqn. 38 gives t_m for a set of isochronic columns with $\lambda = 20000$ as 20 s. The run time is therefore 6×20 s $= 2$ min. Thus using the isochronic set it would be necessary to carry out 30 injections per hour. If N^* were 1000 then each injection would be of about 4 mg whereas with $N^* = 50$ then 0.5 g per run for each cm^2 of column section.

A major factor in any chromatographic separation is sample dilution. This is particularly relevant in PLC where it will be necessary in most cases to isolate the separated materials from eluent. It is a straightforward matter to calculate the mean sample concentration in collected eluent for the various cases considered in Table I. The results are shown in Table II which gives the concentrations of sample eluted at with $k_0 = 4$ when collection is taken over the base peak width. The insensitivity of the collected concentration to the exact geometry of the column is again most notable. Surprisingly there is rather little loss of concentration when long columns with relatively large particles are used for quite high efficiency separations (last entry Table II). Nevertheless Table II emphasises that the maximum concentrations which can be expected in PLC at the column outlet range from some 0.3 to 3 g/l as N^* decreases from 2000 to 50.

On the broad subject of cost of separating materials by PLC, it is clear that both column packing materials and eluents must be of the highest quality. A given weight of packing material will process between 1–10% of its own weight of solute per hour; and a given yield of purified solute will require between 5000 and 300 times its own weight or volume of eluent for elution. Thus only materials with a value of say 1000–10000 times that of common bulk organic chemcials can be candidates for production LC. Minimum production costs in PLC are thus likely to be in the range of \$1 to \$10 per gram, similar to those of high-grade chromatographic packing materials even if the capital cost of the equipment is discounted.

CONCLUSIONS AND LIMITATIONS

(1) For many sorbent–eluent combinations the distribution of a solute follows a Langmuir type isotherm up to concentrations where deviation from linearity is around 20%. Under these circumstances the peak profile is very close to triangular.

(2) Under these conditions there will inevitably be some interference between competing solutes. Such interferences cannot be predicted or dealt with simply and have been ignored in our treatment. Their effect is likely to be secondary especially if solutes are fairly well separated (large α values).

(3) With triangular peak profiles the peak base width, in the absence of kinetic dispersion, increases with the square root of the distance migrated. Accordingly optimisation can be carried out using similar procedures to those employed in optimising kinetic performance.

(4) Optimisation for maximum throughput under conditions of restricted pres-

sure drop requires a balancing of kinetic and thermodynamic dispersion. The theoretical analysis shows that maximum throughput occurs when the kinetic dispersion is half the thermodynamic dispersion.

(5) The maximum throughput, T_{opt}, is determined almost exclusively by the minimum number of theoretical plates which provides acceptable resolution of the components of interest N^*. It also depends upon the operating parameters: pressure drop, solute diffusion coefficient, eluent viscosity and column resistance parameter.

(6) For typical values of operating parameters, assuming a Langmuir isotherm and a molecular weight of 200 g mol^{-1}, it is found that the maximum practical throughput, defined as injected quantity/elution time of solute with $k_0 = 5$ is given by

$$\log_{10}\left\{\frac{PT}{\text{g cm}^{-2}\,\text{h}^{-1}}\right\} = 3.84 - 1.58 \log N^*$$

(7) Optimum throughput is obtained for a specific ratio of d_p^2/L which depends upon N^* and the operating parameters. For a given N^* there is a wide range of d_p and L which give the same N^*.

(8) The optimum throughput for a given N^* is obtained for a specific ratio of d_p^2/L and is almost independent of the actual values of d_p and L.

(9) Likewise sample dilution for optimum conditions for a given N^* is independent of the actual values of d_p and L.

(10) It is recognised that the whole of the above treatment makes major assumptions about the nature of the partition isotherm of a typical solute and ignores interferences of solutes which could produce distortion of isotherms. We do, however, claim that the broad results provide a useful and realistic framework for optimising throughput in preparative liquid chromatography.

GLOSSARY OF SYMBOLS

A	constant in plate height eqn. 49, value 1
A_m	cross sectional area of eluent in column
B	constant in plate height eqn. 49, value 2
C	constant in plate height eqn. 49, value 0.1
C'	constant in modified plate height eqn. 55
C	concentration: total amount of solute per unit volume of column bed
C_m, C_s	concentrations: amount of solute in eluent phase, and stationary phase per unit volume of column bed
C_0	initial concentration of solute in column immediately following injection
C_m^*	maximum concentration of solute in mobile phase in a chromatographic band
C_s^∞	concentration of solute in stationary phase corresponding to monolayer coverage on adsorbent per unit volume of column bed
D_m	diffusion coefficient of solute in eluent
d_p	mean particle diameter
G	constant in modified plate height eqn. 56
H	plate height

H_0	kinetic contribution to plate height corresponding to an analytical sample
H_{th}	thermodynamic contribution to plate height
H_{total}	total plate height
h, $h(v)$	reduced plate height, value of h at specified reduced velocity
k	column capacity ratio
k_0	column capacity ratio at zero concentrations of solute
k_{C_m}	column capacity ratio for a concentration C_m in tail of a peak
k_{front}	column capacity ratio for a front
k_f	column capacity ratio corresponding to end of cycle in a series of repetitive PLC runs
K	equilibrium distribution coefficient for an adsorbent
L	column length
N	plate number
N^*	minimum number of plates required to provide adequate resolution in a preparative run
n	constant in modified plate height eqn. 56
Δp	pressure drop
PT, PT_{opt}	practical throughput, optimum practical throughput
Q	quantity injected
q	configurational factor (in eqn. 35)
R_F, R_{F_0}	retention ratio, and retention ratio at zero concentration of solute
T, T_{opt}	throughput and optimum throughput
t_m	elution time of unretained solute
t_{cycle}	cycle time in PLC
u	eluent linear velocity
V_{inj}	volume of injected sample
V_{R1}, V_{R2}	retention volumes of solutes 1 and 2
V_m	volume of eluent phase in column
V_s	volume of stationary phase in column
w_z	base peak width measured as a distance within the column
x, X	dummy variables
z	distance from start of column
Δz	distance measured from centre of mass of peak
z_0	distance migrated by low concentration side of peak
$z^{\ominus}$	distance migrated by unretained solute or solvent front
z_{cm}	distance migrated by centre of mass of peak
z_{max}	distance migrated by maximum concentration in peak
z_{inj}	length of column occupied by peak immediately following injection
α	parameter in Langmuir isotherm, relative retention ratio
β	parameter given by $\alpha k_0/(1+k_0)$
γ	constant relating plate height to Q
η	eluent viscosity
θ	fractional surface coverage
λ	reduced column length, L/d_p
v, v_{opt}	reduced eluent velocity, optimum reduced velocity
φ	column flow resistance factor
ψ	constant $k_0/(1+k_0)$

σ, σ_z standard deviation of peak measured as elution volume and as distance in column

REFERENCES

1 J. H. Knox and M. Saleem, *J. Chromatogr. Sci.*, 7 (1969) 614–622.
2 J. H. Knox and M. T. Gilbert, *J. Chromatogr.*, 186 (1979) 405–418.
3 I. Halàsz, H. Schmidt and P. Vogtel, *J. Chromatogr.*, 126 (1967) 19–33.
4 L. R. Snyder, *J. Chromatogr. Sci.*, 15 (1977) 441–449.
5 G. Guiochon, in Cs. Horváth (Editor), *High Performance Liquid Chromatography*, Vol. 2, Academic Press, New York, London, 1980, pp. 1–56.
6 R. Rosset, M. Caude, J. Desbarres and E. Schmidt, *Analusis*, 8 (1980) 213–223.
7 K. P. Hupe and H. H. Lauer, *J. Chromatogr.*, 203 (1981) 41–52.
8 C. N. Reilley, G. P. Hildebrand and J. W. Ashley, Jr., *Anal. Chem.*, 34 (1962) 1198.
9 B. Coq, G. Cretier and J. L. Rocca, *J. Chromatogr.*, 186 (1979) 457.
10 R. P. W. Scott and P. Kucera, *J. Chromatogr.*, 119 (1976) 467.
11 R. A. Barford, R. McGraw and H. L. Rothbart, *J. Chromatogr.*, 166 (1978) 365–372.
12 P. C. Haarhoff and H. J. van der Linde, *Anal. Chem.*, 38 (1966) 573.
13 J. F. K. Huber and R. G. Gerritse, *J. Chromatogr.*, 58 (1971) 137.
14 A. W. J. de Jong, H. Poppe and J. C. Kraak, *J. Chromatogr.*, 209 (1981) 432–436.
15 J. H. Knox and R. Kaliszan, *J. Chromatogr.*, 349 (1985) 211–234.
16 G. Cretier and J. L. Rocca, *Chromatographia*, 18 (1984) 623–627.
17 H. Poppe and J. C. Kraak, *J. Chromatogr.*, 255 (1983) 395.
18 A. W. J. de Jong, J. C. Kraak, H. Poppe and F. Nooitgedacht, *J. Chromatogr.*, 193 (1980) 181–185.
19 B. Coq, G. Cretier and J. L. Rocca, *Anal. Chem.*, 54 (1982) 2271–2277.
20 F. Eisenbeiss, S. Ehlevding, A. Wehrli and J. F. K. Huber, *Chromatographia*, 20 (1985) 657–663.
21 J. C. Smit, H. C. Smit and E. M. de Jaeger, *Anal. Chim. Acta*, 122 (1980) 1.
22 A. W. J. de Jong, H. Poppe and J. C. Kraak, *J. Chromatogr.*, 148 (1978) 127–141.
23 R. A. Wall, *J. Liq. Chromatogr.*, 2 (1979) 775–798.
24 H. M. Pyper and J. H. Knox, *Ph.D. Thesis*, University of Edinburgh, 1984.
25 P. Gareil, L. Personnaz, J. P. Feraud and M. Caude, *J. Chromatogr.*, 192 (1980) 53–74.
26 J. H. Knox, in C. F. Simpson (Editor), *Techniques in Liquid Chromatography*, Wiley, London, New York, 1982, p. 31.
27 J. H. Knox, *J. Chromatogr. Sci.*, 15 (1977) 352.

Journal of Chromatography, 363 (1986) 31–36
Elsevier Science Publishers B.V., Amsterdam — Printed in The Netherlands

CHROM. 18 599

Note

Process scale high-performance liquid affinity chromatography

Y. D. CLONIS
The Biotechnology Centre, University of Cambridge, Downing Street, Cambridge CB2 3EF (U.K.)
K. JONES
Phase Separations Ltd., Deeside Ind. Estate, Queensferry, Clwyd CH5 2LR (U.K.)
and
C. R. LOWE*
The Biotechnology Centre, University of Cambridge, Downing Street, Cambridge CB2 3EF (U.K.)

The applicability of triazine dyes as group-specific ligands in affinity chromatography has been well documented over many years. Different dyes immobilised to carbohydrate polymers have been employed to purify a plethora of proteins and enzymes both at the analytical [1–7] and preparative scales [2,5,7]. More recently, triazine dyes immobilised to bonded silica matrices have been used in high-performance liquid affinity chromatography (HPLAC) to isolate and purify a number of enzymes[8–10].

We now report preliminary details of the first application of process scale HPLAC using a 3.3-l column of silica-immobilised Procion Blue MX-R for the purification of rabbit muscle L-lactate dehydrogenase from a crude extract.

This system, in its non-optimised form, processes a minimum of 1.8 g crude protein per cycle time of approximately 1 h and affords enzyme of specific activity 450 U/mg in 46% overall yield with a 8.6-fold purification.

EXPERIMENTAL

Materials

γ-Glycidoxypropyltrimethoxysilane was purchased from Aldrich (U.K.); crude rabbit muscle L-lactate dehydrogenase (Type I, 40–100 U/mg) and sodium pyruvate were obtained from Sigma (U.K.); NADH was purchased from Boehringer (U.K.); Procion Blue MX-R was a gift from Dr. C. V. Stead (ICI Organics Division, Blackley, U.K.) and spherical silica (Spherisorb VLS; mean pore size 280 Å, mean particle diameter 20 μm) was a gift from Dr. K. Jones (Phase Separations, Clwyd, U.K.).

Synthesis of silica-immobilised Procion Blue MX-R

Spherical silica (2.5 kg) was suspended in a mixture of 16.7 l of 0.1 *M* sodium acetate buffer (pH 5.5) and γ-glycidoxypropyltrimethoxysilane (1.3 l) and heated at 90°C for 3–4 h under reduced pressure and gentle rotation. The epoxy-silica was washed with water (20 l) on a sintered funnel through a Whatman paper filter and then hydrolysed to the corresponding diol-silica at pH 3.0 (18 l of 1 m*M* hydrochloric acid) for 1 h at 90°C under reduced pressure and gentle rotation. The diol-silica was

0021-9673/86/$03.50

washed with water (20 l) and acetone (10 l) and dried under reduced pressure to yield diol-bonded silica containing 5.5% carbon. Procion Blue MX-R (130 g) in a solution of 0.1 *M* sodium bicarbonate (9.1 l) was introduced into a flask containing diol-silica (1.1 kg dry weight) and the suspension rotated under reduced pressure at 35–40°C for 22 h. The blue-silica was washed with water (10 l), 1 *M* potassium chloride solution (10 l) and water until the effluents were free of dye. The adsorbent was washed with acetone (20 l) and dried under reduced pressure to yield silica-immobilised Procion Blue MX-R containing 2.9 μmol dye per gram dry weight of silica. The molar extinction coefficient of Procion Blue MX-R was taken as 10 500 l mol^{-1} cm^{-1}. The procedure for the preparation of silica-immobilised Procion Blue MX-R is shown in Fig. 1.

Chromatographic procedures

The Procion Blue MX-R silica was packed with axial compression into a stainless-steel column with adjustable bed length [Chromatelf (Elf Solaize, St. Symphorien D'Ozou, France) system LC150 (Fig. 2)] to yield a 3.3-l dyed-silica HPLAC adsorbent of 15 × 18.8 cm bed dimensions.

A dialysed and filtered (Millipore, fibre glass) crude preparation of rabbit muscle L-lactate dehydrogenase (61 790 U; 1.8 g protein) in 100 ml of 30 m*M* sodium phosphate buffer (pH 7.0) was loaded onto the silica-immobilised Procion Blue MX-R column (15.0 × 18.8 cm, 3.3 l, 2.9 μmol dye per gram of silica) which had been equilibrated previously in 30 m*M* sodium phosphate buffer (pH 7.0). Unbound proteins were washed off with irrigating buffer until the adsorption at 280 nm was reduced to zero whence bound L-lactate dehydrogenase was eluted with a pulse of

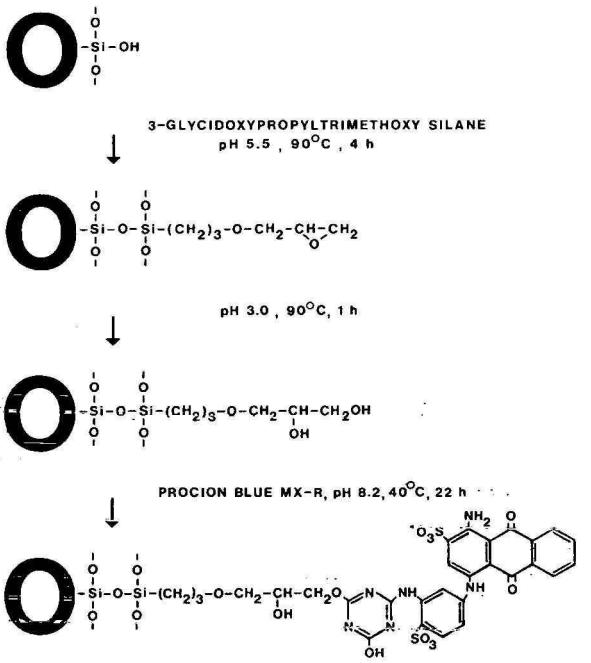

Fig. 1. Procedure for the preparation of silica-immobilised Procion Blue MX-R.

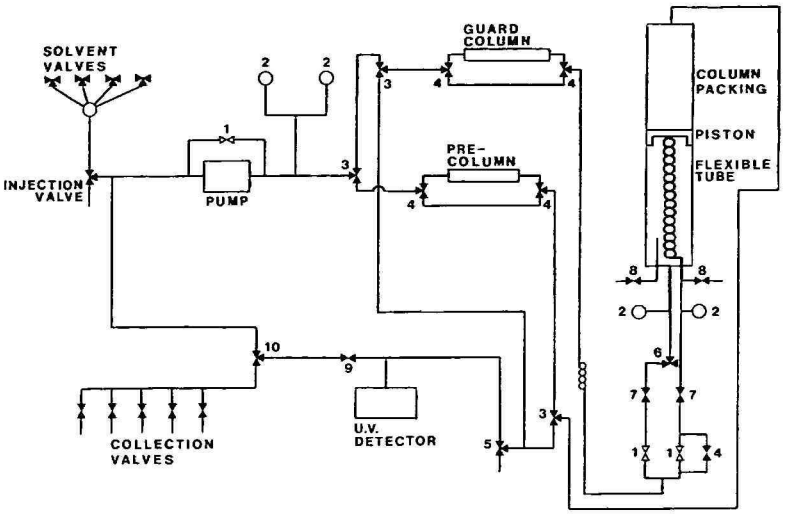

Fig. 2. Chromatelf LC150 System for process scale HPLAC. 1 = Check valve; 2 = pressure gauge; 3 = backflush valve; 4 = bypass valve; 5 = compressed air valve; 6 = purge compression valve; 7 = stop valve; 8 = purge air valve; 9 = needle valve; 10 = recycling valve.

NADH (7 m*M*) in the same buffer (10 ml), as shown in Fig. 3. Fractions (2 l) were collected at a flow-rate of 32.4 l/h. The protein content of each fraction was monitored by its absorbance at 280 nm whereas L-lactate dehydrogenase activity was monitored by following the oxidation of NADH by pyruvate at 340 nm. The molar extinction coefficient of NADH was taken as 6220 l mol^{-1} cm^{-1}.

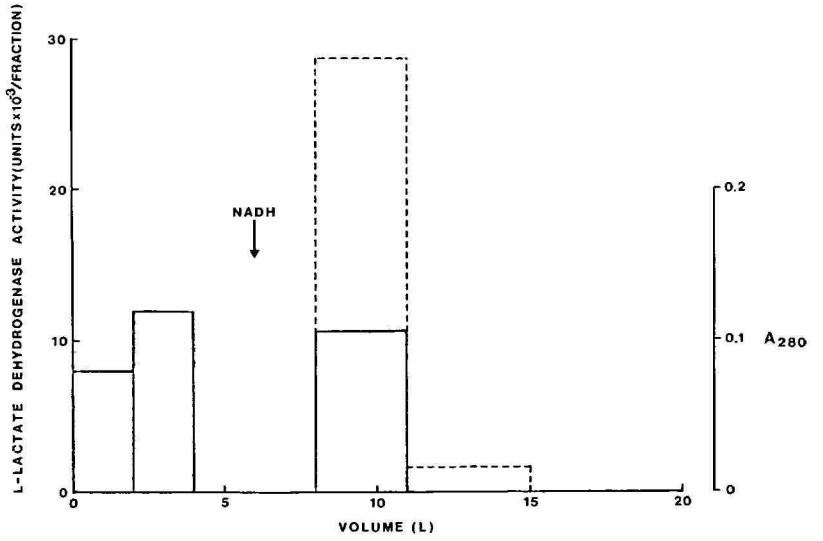

Fig. 3. Process scale purification of L-lactate dehydrogenase from a crude rabbit extract. ———, Absorbance at 280 nm; – – –, enzyme activity.

TABLE I

SUMMARY OF PURIFICATION OF L-LACTATE DEHYDROGENASE

	Volume (ml)	*Protein (mg)*	*Total activity** *(U)*	*Specific activity** *(U/mg)*	*Purification (fold)*	*Yield (%)*
Crude rabbit muscle preparation	100	1800	61 740	34.3	1	100
NADH eluate	3100	97	28 710	296 (450)**	8.6	46.5

* Enzyme assays were performed at 20°C unless stated otherwise.
** Specific activity at 37°C.

Assays

L-lactate dehydrogenase activity was monitored at 340 nm by the oxidation of NADH to NAD^+ with the concomitant conversion of pyruvate to lactate at pH 7.0[6]. Protein concentration was determined by the method of Bradford[11] using Coomassie Brilliant Blue G-250. Bovine serum albumin (fraction V) was used as the protein standard.

RESULTS AND DISCUSSION

The high reactivity of Procion Blue MX-R, a dichlorotriazinyl structural analogue of Cibacron Blue F3G-A, permitted efficient and facile dye coupling directly to diol-silica. This procedure circumvented the problems normally encountered with the immobilisation of monochlorotriazinyl dyes such as Cibacron Blue F3G-A and the Procion H-series[9]:

(i) low substitution when the dyes were coupled directly to diol-silica under mild alkaline conditions, and

(ii) conversion of the parent dye to the corresponding aminoalkyl dye prior to coupling to epoxy-silica.

The blue adsorbent was packed into a 2 m × 15 cm stainless-steel HPLC column with axial compression by exploiting the unique design of the Chromatelf system (Fig. 2). Packing was achieved via a mobile piston, with which the length of the column could be adjusted to afford any bed volume up to 23 l, but with a fixed diameter of 15 cm. Process scale HPLAC was assessed with a 3.3-l column of Procion Blue MX-R silica for the purification of rabbit muscle L-lactate dehydroghenase in one step from a crude rabbit muscle preparation. The adsorbent was loaded with a crude enzyme preparation (1.8 g protein, 61 740 U enzyme activity) at a flow-rate of 32.4 l/h (3.0 ml min^{-1} cm^{-2}). The majority of the inert proteins washed through unretarded whereas L-lactate dehydrogenase was bound and subsequently eluted specifically with a pulse of the competitive ligand, NADH (7 m*M*, 10 ml). This procedure afforded enzyme of specific activity 450 U/mg protein, purified 8.6-fold with an overall yield 46% (Table I). These results were obtained with a non-optimised system operating well below the theoretical capacity of the adsorbent. It is believed that the working capacity of this adsorbent, *i.e.* the maximum amount of total protein that could be loaded for which all the enzyme present is adsorbed, could be increased substantially on optimisation of the adsorbent and operational parameters. Nevertheless, the system described in this paper is capable of processing a minimum of 1.8 g of total protein per cycle (1 h), affording 97 mg of 8.6-fold purified L-lactate dehydrogenase. We believe that this report describes the first example of process scale HPLAC applied in enzyme purification technology on silica adsorbents.

ACKNOWLEDGEMENTS

The authors are indebted to Chromatelf (Centre de Recherche, Elf Solaize, BP22, F69360, St. Symphorien D'Ozou, France) for the loan of the Chromatelf LC150 chromatographic system and to Dr. D. Taylor for his assistance in locating the instrument in the Department of Chemistry, UMIST, Manchester, U.K.

REFERENCES

1 J. K. Baird, R. F. Sherwood, R. J. G. Carr and A. Atkinson, *FEBS Lett.*, 70 (1976) 61–66.
2 C. J. Bruton and T. Atkinson, *Nucl. Acids Res.*, 7 (1979) 1579–1591.
3 P. D. G. Dean and D. H. Watson, *J. Chromatogr.*, 165 (1979) 301–319.
4 C. R. Lowe, M. Hans, N. Spibey and W. T. Drabble, *Anal. Biochem.*, 104 (1980) 23–28.
5 Y. D. Clonis and C. R. Lowe, *Biochim. Biophys. Acta*, 659 (1981) 86–98.
6 Y. D. Clonis, *J. Chromatogr.*, 236 (1982) 69–80.
7 C. R. Lowe, in A. Wiseman (Editor), *Topics in Enzyme & Fermentation Biotechnology*, Vol. 9, Ellis Horwood, Chichester, U.K., 1984, pp. 78–161.
8 C. R. Lowe, M. Glad, P.-O. Larsson, S. Ohlson, D. A. P. Small, T. Atkinson and K. Mosbach, *J. Chromatogr.*, 215 (1981) 303–316.
9 D. A. P. Small, T. Atkinson and C. R. Lowe, *J. Chromatogr.*, 216 (1981) 175–190.
10 D. A. P. Small, T. Atkinson and C. R. Lowe, *J. Chromatogr.*, 266 (1983) 151–156.
11 M. Bradford, *Anal. Biochem.*, 72 (1976) 248–254.

Journal of Chromatography, 363 (1986) 37–56
Elsevier Science Publishers B.V., Amsterdam — Printed in The Netherlands

CHROM. 18 613

PHYSICAL AND MATHEMATICAL MODELLING TO AID SCALE-UP OF LIQUID CHROMATOGRAPHY

G. H. COWAN*, I. S. GOSLING, J. F. LAWS and W. P. SWEETENHAM
BIOSEP, Biotechnology Group, Building 353, Harwell Laboratory, Harwell, Oxon OX11 ORA (U.K.)

SUMMARY

A review of previous work indicates that the mathematical modelling of adsorption rate processes is well established and provides a basis for predictive methods for scale-up. Small-scale experiments to provide isotherm and kinetic data for code prediction purposes are described and pilot-scale equipment to provide results for code predictions are outlined. Predictions of the performance of a packed-bed adsorption column using numerical methods incorporated in the FACSIMILE code show good agreement with results from an analytic solution, and with the experimental data of Chase for affinity adsorption of lysozyme on Blue Sepharose CL-6B. This is part of a programme aimed at validating the FACSIMILE code for application to the design, performance prediction, optimization and scale-up of industrial adsorption and chromatography equipment.

INTRODUCTION

There is considerable industrial interest in the scale-up of adsorption and chromatographic techniques for the recovery, separation and purification of biochemical components from liquid feedstocks. This leads to a requirement for computer methods for the design, performance prediction and optimization of adsorption equipment. Before general application of such computer programs, it is necessary that predictions from codes be validated against relevant experimental and operational data, to give confidence in application of the codes to scale-up.

In this paper, previous work on the mathematical modelling of adsorption rate processes is briefly reviewed, and details are given of the computer code FACSIMILE, which is being developed for the prediction of such processes, in particular for scale-up and performance studies. Complementary to the mathematical modelling work, small-scale experiments to provide adsorption isotherm and kinetic data for use in making predictions with the FACSIMILE code, and pilot-scale equipment to provide experimental results to check the code predictions, are described.

Comparisons are given between FACSIMILE predictions for the mathematical modelling of a packed-bed adsorption column and results from the analytic solution that can be derived in the case of no axial diffusion, and with experimental

data from the literature for the adsorption of lysozyme on Sepharose CL-6B–Cibacron Blue affinity adsorbent in a packed column.

PREVIOUS WORK

Useful reviews of the rate theories of adsorption are given by Yang and Tsao[1], Vermeulen *et al.*[2] and Ruthven[3].

For a packed-bed column, the mass balance for the mobile phase can be written as

$$D \cdot \frac{\partial^2 c}{\partial z^2} - V \cdot \frac{\partial c}{\partial z} - M = \frac{\partial c}{\partial t} \tag{1}$$

where D is the axial dispersion coefficient, V is the linear velocity, c is the solute concentration in the fluid stream, M is the rate of interface mass transfer, z is the axial co-ordinate, and t is time. Differences in rate theory models are mainly due to the variation in the rate equations for interface mass transfer or for the specification of M in eqn. 1. The rate of interface mass transfer may be formulated for (i) fluid film diffusion rate controlling, (ii) surface adsorption reaction rate controlling, and (iii) particle and/or pore diffusion rates controlling; the various mass transfer steps are depicted in Fig. 1.

For film diffusion controlling, Furnas[4] has given solutions with the assumptions of plug flow and linear isotherm, and Michaels[5] obtained the exact solution for a range of favourable equilibrium. Thomas[6] has given analytical solutions for surface adsorption reaction rate controlling for fixed-bed ion exchange, neglecting axial dispersion.

When the particle and/or pore diffusion rate is controlling, two types of approach have been used. These are: (i) the homogeneous solid model and (ii) the porous particle model. The homogeneous solid model treats the particle as a homogeneous matrix, irrespective of its porous structure. A number of workers have obtained analytical solutions by assuming a homogeneous model: Rosen[7,8] and Tien and Thodos[9], based on linear isotherms; and Cooper[10] and Ozil and Bonnetain[11], based on irreversible isotherms. More recently, Rice[12] has given analytical solutions for batch, packed-tube and radial flow adsorbers by assuming a linear isotherm, together with experimental data to validate the predictions for batch and packed-tube systems. Numerical results have been obtained by Tien and Thodos[13], Ying and Weber[14] and Weber and Liu[15], by assuming Freundlich isotherms; and by Westmark[16], for a linear isotherm.

Due to its realistic description of the porous feature of the packing used, the porous particle model has received considerable attention. Kasten *et al.*[17] obtained an analytical solution by assuming a linear isotherm, as did Masamume and Smith[18–20] for cases with pore diffusion and surface adsorption resistances considered simultaneously, but neglecting axial dispersion. Analytical solutions for irreversible isotherms have been obtained by Weber and Chakravorti[21] and by McKay and Allen[22]. Numerical solutions have been obtained for non-linear isotherm systems by Lee and Weber[23,24] and by Meyer and Weber[25]. Fleck *et al.*[26] provide numerical solutions for fixed-bed adsorption or ion exchange for Langmuir and Freundlich

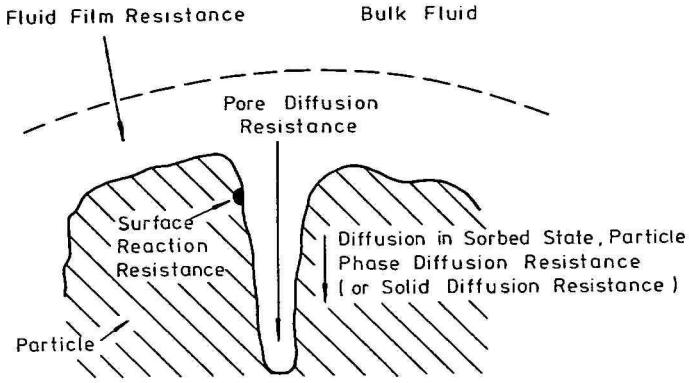

Fig. 1. The physical nature and location of individual steps in mass transfer of a solute from a fluid to a solid particle.

isotherms. Other numerical solutions have been given by Neretnieks[27], Liapis and Rippin[28], Svedberg[29], Costa and Rodrigues[30], Raghaven and Ruthven[31], Leyva-Ramos and Geankoplis[32], Mehrotra and Tien[33] and Rasmuson[34].

Simplified models have also been used effectively where the assumption is made that the solid adsorbent matrix is homogeneous, not only in structure but also in concentration, which is then represented by the mean concentration within the particle. The interface mass transfer equations then become simple functions of time and position only, and are no longer controlled by the momentary rate of particle diffusion, which is dependent on the shape of the unsteady concentration profile within the particle. Yang and Tsao[1] categorize the various simplified rate equations into three types: (i) the kinetic rate expression type; (ii) the linear driving force type; and (iii) miscellaneous, including constant pattern behaviour.

For the kinetic rate expression models, the adsorption process is treated as a reversible or irreversible chemical reaction. Analytical solutions for this case have been given by Thomas[6,35]. Other solutions have been presented by Heister and Vermeulen[36], Goldstein[37], Lapidus and Amundson[38] and Dranoff and Lapidus[39]. Chase[40,41] neglecting axial dispersion, has adapted Thomas' solution to the prediction of the performance of preparative affinity separation for biological macromolecules in packed columns for a favourable isotherm of the Langmuir type.

In the linear driving force model, the rate of interface mass transfer is assumed to be proportional to the distance the system is from equilibrium. Linear driving force models have been developed by Heister and Vermeulen[36], Heister *et al.*[42], Chen *et al.*[43] and Hashimoto *et al.*[44,45], covering linear, Langmuir and Freundlich isotherms. Hsieh *et al.*[46] give details of a method for prediction of multi-component liquid phase adsorption in a fixed bed, by assuming a Langmuir isotherm and the linear driving force approximation. Garg and Ruthven[47], Peel and Benedek[48], Yoshida *et al.*[49] and Leaver[50] have studied the use of linear driving force approximations for intraparticle diffusion mass transfer.

It is often observed in frontal analysis column operation with very favourable isotherm systems, that the shape of the wave front becomes essentially time independent, or column length independent after a certain distance from the entrance. Yang

and Tsao[1] point out that this behaviour was first noted by Bohart and Adams[51], Wicke[52], Sillen[53] and Sillen *et al.*[54]. Hall *et al.*[55], assuming Langmuir isotherms, give numerical solutions for fixed-bed adsorption under constant pattern conditions taking into account both solid diffusion and pore diffusion. Katoh *et al.*[56] have developed numerical methods of prediction of breakthrough curves and elution profiles for packed-bed affinity chromatography columns for constant pattern conditions and the Freundlich isotherm.

The review shows that the mathematical modelling of adsorption rates processes is well established and provides a basis for the application of the FACSIMILE code to different problems.

Any mathematical model that is proposed has to be evaluated by comparing its predictions with experimental results. For application of the models in codes such as FACSIMILE, specific information on equilibrium and kinetics are required either from the literature or from small-scale experiments. The section below outlines some of the experiments that can be used to generate useful data, and includes some preliminary results. The following section then details the testing of FACSIMILE. This testing includes the use of data from the literature.

SMALL-SCALE EXPERIMENTS TO PROVIDE EQUILIBRIUM AND KINETIC DATA AND PILOT-SCALE EXPERIMENTS FOR CODE VALIDATION

There are two types of experiments that are concerned with the modelling of any adsorption process. The first investigates the equilibrium situation, usually expressed in terms of adsorption isotherms, and the second investigates the time course of the approach to equilibrium; the kinetics. A programme of experimental work is in progress, aimed at providing a wide range of data to validate the FACSIMILE code. The particular system under study is the adsorption of aspartic acid onto an ion exchanger. Duolite A162; some of the experimental details are given below.

Measurement of adsorption isotherms

Adsorption isotherms were generated by contacting solutions of different concentrations of aspartic acid with known weights of adsorbent, at a constant temperature, until equilibrium was attained. The amount of material adsorbed, the capacity, is plotted against the equilibrium solution concentration, as shown in Fig. 2. This was a typical result and shows the isotherms following a characteristic Langmuir-type pattern, which can also be modelled by a forward and reverse reaction model[40]. The isotherm shape illustrates that the experimental system under investigation shows consistency with the model used by Chase[40]. This is important, because checking the validity of a particular proposed model is a significant part in the overall process of mathematical modelling.

Kinetics of adsorption

There are several possible rate-limiting steps in any adsorption process, arising from the resistances to the transport of material from the bulk liquid to the interior of the adsorbent particles, as shown in Fig. 1. The kinetics of these steps can be measured in several ways, the simplest of which is to monitor the uptake of adsorbate in a stirred cell, illustrated in Fig. 3. The result from this is shown in Fig. 4. Providing

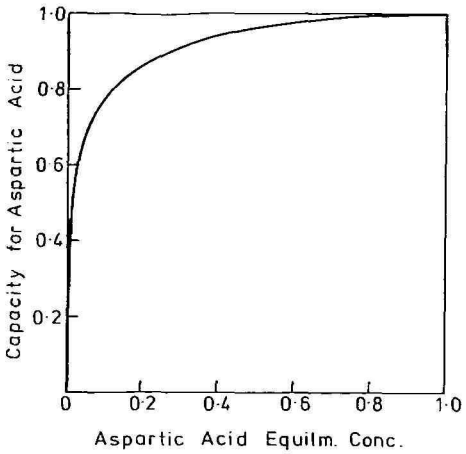

Fig. 2. Dimensionless adsorption isotherm for aspartic acid onto Duolite A162.

the agitation is sufficient; no significant concentration gradients arise in the bulk liquid, thereby negating the effects of that particular resistance and thus slightly simplifying the process description.

Most adsorption processes are performed in columns and although a stirred cell provides useful information, experiments examining column operations are necessary. The simplest apparatus for doing this is shown in Fig. 5, where the column output is monitored in response to either step or pulse changes in input conditions.

Pilot-scale experiments

Small-scale experiments provide a means of characterizing the adsorbent

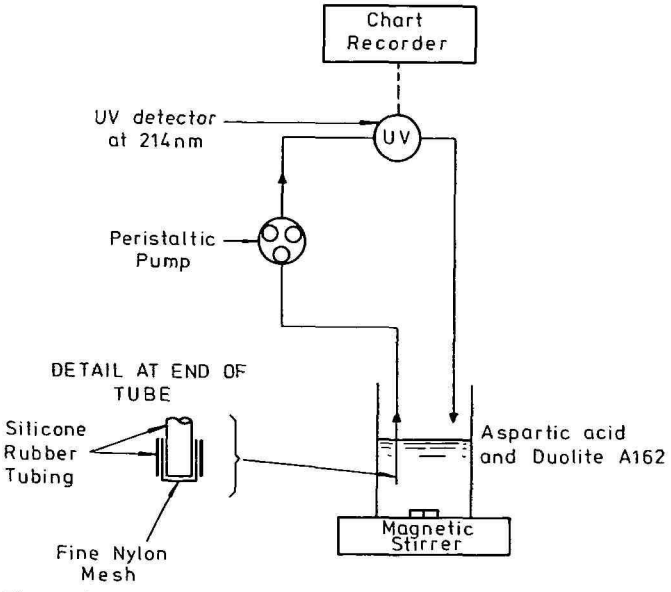

Fig. 3. Diagram of apparatus for stirred cell experiments.

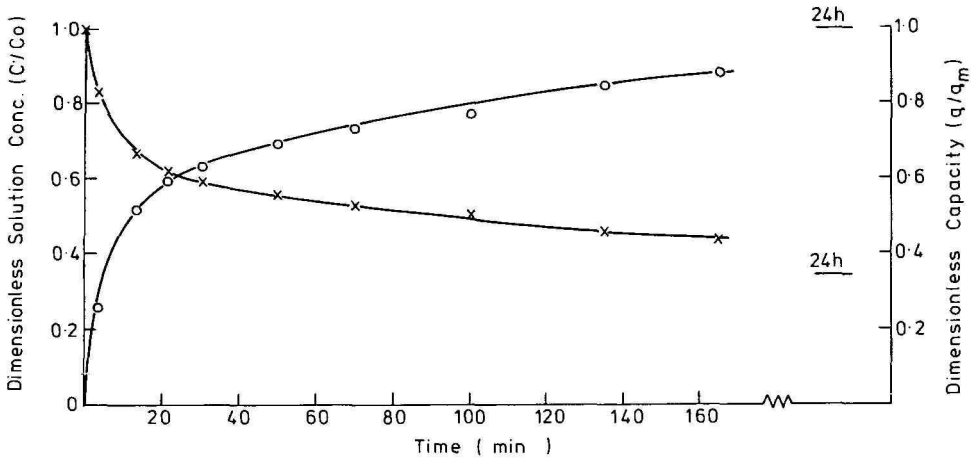

Fig. 4. Kinetics of aspartic acid adsorption, in a stirred cell: C_0 = initial solution concentration; q_m = capacity at equilibrium.

within a limited microenvironment and the results will be applicable to any scale of operation, to a certain extent. Regardless of scale, the adsorbent will always be operating in a microenvironment so, provided that these conditions are known, the adsorbent performance can be predicted from the results of small-scale experiments. The major differences in scale-up are the hydrodynamic variations that arise from poor distribution, and pilot-scale equipment is under construction (Fig. 6) to evaluate these effects. This pilot-scale equipment will also be used to validate computer predictions of scale-up, based on results from the small-scale experiments.

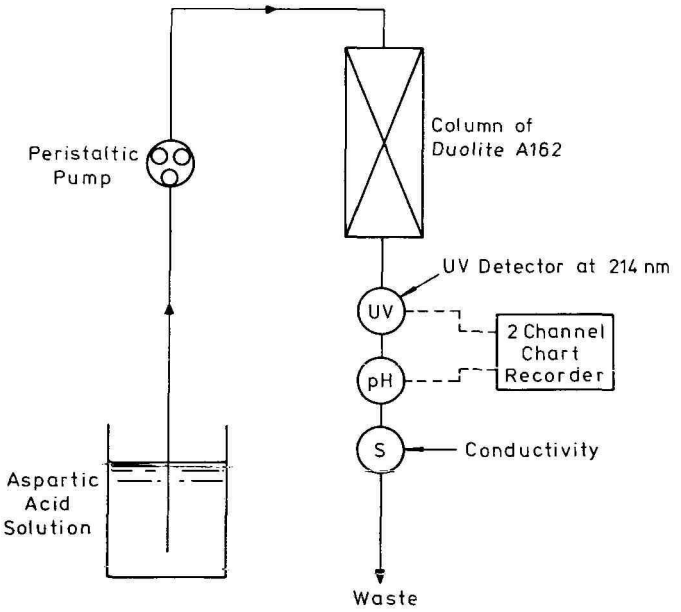

Fig. 5. Diagram of apparatus for column experiments.

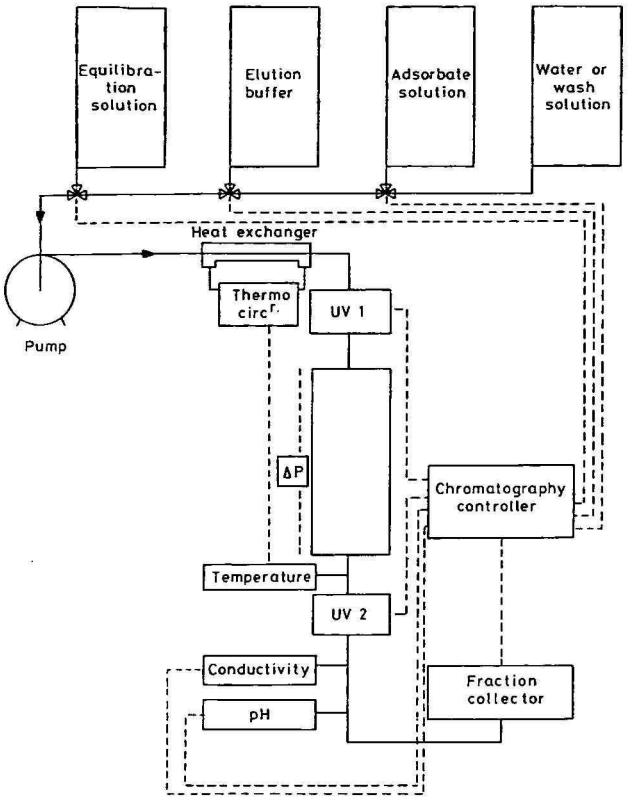

Fig. 6. Adsorption column performance rig (schematic).

PREDICTION OF PACKED-BED COLUMN PERFORMANCE

With information available on the equilibrium and kinetic characteristics from small-scale experiments, it is possible to predict the performance of adsorption processes using the FACSIMILE code. This code has been developed at Harwell. Computer models using FACSIMILE for general prediction of adsorption and chromatographic systems are being written. There is particular emphasis on writing models suitable for predicting scale-up. The code solves the mass balance and mass transfer rate equations for a given adsorption system with specified initial conditions. The numerical methods used in FACSIMILE are outlined here, with reference to the prediction of packed-bed adsorption column performance, and predictions are compared with the experimental data of Chase[40] for an affinity chromatography application.

The FACSIMILE program

FACSIMILE is a computer program designed for solving ordinary differential equations such as those which arise from problems involving mass action kinetics. The equations are described to FASCIMILE in a high-level language. To solve a

particular system, a program is written in the FACSIMILE data language. This program should specify all the rate equations for a system. A particular problem is solved by supplying FACSIMILE with this program and with the values for all the parameters for the particular problem.

Because of the power of the FACSIMILE data language, almost any model for a particular system can be described to FACSIMILE. The kernel of FACSIMILE is the Harwell Library subroutine DC03AD. This is a routine for solving sets of stiff ordinary differential equations. The class of stiff differential equations includes those which arise from reaction kinetics where there are processes proceeding at different rates. DC03AD uses a numerical method, which is efficient at solving such equations. From experience of solving real problems, the routine has been found to be robust and reliable. FACSIMILE is written in Fortran 77 and can be run on any computer with a good Fortran 77 compiler. FACSIMILE is described in a Harwell report[57].

The experimental data

This work takes data from experiments conducted by Chase[40]. Chase measured the adsorption of lysozyme in a 0.05 *M* Tris–HCl buffer at pH 7.2 onto Cibacron Blue supported on Sepharose CL-6B. For each experiment, Chase has supplied the values of adsorbate concentration at the outlet of the column against time, *i.e.* values on the breakthrough curve. The results given here are in two sets. In the first set, the only difference between the experiments was the length of the column. The second set of data contains values from an experiment that used a lower fluid speed than the first set of experiments.

The mathematical model

Chase[40] suggested a set of equations to describe this system. The equations are of the form described in eqn. 1. The system is modelled as a reversible mass transfer reaction in which the free adsorbate becomes bound to the adsorbent. The forward rate of the reaction is proportional to the amount of free adsorbate multiplied by the amount of adsorbent free to bind with the adsorbate. The reverse rate is proportional to the amount of adsorbate bound to the adsorbent, *i.e.*

$$C \underset{K_2}{\overset{K_1(Q_m - q)}{\rightleftharpoons}} Q \tag{2}$$

where C is the free adsorbate, Q is the bound adsorbate, Q_m is the maximum capacity of the adsorbent and K_1 and K_2 are constants.

The solution of free adsorbate flows down the column, of length L, with speed V; V is sometimes called the interstitial velocity. The free adsorbate also diffuses through the solution with coefficient D. The differential equations suggested by Chase are expressed here, using the symbols t for time and z for distance down the column; $c(z,t)$ is used for the concentration of free adsorbate, as a function of distance and time, and $q(z,t)$ is used for the concentration of bound adsorbate, also as a function of distance and time. The differential equations are

$$\frac{\partial c}{\partial t} = D\frac{\partial^2 c}{\partial z^2} - V\frac{\partial c}{\partial z} - K_1 c\,(Q_m - q) + K_2 q \tag{3}$$

$$\frac{\partial q}{\partial t} = K_1 c(Q_m - q) - K_2 q \tag{4}$$

One of the boundary conditions for c is that before the process starts, at time $t = 0$, the value of c is zero all along the column except at the inlet, *i.e.*

$$c(z,0) = \begin{cases} 0, & z > 0 \\ C_0, & z = 0 \end{cases}$$

Another boundary condition is that, at all times, the value of c at the inlet is C_0 so $c(0,t) = C_0$, $t \geqslant 0$. In the case of diffusion, $D \neq 0$, another condition is needed; it is assumed that at any particular value of t, t_1 say, there is some large value of z, z_1 say, such that for all values of $z > z_1$, $c(z,t_1) = 0$.

The boundary condition for q is that at time $t = 0$, $q = 0$ all along the column, *i.e.* $q(z,0) = 0$, $z \geqslant 0$.

These equations assume that the adsorbate in solution is well mixed radially. The fluid speed V is the true fluid speed, not the superficial speed. So V can be expressed as:

$$V = \frac{\text{fluid volume entering the column in unit time}}{\text{cross-section area of column} \times \text{porosity}}$$

The concentrations c, q, C_0 and Q_m are measured in moles of adsorbate divided by the volume of fluid containing that amount of adsorbate.

Thomas' analytic solution

If the assumption is made that diffusion is zero, there is an analytical solution for these equations with these boundary conditions. The results in this section include a comparison between the predictions from FACSIMILE and the predictions from Thomas' solution using the same parameters. This analytic solution is quoted in Appendix 1.

Solving the model using FACSIMILE

FACSIMILE provides a tool for solving the above equations without needing to assume $D = 0$. Chase assumed that diffusion was negligible and, using this assumption, the differential equations were solved using FACSIMILE and using Thomas' solution. This allowed comparison between the answers gained from using FACSIMILE, the experimental data and the analytical solution. The following describes some results which can be deduced from assuming that, in the case of negligible diffusion, the concentration has a constant pattern. These results were used to speed up the calculations performed by FACSIMILE without forcing FACSIMILE to produce a solution with a constant pattern.

The constant pattern assumption

Away from the column inlet, Thomas' solution is similar to a wave moving down the column at fixed speed. This is known as a constant pattern.

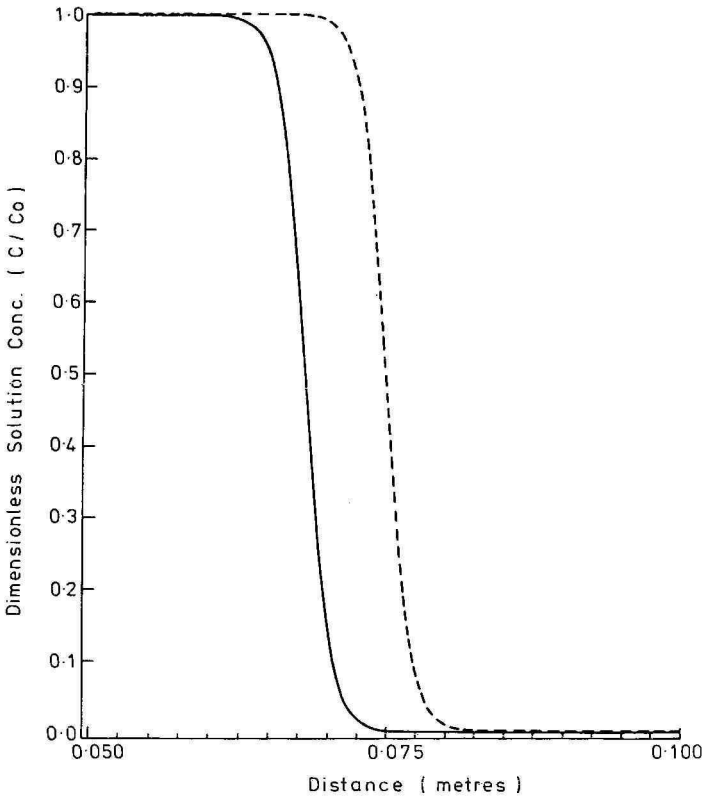

Fig. 7. Results assuming a constant pattern (Thomas' solution) for two different times.

Fig. 7 shows Thomas' solution plotted as concentration against distance at two different times during the experiment. As illustrated in Fig. 7, along the section of column between the column inlet and one end of the wave-front the concentration of free adsorbate is constant. Equally, from the other end of the wave-front to the column outlet the concentration is also zero. Therefore, at any particular time, only a section of the column needs to be modelled in detail. This section is called here a grid. The grid needs to be long enough to include all of the wave-front. It also needs to move so as to include all of the wave-front at any given time.

Appendix 2 considers the constant pattern assumption. In it, is the derivation for the speed of the wave-front, by assuming a constant pattern. This speed is:

$$U = \frac{VC_0}{C_0 + Q_0} \tag{5}$$

where Q_0 is defined by:

$$Q_0 = \frac{C_0 Q_m}{K_2/K_1 + C_0} \tag{6}$$

The same section also derives an expression for l, the length of grid needed to model the wave-front.

The equations used within the grid

The next task is to decide how to model the section of column covered by the grid. The grid is divided into a one-dimensional set of cells. In each cell, the mass transfer reaction between the free adsorbate and the bound adsorbate are provided to FACSIMILE. The flow of solution through the grid and diffusion along the grid are modelled by transfer of species between neighbouring cells. If there are n cells, then, using c_i and q_i for the concentrations of free and bound adsorbate in cell i, the ordinary differential equations for each cell are:

$$\frac{dc_i}{dt} = \frac{D}{h^2}(c_{i-1} + c_{i+1} - 2c_i) - \frac{V}{h}(c_{i-1} - c_i) - K_1c_i(Q_m - q_i) + K_2q_i \quad (7)$$

and

$$\frac{dq_i}{dt} = K_1c_i(Q_m - q_i) - K_2q_i \quad (8)$$

for $1 \leqslant i \leqslant n$ and where c_0, c_{n+1}, q_0 and q_{n+1} are defined by $c_0 = C_0$, $c_{n+1} = 0$, $q_0 = 0$ and $q_{n+1} = 0$.

Note that a central difference is used for the diffusion term and a backward difference is used for the advection term. This makes the method stable. This form of discretization ensures local conservation of adsorbate. In other words, the equations, which are solved using FACSIMILE, ensure that the difference between the amount of adsorbate entering a section of column and the amount leaving that section is equal to the increase in adsorbate in that section of column.

Integrating the equations

The model works in two phases. In the first phase, the grid is stationary with one end at the inlet of the column. The differential equations within the grid are then integrated until the concentrations of free adsorbate in the cells at the centre of the grid have reached half of their equilibrium values. By this stage, the value of the concentrations in the cells adjacent to the column inlet should have reached their equilibrium values. The constant pattern assumption is now valid and, in phase two, the integration continues with the grid moving along the column at a fixed speed until it has passed the end of the column. This means that the speed of the free adsorbate relative to the grid is $V - U$ and the bound adsorbate is moving in the opposite direction at speed U relative to the grid. There are no special boundary conditions at the end of the column and so the same equations can be solved while the grid passes over the end of the column.

If there is no diffusion, the length used for the grid is the minimum required, calculated using the constant pattern assumption. If the diffusion is small but not zero, the same method works but diffusion means that the wave-fronts for the concentrations of free and bound adsorbate broaden slowly as they move down the column. So the grid length is chosen to be larger than the minimum required. If diffusion is large, the grid covers the entire column and never needs to move.

Note that the results of the constant pattern assumption were only used to find values for the grid length and speed. The equations are still solved properly on the grid and the assumptions can be checked as the calculation proceeds. The moving grid is just used to speed-up FACSIMILE's calculations, it does not affect the answers. The same answers could be obtained using a grid which covered the entire column and which had more cells so that the size of each cell was the same.

Results for the first set of experiments

Fig. 8 plots the breakthrough curves for the first set of experiments. These are on five columns of different length, with all other parameters the same. The parameters are: $Q_m = 8.75 \cdot 10^{-4}$ mol/l, $K_1 = 2.86 \cdot 10^2$ l/(mol s), $K_2 = 5.0 \cdot 10^{-4}$/s, $C_0 = 7.1 \cdot 10^{-6}$ mol/l, $V = 2.24 \cdot 10^{-4}$ m/s, $D = 0$ m^2/s. The column lengths were 14, 41, 66, 104 and 161 mm.

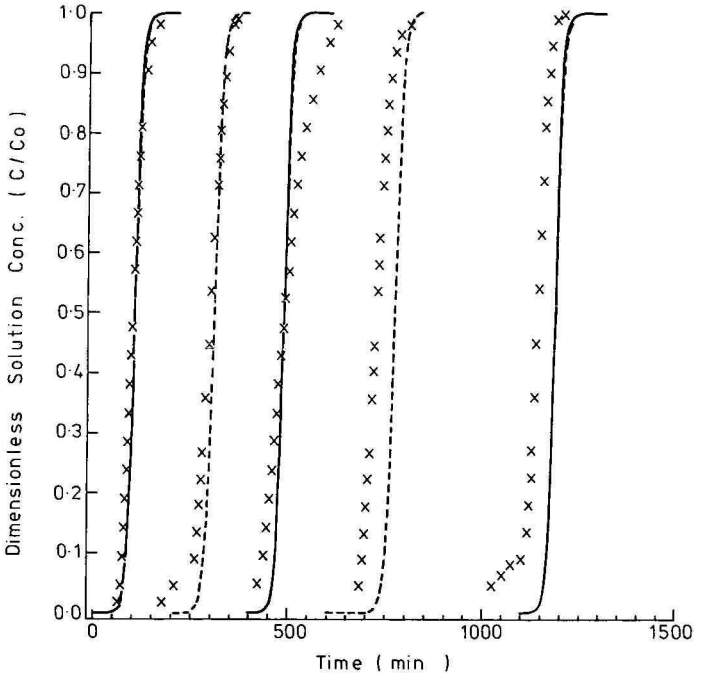

Fig. 8. Breakthrough curves for five columns of different length. (——) Thomas' solution, (--------) FACSIMILE, (×) experimental data.

The five dashed lines are predictions gained from FACSIMILE for the five different column lengths. The leftmost line is for the 14-mm column and the lines are in order of column length. The three solid lines are the analytical results from Thomas' solution for the first, third and fifth columns. The five sets of crosses are the experimental results on the breakthrough curves. FACSIMILE's results agree very well with Thomas' solution and are similar to the experimental results. The fact that results gained from using FACSIMILE are very close to those gained from Thomas' solution means that in this case, where diffusion is ignored, FACSIMILE is certainly

solving the equations accurately. This gives confidence in FACSIMILE's predictions in cases where Thomas' solution does not hold.

The predicted breakthrough curves are very sensitive to the parameters used in the calculation. Fig. 9 gives the same results calculated using a value for the adsorbent capacity about 4% smaller than that suggested by Chase. This new value of Q_m is $8.45 \cdot 10^{-4}$ mol/l. The predicted curves fit the experimental results more closely and it is unlikely that the capacity is known to within 4%.

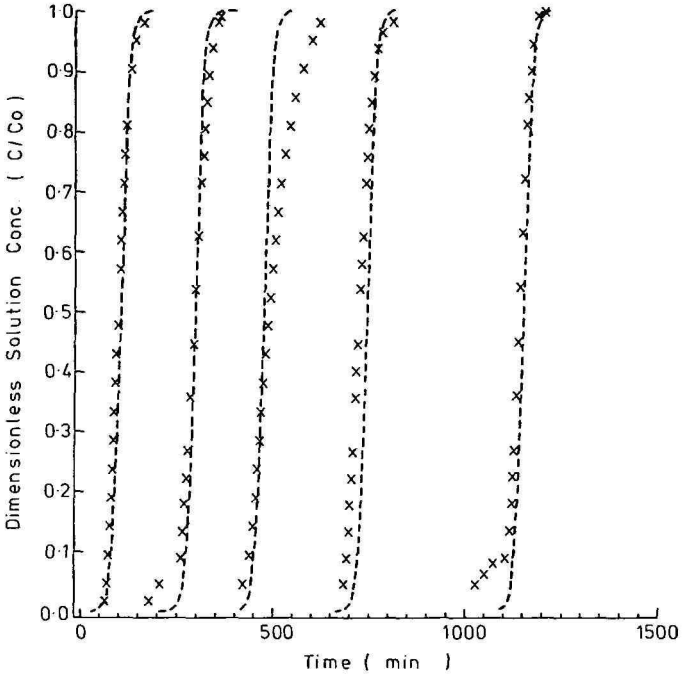

Fig. 9. Breakthrough curves for five columns of different length. Examination of parameter sensitivity of Q_m. (------) FACSIMILE, (×) experimental data.

Results from the second set of data

The second set of data comes from an experiment where the fluid speed was $4.62 \cdot 10^{-5}$ m/s and the column length (L) was 0.032 m. This was modelled using FACSIMILE and Chase's suggested values for the other parameters. These parameters are $Q_m = 8.75 \cdot 10^{-4}$ mol/l, $K_1 = 2.86 \cdot 10^2$ l/(mol s), $K_2 = 5.0 \cdot 10^{-4}$/s, $C_0 = 7.1 \cdot 10^{-6}$ mol/l, $D = 0$ m²/s. The experimental data are the crosses on Fig. 10 and the prediction for these parameter values is the dashed line.

From the experimental data, the breakthrough curve appears broader than that predicted using these parameter values. Also, the breakthrough occurs earlier than predicted. A second model was run using parameters chosen to fit the experimental data more closely.

To make the breakthrough occur at the correct time, the speed of the wavefront needs to be increased. This can be done either by altering the fluid speed V or

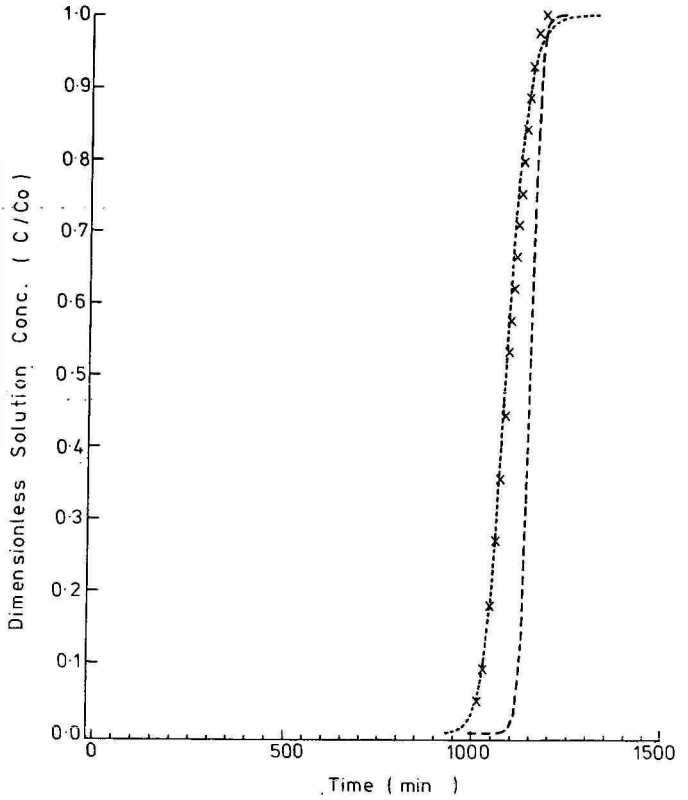

Fig. 10. Breakthrough curve for column of length 0.032 m. (– – –) FACSIMILE prediction, (×) experimental data, (---------) FACSIMILE prediction, but including diffusion.

the bed capacity Q_m, depending on which value was measured more accurately. In this case, V was altered to $4.89 \cdot 10^{-5}$ m/s.

To broaden the breakthrough curve, a diffusion coefficient D of $3 \cdot 10^{-8}$ m^2/s was used. This is reasonable as a value to include both the effect of diffusion through the solute and the increased dispersion caused by the adsorbent around which the solute flows.

The prediction gained using FACSIMILE with this altered set of parameters is the dotted line in Fig. 10.

CONCLUSION

It has been shown that the FACSIMILE computer code accurately solves the mathematical model used to describe the affinity adsorption process. Although in the example the model incorporated a simplified kinetic rate equation, FACSIMILE has the potential to predict a wide range of adsorption and chromatography systems for performance, optimization and design purposes. This includes the potential to solve more-complex mass transfer rate models, which include dispersion, coupled with the

ability to cover the whole process cycle: adsorption, washing, elution and regeneration. To gain physical understanding of the relevant adsorption process and to gain accuracy of prediction, it is desirable to provide information on isotherms and kinetics from small-scale experiments of the type described in this paper. The comparison of the FACSIMILE predictions with the affinity adsorption data gives a first check of the code, but further comparison with data from small-scale rigs, and industrial equipment, will validate the code to give confidence in the application to scale-up of adsorption and chromatographic processes.

ACKNOWLEDGEMENTS

Acknowledgement is made to BIOSEP, Harwell Laboratory, Harwell, Oxfordshire, OX11 0RA, U.K. for permission to publish the work presented in this paper. Acknowledgement is also made to Dr. H. A. Chase of the Department of Chemical Engineering, Cambridge University, Cambridge for providing actual experimental data for the affinity adsorption of lysozyme on Blue Sepharose CL-6B, to enable comparisons to be made with predictions from the FACSIMILE code.

APPENDIX 1 — THOMAS' SOLUTION

If the assumption is made that axial diffusion is zero, the mathematical equations for this system become:

$$\frac{\partial c}{\partial t} = -V\frac{\partial c}{\partial z} - K_1 c(Q_m - q) + K_2 q \tag{A1}$$

$$\frac{\partial q}{\partial t} = K_1 c(Q_m - q) - K_2 q \tag{A2}$$

There is an analytic solution to these equations, which was quoted by Thomas[53]. The solution is quoted here using the notation of this paper, which is different from Thomas' original notation. The solution for the concentration of C at time t and position z is given by:

$$\frac{c(x,y)}{C_0} = \frac{I_0(2\sqrt{ABxy}) + \varphi(\alpha y,\beta x)}{I_0(2\sqrt{ABxy}) + \varphi(\alpha y,\beta x) + \varphi(Bx,Ay)} \quad \text{for } x \geqslant 0,\ y \geqslant 0 \tag{A3}$$

As before, z is the position along the column; $z = 0$ at the inlet. t is the time measured from when the solution entered the column. At a particular position z and a particular time t, x is the time it would take an unadsorbed component of the solution to reach the current position after entering the column. y is the difference between the current time and the time at which an unadsorbed component would have reached the current position. Thus x and y are: $x = z/V$ and $y = t - z/V$. y less than zero means that an unadsorbed component would not yet have reached the current position, so $y < 0 \Rightarrow c(x,y) = 0$.

x is always positive for positions within the column. The constants A, B, α and β are defined thus: $A = K_2$, $B = K_1 Q_m$, $\alpha = K_1 C_0 + K_2$, $\beta = \dfrac{K_2 K_1 Q_m}{K_1 C_0 + K_2}$. The function I_0 is the zeroth-order imaginary Bessel function.

APPENDIX 2 —RESULTS FROM ASSUMING A CONSTANT PATTERN

In general, the concentration of adsorbate in solution is a function of both time and position along the column. The constant pattern means that this function can be expressed as a function of one variable whose argument is $z - Ut$, *i.e.* $c(z,t) \approx f(z - Ut)$, for some function f and some constant U. U is the speed of the wave-front and f is its shape.

Let the cross-section area of the fluid be A, then the amount of free adsorbate which flows into the column in time δt is $C_0 V A \delta t$. In time δt, the extra adsorbate goes into increasing the nett amount of free adsorbate in the column, *i.e.* moving the wave-front of c down the column, and into increasing the amount of adsorbate bound to the adsorbent, *i.e.* moving the wave-front of q down the column. These two increases require an increase in total adsorbate of $\delta z A(C_0 + Q_0)$. The increase of total adsorbate in the column must equal the amount of free adsorbate flowing into the column; thus the speed of the wave front is:

$$U = \frac{\delta z}{\delta t} = \frac{V C_0}{C_0 + Q_0}$$

Consider the concentration of the adsorbate bound to the adsorbent. At equilibrium, for any part of the column, the concentration of the free adsorbate is C_0, the concentration at the inlet. So the concentration of bound adsorbate can be obtained from the isotherm. Let Q_0 be the equilibrium value of the concentration of the bound adsorbate, then:

$$Q_0 = \frac{C_0 Q_m}{K_2/K_1 + C_0}$$

Next, the assumption is made that the bound adsorbate also moves at a fixed speed and also has a fixed shape. The speeds of the two wave-fronts must then be the same for otherwise one would get completely ahead of the other. So, after a long time, at some point along the column, either the concentration of the free adsorbate would be at its equilibrium value while the concentration of the bound adsorbate was still zero or the concentration of the bound adsorbate would be at its equilibrium value while the concentration of the free adsorbate was still zero. Neither of these is possible, so assuming that both wave-fronts move at fixed speeds means that they must both move at the same speed. So, the further assumption is made that there exists a function g such that $q(z,t) \approx g(z - Ut)$. This value of U is the speed at which the grid should move once the solution has reached the constant pattern stage.

Using the value for U eqns. A1 and A2 can be rewritten in terms of f. Let $\zeta = z - Ut$, then:

$$\frac{\partial c}{\partial t} = - U \frac{df}{d\zeta}$$

$$\frac{\partial c}{\partial z} = \frac{df}{d\zeta}$$

and

$$\frac{\partial q}{\partial t} = - U \frac{dg}{d\zeta}$$

These turn eqns. A1 and A2 into:

$$-(V - U) \frac{df}{d\zeta} - K_1 f(Q_m - g) + K_2 g = 0$$

$$U \frac{dg}{d\zeta} + K_1 f(Q_m - g) - K_2 g = 0$$

Addition of these equations gives:

$$(V - U) \frac{df}{d\zeta} = U \frac{dg}{d\zeta}$$

For $\zeta \ll 0, f = C_0$ and $g = Q_0$, so by integration

$$(V - U)(f - C_0) = U(g - Q_0)$$

Note that

$$\frac{U}{(V - U)} Q_0 = \left(\frac{VC_0}{C_0 + Q_0}\right)\left(\frac{VQ_0}{C_0 + Q_0}\right)^{-1} Q_0 = C_0$$

Thus, g can be expressed in terms of f:

$$g(\zeta) = \frac{Q_0}{C_0} f(\zeta)$$

This gives an ordinary differential equation for f:

$$(V - U) \frac{df}{d\zeta} = K_1 f\left(Q_m - \frac{Q_0}{C_0} f\right) + K_2 \frac{Q_0}{C_0} f$$

The solution to this is:

$$f(\zeta) = \frac{C_0}{(1 + e^{(\zeta - \zeta_0) C_0 K_1 / U})}$$

and therefore the equation for g is:

$$g(\zeta) = \frac{Q_0}{(1 + e^{(\zeta - \zeta_0)C_0K_1/U})}$$

The value of ζ_0 is determined by the equation:

$$z - Ut = \zeta = \zeta_0 \Rightarrow \frac{c}{C_0} = \frac{1}{2}$$

Note that $\zeta \to -\infty \Rightarrow f \to C_0$ and $\zeta \to \infty \Rightarrow f \to 0$, and similarly for g.

These formulae for the shapes of the wave-fronts make it possible to calculate the length of grid needed to model the system.

To use such a grid assumes that along all of the column, from the column inlet to one end of the grid, both the concentration of free adsorbate and the concentration of bound adsorbate are practically at their equilibrium values. It also assumes that from the other end of the grid to the column outlet both of these concentrations are practically zero. To find the grid length, some ratio R is needed which specifies how closely these assumptions are met. The first requirement is that between the grid and the inlet, the error in c from its correct value of C_0 is less than R, *i.e.*

$$\frac{C_0 - c}{C_0} < R$$

The other requirement is that between the end of the grid and the outlet, the error in assuming $c = 0$ is:

$$\frac{c}{C_0} < R$$

Having decided upon some small number for R which is small compared to one, 0.0001 is a reasonable value, the minimum value required for the grid length l is given by:

$$l \approx -2\ln(R)\frac{U}{C_0K_1}$$

It is interesting to look at the width of the breakthrough curve. This can be taken to be the time interval for the value of c at the outlet of the column to rise from C_0R to $C_0(1 - R)$. This time interval is given by:

$$\frac{l}{U} = \frac{-2\ln(R)}{C_0K_1}$$

Thus, given the assumptions made about a constant pattern, the width of the breakthrough curve is independent of both the speed of fluid flowing through the column and the capacity of the adsorbent.

REFERENCES

1 C. Yang and G. T. Tsao, in A. Fiechter (Editor), *Chromatography, Advances in Biochemical Engineering 25*, Springer-Verlag, Berlin, Heidelberg, 1982, p. 2.
2 T. Vermeulen, M. D. Le Van, N. K. Heister and G. Klein, in R. H. Perry, D. W. Green and J. O. Maloney (Editors), *Perry's Chemical Engineers' Handbook*, McGraw-Hill, New York, London, Paris, 6th ed., 1984, Section 16, p. 16.1.
3 D. M. Ruthven, *Principles of Adsorption and Adsorption Processes*, Wiley, New York, Chichester, Brisbane, Toronto, Singapore, 1984.
4 C. C. Furnas, *Trans. Am. Inst. Chem. Eng.*, 24 (1930) 142.
5 A. S. Michaels, *Ind. Eng. Chem.*, 44 (8) (1952) 1922.
6 H. S. Thomas, *J. Am. Chem. Soc.*, 66 (1944) 1664.
7 J. B. Rosen, *J. Chem. Phys.*, 20 (1952) 387.
8 J. B. Rosen, *Ind. Eng. Chem.*, 46 (1954) 1590.
9 C. Tien and G. Thodos, *AIChE J.*, 6 (1960) 364.
10 R. S. Cooper, *Ind. Eng. Chem., Fundam.*, 4 (1965) 308.
11 P. Ozil and L. Bonnetain, *Chem. Eng. Sci.*, 32 (1977) 303.
12 R. G. Rice, *Chem. Eng. Sci.*, 1 (1982) 83.
13 C. Tien and G. Thodos, *AIChE J.*, 5 (1959) 373.
14 W. C. Ying and W. J. Weber, *33rd Annual Industrial Waste Conference, Purdue University, Lafayette, Indiana, 1978*, Ann Arbor Sci. Publ., Ann Arbor, MI, 1979.
15 W. J. Weber and K. T. Liu, *Chem. Eng. Commun.*, 6 (1980) 49.
16 M. Westermark, *J. Water Pollut. Control Fed.*, 40 (1975) 704.
17 P. R. Kasten, L. Lapidus and N. R. Amundsen, *J. Phys. Chem.*, 56 (1952) 683.
18 S. Masamume and J. M. Smith, *AIChE J.*, 11 (1965) 34.
19 S. Masamume and J. M. Smith, *AIChE J.*, 22 (1975) 41.
20 S. Masamume and J. M. Smith, *Ind. Eng. Chem. Fundam.*, 3 (1969) 179.
21 T. M. Weber and R. K. Chakravorti, *AIChE J.*, 20 (1974) 228.
22 G. McKay and S. J. Allen, *Can. J. Chem. Eng.*, 62 (1984) 340.
23 R. G. Lee and T. W. Weber, *Can. J. Chem. Eng.*, 47 (1969) 54.
24 R. G. Lee and T. W. Weber, *Can. J. Chem. Eng.*, 47 (1969) 60.
25 G. A. Meyer and T. W. Weber, *AIChE J.*, 13 (1967) 457.
26 R. D. Fleck, D. J. Kirwan and K. R. Hall, *Ind. Eng. Chem. Fundam.*, 12 (1) (1973) 95.
27 I. Neretnieks, *Chem. Eng. Sci.*, 31 (1976) 107.
28 A. I. Liapis and D. W. T. Rippin, *Chem. Eng. Sci.*, 32 (1977) 619.
29 U. G. Svedberg, *12th Symp. Computer Appl. Chem. Eng., Montreux, April 8–11, 1979.*
30 C. Costa and A. Rodrigues, *Chem. Eng. Sci.*, 6 (1985) 983.
31 N. S. Raghaven and D. Ruthven, *Chem. Eng. Sci.*, 39 (7/8) (1984) 1201.
32 R. Leyva-Ramos and C. J. Geankoplis, *Chem. Eng. Sci.*, 50 (5) (1965) 7.
33 A. K. Mehrotra and C. Tien, *Can. J. Chem. Eng.*, 62 (1984) 632.
34 A. Rasmuson, *Chem. Eng. Sci.*, 40 (4) (1985) 621.
35 H. C. Thomas, *Ann. N.Y. Acad. Sci.*, 49 (1948) 161.
36 N. K. Heister and T. Vermeulen, *Chem. Eng. Progr.*, 48 (10) (1952) 505.
37 S. Goldstein, *Proc. R. Soc. London*, A219 (1953) 151, 171.
38 L. Lapidus and N. R. Amundson, *J. Phys. Chem.*, 56 (1952) 984.
39 J. S. Dranoff and L. Lapidus, *Ind. Eng. Chem.*, 53 (1) (1961) 71.
40 H. A. Chase, *J. Chromatogr.*, 297 (1984) 179.
41 H. A. Chase, *Chem. Eng. Sci.*, 39 (7/8) (1984) 1099.
42 N. K. Heister, Shirley B. Radding, R. L. Nelson, Jr. and T. Vermeulen, *AIChE J.*, 2 (3) (1956) 404.
43 J. W. Chen, J. A. Burge, F. L. Cunningham and J. I. Northam, *Ind. Eng. Chem. Process Des. Dev.*, 7 (1) (1968) 26.
44 K. Hashimoto and K. Miura, *J. Chem. Eng. Jpn.*, 9 (5) (1976) 388.
45 K. Hashimoto, K. Miura and M. Tsukano, *J. Chem. Eng. Jpn.*, 10 (1) (1977) 27.
46 J. S. C. Hsieh, R. M. Turian and C. Tien, *AIChE J.*, 23 (3) (1977) 263.
47 D. R. Garg and D. M. Ruthven, *AIChE J.*, 21 (1) (1975) 200.
48 R. G. Peel and A. Benedek, *Can. Ind. Chem. Eng.*, 59 (1981) 688.
49 H. Yoshida, T. Kataska and D. M. Ruthven, *Chem. Eng. Sci.*, 39 (10) (1984) 1489.

50 G. Leaver, *Ph.D. Thesis*, University of Wales, 1984.
51 G. S. Bohart and E. Q. Adams, *J. Am. Chem. Soc.*, 42 (1920) 523.
52 E. Wicke, *Kolloid-Z.*, 86 (1939) 167, 289.
53 L. G. Sillen, *Ark. Kemi Mineral Geol.*, A22 (1946).
54 L. G. Sillen and E. Akedahl, *Ark. Kemi Mineral Geol.*, A22 (1946).
55 K. R. Hall, L. C. Eagleton, A. Acrivos and T. Vermeulen, *Ind. Eng. Chem. Fundam.*, 5 (1966) 212.
56 S. Katoh, T. Kambayashi, D. Ryuichi and Y. Fumitake, *Biotech. Bioeng.*, XX (2) (1978) 267.
57 A. R. Curtis and W. P. Sweetenham, *FACSIMILE Release H User's Manual*, AERE R.11771, U.K. Atomic Energy Authority, Oxon, October 1985.
58 H. A. Chase, personal communication.

Journal of Chromatography, 363 (1986) 57–69
Elsevier Science Publishers B.V., Amsterdam — Printed in The Netherlands

CHROM. 18 665

SEMIPREPARATIVE SEPARATION OF TERPENOIDS FROM ESSENTIAL OILS BY HIGH-PERFORMANCE LIQUID CHROMATOGRAPHY AND THEIR SUBSEQUENT IDENTIFICATION BY GAS CHROMATOGRAPHY–MASS SPECTROMETRY

Ph. MORIN
École Nationale Supérieure des Industries Agricoles et Alimentaires, 1 Avenue des Olympiades, 91305 Massy (France)
M. CAUDE
Laboratoire de Chimie Analytique, École Supérieure de Physique et de Chimie de Paris, 10 Rue Vauquelin, 75005 Paris (France)
H. RICHARD
École Nationale Supérieure des Industries Agricoles et Alimentaires, 1 Avenue des Olympiades, 91305 Massy (France)
and
R. ROSSET
Laboratoire de Chimie Analytique, École Supérieure de Physique et de Chimie de Paris, 10 Rue Vauquelin, 75005 Paris (France)

SUMMARY

After mobile phase optimization (composition and elution profile) on an analytical scale with a standard mixture of mono- and sesquiterpenoids, the prefractionation of an essential oil has been carried out by semipreparative liquid chromatography. Reversed-phase chromatography on an octadecyl-bonded silica was used and the separation of the essential oil into several fractions was achieved within 20 min in a single experiment. The fractions were oxygenated monoterpenes, monoterpene hydrocarbons, sesquiterpene hydrocarbons and oxygenated sesquiterpenoids. Thus, liquid chromatographic separations of essential oils can be achieved, at room temperature, avoiding the risk of thermal rearrangement and decomposition which can occur in gas chromatographic separations. The fractions obtained were easily analysed by gas chromatography–mass spectrometry and several minor components, in particular sesquiterpenoids, were identified.

INTRODUCTION

Essential oils are complex mixtures of terpene compounds containing around 100 components. Whereas gas chromatography–mass spectrometry (GC–MS) is the method of choice for analysing the volatile components of these essential oils, the presence of so many components makes GC analysis in a single experiment very

0021-9673/86/$03.50

difficult, due to the overlap of some peaks and the loss of resolution particularly with minor compounds.

Traditional methods for prefractionation of terpene mixtures, *e.g.*, vacuum distillation and preparative GC cannot be achieved without thermal degradation[1,2], and column liquid chromatography is time consuming and has a low resolution[3].

The high-performance liquid chromatography (HPLC) technique is well adapted to thermosensitive compounds like terpenoids; experiments are done at room temperature directly on plant extracts, without derivatization procedures. Moreover, the molecular interactions are increased at room temperature and the selectivity of the separation is improved. The lack of an universal and sensitive detector is however a serious limitation in the HPLC separation of these compounds which, unfortunately, have no good chromophoric groups.

For instance, O'Connors and Goldblatt[4] studied the UV absorption spectra of several monoterpene hydrocarbons. The spectra of the saturated compounds (*cis*- and *trans-p*-menthane, pinane and tricyclene) exhibit no characteristic absorption above 200 nm. The spectra of unsaturated compounds (α- and β-pinenes, camphene, Δ^3-carene, limonene, terpinolene and γ-terpinene) exhibit some absorption only at 220 nm with no characteristic bands; their absorptivity is low at this wavelength ($\varepsilon \approx 100$–200 l mol^{-1} cm^{-1} for monounsaturated and $\varepsilon \approx 250$–400 l mol^{-1} cm^{-1} for polyunsaturated compounds).

Many papers have been published on the analytical separation of terpenoids by HPLC (Table I), but most concern separations of synthetic mixtures. In a general paper on the separation of terpenoids by HPLC[5], the main chromatographic methods (adsorption, reversed-phase, exclusion, ligand exchange) used for separation of terpene compounds are discussed and detection systems (UV–visible absorption, Fourier transform IR, fluorimetry and electrochemical detection) are compared in respect of their selectivity and sensitivity.

Otherwise, few fundamental works have been published on the semipreparative

TABLE I

ANALYTICAL SEPARATIONS OF TERPENOIDS BY HPLC

Terpenoids	*UV detection wavelength (nm)*	*Chromatographic method*	*Ref.*
Limonene, menthone, citral	215	Reversed phase	6
Nerol, geraniol, linalol, citral, farnesol	254	Reversed phase	7
Sesquiterpene hydrocarbons	220	Reversed phase	8
Sesquiterpene lactones	210	Reversed phase	9
	215	Reversed phase	10
Diterpenes	230	Reversed phase	11
	220	Reversed phase	12
Diterpene acids	220	Reversed phase	13
Triterpenols	215	Reversed phase	14
Isoprenoid benzoates and naphthoates	214	Reversed phase	15
Monoacid sesquiterpenes	220	Adsorption	16
Eugenol, cinnamaldehyde	260	Adsorption	17
Triterpenes	210	Adsorption	18

(or preparative) liquid chromatography of terpenoids[22–24,28]; some of them are described in Table II.

The present study describes the usefulness of semipreparative liquid chromatography for the prefractionation of complex mixtures of components with a large range of polarity. In this way, minor components are more easily identified by GC–MS.

EXPERIMENTAL

Liquid chromatography

Analytical separations were performed on a 250 mm × 4.6 mm I.D. columns packed with octadecyl-bonded silica Nucleosil C_{18} (7 μm), LiChrosorb RP-18 (10 μm) or Zorbax C_{18} (7–8 μm); semipreparative separations were performed on a 250 mm × 9.2 mm I.D. column packed with 7–8 μm octadecyl-bonded silica (Zorbax C_{18}), using a Model 5060 pump (Varian, Palo Alto, CA, U.S.A.). Injections were made through a sample loop (volume: 10 μl in analytical and 420 μl in semipreparative work) with a conventional Model 7010 injection valve (Rheodyne, Berkeley, CA, U.S.A.). Detection was performed with a UV spectrophotometer (Pye Unicam, Cambridge, U.K.) at 220 nm.

Gas chromatography

The HPLC fractions were extracted with pentane–diethyl ether (1:1), dried over sodium sulphate and the organic extract was evaporated with a rotating bath. The extracts were directly analysed with a Carlo Erba chromatograph, Fracto Vap Series 4160, equipped with a split injector (1:100), a flame ionization detector and a 25 m × 0.32 mm I.D. fused-silica DB 5 (J & W) column. The oven temperature was programmed from 60 to 220°C at 4°C/min and held for 10 min at 220°C.

Gas chromatography–mass spectrometry

The different fractions of essential oils were analysed using an Hewlett-Packard capillary GC–quadrupole MS system (Model 5995 B) fitted with a 25 m × 0.32 mm I.D. fused-silica DB 5 (J & W) column coupled to the source. The GC oven was programmed from 60 to 220°C at 4°C/min with helium as carrier gas. Typical MS operating conditions were used and mass spectra were obtained by scanning from 40 to 400 a.m.u. with a selected ion monitoring (SIM) technique on the fragment at *m/e* 43. The mass spectrometer was operated at 70 eV. Peak assignments were made by comparing spectra of unknown terpenoids with those present in our mass spectra library.

Solvents and reagents

Mobile phases were prepared by mixing water and acetonitrile. The water used was specially twice distilled and the solvent was obtained from SDS (Peypin, France). The capacity factors, k', were calculated with a column dead volume, t_0, measured by injection of nitrate.

Solutes

The different samples of terpenoids (Table III) were purchased from several

TABLE II

SEMIPREPARATIVE OR PREPARATIVE SEPARATIONS OF TERPENOIDS BY LC

Terpenoids	*Chromatographic method*	*Stationary phase*	*Column dimensions*	*Flow-rate (ml/min)*	*Sample size*	*Ref.*
Linalyl acetate purification	Adsorption	Spherosil XOA-400	50 cm × 23 mm I.D.	23	500 mg	19
Farnesol isomers	Adsorption	Silica gel	30 cm × 5 cm I.D.	250	3 g	20
Sesquiterpene lactones	Reversed phase	Ultrasphere ODS with an Altex precolumn	25 cm × 10 mm I.D.	4	–	21
Mono- and sesquiterpenoids	Reversed phase	LiChroprep RP-18 (40 μm)	24 cm × 10 mm I.D.	8	0.5 ml	16
Farnesol isomers	Exclusion	Styrene–divinylbenzene copolymer gel	60 cm × 21 mm I.D.	6	200 mg	25
	Adsorption	Prep-Pak 500 silica cartridge	–	350	2.4 g	26
(−) Menthone, (+)isomenthone	Exclusion	Partisil 10 (Whatman)	30 cm × 7.7 mm I.D.	–	50 mg	27

TABLE III

FORMULAE OF THE MOLECULES SEPARATED BY HPLC OR GC

Monoterpene alcohols

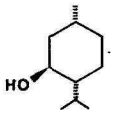

isomenthol

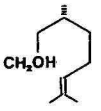

(+)citronellol

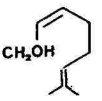

nerol

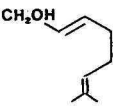

geraniol

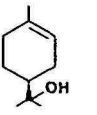

α-terpineol

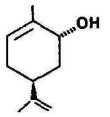

cis-carveol

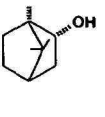

borneol

Monoterpene ketones

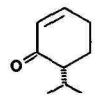

(−)piperitone

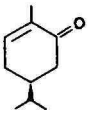

(+) carvone

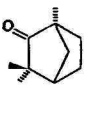

fenchone

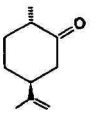

(−)dihydrocarvone

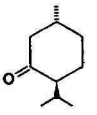

(−) menthone

Monoterpene esters

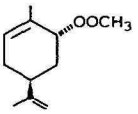

carvyl acetate

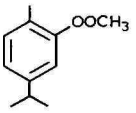

carvacryl acetate

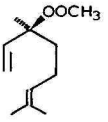

linalyl acetate

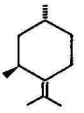
isopulegyl acetate

Monoterpene hydrocarbons


α-pinene

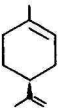
limonene

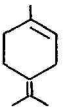
terpinolene

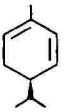
α-phellandrene

Sesquiterpene alcohols

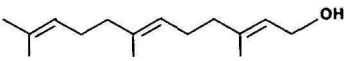

farnesol

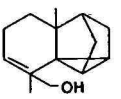

santalol

Sesquiterpene hydrocarbons

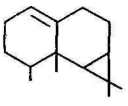
calarene

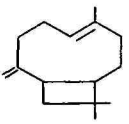
caryophyllene

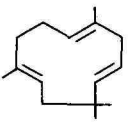
humulene

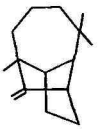
longifolene

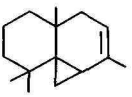
thujopsene

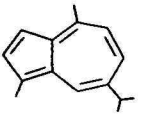
guiazulene


longipinene

companies; isomenthol, citronellol, carveol, fenchone, dihydrocarvone, menthone, carvyl acetate, isopulegyl acetate, guiazulene, humulene from EGA-Chimie France (Aldrich, Strasbourg, France); nerol, borneol, geraniol, terpineol, carvone, linalyl acetate, calarene, α-pinene, limonene, α-phellandrene, farnesol, caryophyllene, longifolene, thujopsene, longipinene from Fluka (Buchs, Switzerland).

The Vervain essential oil (29) was a generous gift from Dr. Garnero (Ets Robertet, Grasse, France) who has identified by classical methods (column LC, GS–MS) the main components of this essential oil[30].

RESULTS AND DISCUSSION

Two chromatographic techniques can be used: adsorption or reversed-phase chromatography. HPLC on silica columns is well known to be a convenient method for resolving compounds with different functional groups[31], while HPLC on octadecyl-bonded silica is well adapted for resolving compounds according to their hydrophobic properties.

An essential oil contains merely monoterpenoids (C_{10} chemical compounds) and sesquiterpenoids C_{15}) which differ in their hydrophobicities. So, reversed-phase chromatography has been chosen.

Analytical separation

A preliminary study with synthetic mixtures containing mono- and sesquiterpenoids was carried out and each group was resolved in order to determine the optimum mobile phase composition for semipreparative separation.

The variation of the capacity factors of several terpenoids, factors on octadecyl-bonded silica *vs.* the binary solvent (acetonitrile–water) composition is shown in Fig. 1. In reversed-phase liquid chromatography, the elution order is generally related to the solute hydrophobicity. Unfortunately, it is difficult to link the retention of terpenoids, to their hydrophobic characteristics, as calculated by Rekker's hydrophobic fragmental constants[32]; terpenoids have generally complex skeletons. However, the retention behaviour follows the classical rule of reversed-phase chromatography and the low selectivity exhibited by monoterpene ester–sesquiterpene alcohol groups was due to the small difference in polarity between these compounds.

Isocratic elution of terpenoids with the same functionality. The analytical separation of a standard mixture of sesquiterpene hydrocarbons, different from those in Fig. 1, containing guiazulene, humulene, caryophyllene, thujopsene, longifolene, calarene and longipinene was achieved on a C_{18} silica phase under isocratic conditions in about 40 min with a fair resolution (Fig. 2).

Gradient elution of terpenoids with various functionalities. The polarity range of terpenoids practically precludes the analysis of an essential oil by HPLC in a single experiment, except with a very long microbore column, packed with small diameter particles, which yields several hundred thousand theoretical plates[33]. Scott and Kucera[34] used this method for the analysis of an essential oil at the expense of long analysis time (32 h).

The retention behaviour of synthetic mixtures of terpenoids was investigated in the binary solvent system (acetonitrile–water) on Zorbax C_{18} (7 μm) silica. Acetonitrile–water (70:30) gives a satisfactory resolution of all the components, but

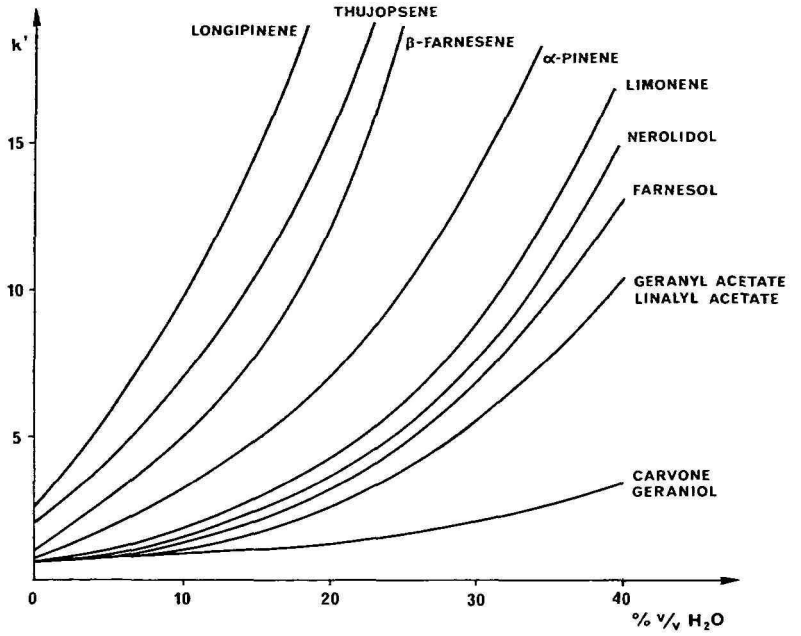

Fig. 1. Variations of the capacity factor, k', for some terpenoids *versus* the mobile phase composition. Column: 250 mm × 4.6 mm I.D. Stationary phase: LiChrosorb RP-18 (10 μm). Mobile phase: acetonitrile–water. Flow-rate: 2 ml min^{-1}. UV detection: 220 nm.

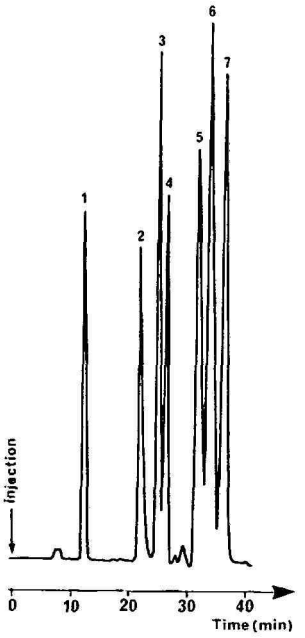

Fig. 2. HPLC resolution of a standard mixture of sesquiterpene hydrocarbons. Column: 250 mm × 4.6 mm I.D. Stationary phase: Nucleosil C_{18} (7 μm). Mobile phase: acetonitrile–water (77.5:22.5). Flow-rate: 2 ml min^{-1}. UV detection: 220 nm. Solutes: 1 = guiazulene; 2 = humulene; 3 = caryophyllene; 4 = *thujopsene*; 5 = *longifolene*; 6 = *calarene*; 7 = *longipinene*.

TABLE IV

CAPACITY FACTORS OF TERPENOIDS IN THE BINARY SYSTEM ACETONITRILE–WATER ON ZORBAX C_{18} SILICA

Solutes	*Acetonitrile–water*		
	77.5:22.5	*70:30*	*Elution gradient**
Monoterpene alcohols	0.4	0.9	0.9
ketones	0.5–0.7	1.0–1.2	1.0–1.2
esters	0.9–1.2	2.0–2.4	1.9–2.2
Sesquiterpene hydrocarbons	2.6	4.6	4.6
Monoterpene hydrocarbons	3.5–6.3	7.0–12.0	6.5–8.9
Sesquiterpene hydrocarbons	13–17	22–30	11.6–13.8

* For elution gradient profile, see Fig. 3.

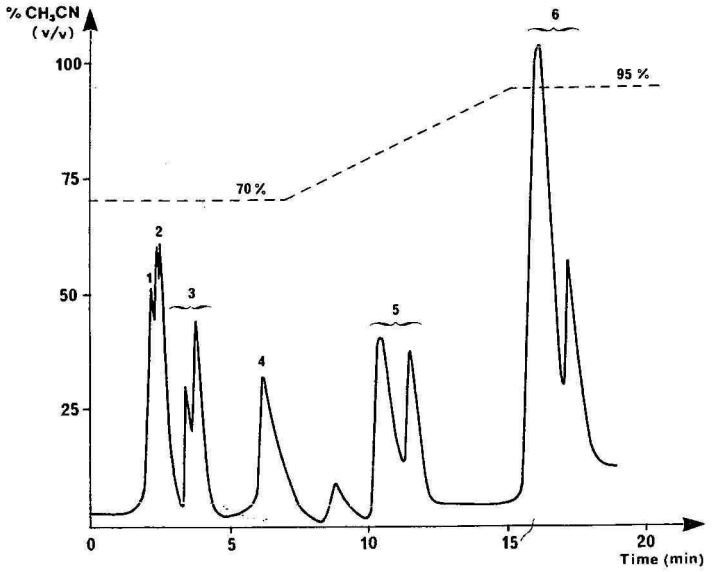

Fig. 3. Analytical HPLC separation of a standard mixture of terpenoids. Column: 250 mm × 9.2 mm I.D. Stationary phase: Zorbax C_{18} (7 μm). Mobile phase: acetonitrile–water; the gradient profile is shown as a dashed line. Flow-rate: 6 ml min^{-1}. Injection volume: 50 μl. UV detection: 220 nm. Solutes: 1 = monoterpene alcohols (isomenthol, citronellol, nerol, borneol, α-terpineol, carveol); 2 = monoterpene ketones (piperitone, carvone, fenchone, dihydrocarvone, menthone); 3 = monoterpene esters (carvyl acetate, carvacryl acetate, linalyl acetate, cinnamyl isobutyrate, isopulegyl acetate); 4 = sesquiterpene alcohols (nerolidol, santalol, patchoulol, farnesol); 5 = sesquiterpene hydrocarbons (caryophyllene, longifolene, bisabolene, β-patchoulene, guiazulene).

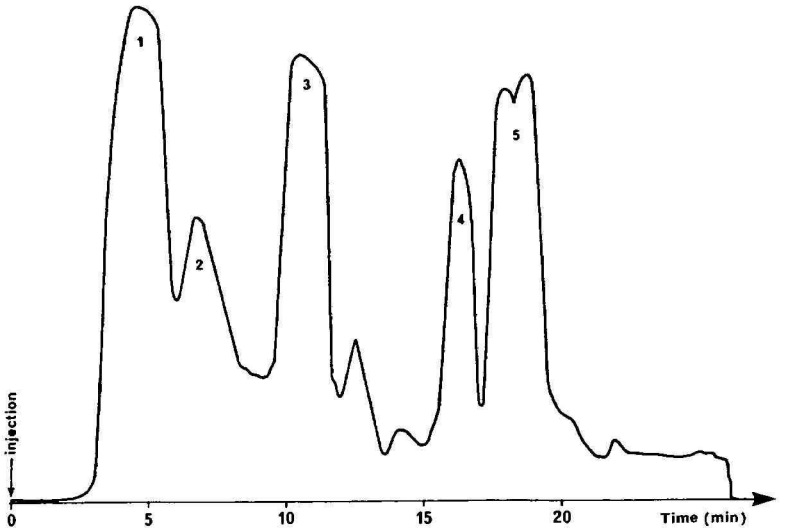

Fig. 4. Semipreparative HPLC separation of a Vervain essential oil. For experimental conditions, see Fig. 3, except: quantity injected, 0.5 ml, and concentration, 50 mg/100 ml.

the peaks eluted last (sesquiterpene and monoterpene hydrocarbons) are too broad and the analysis time too long (Table IV). So, this complex separation requires the use of gradient elution in order to keep the capacity factors in the optimum range (Fig. 3). The peaks are generally broad, but we must bear in mind that several compounds are present within each peak.

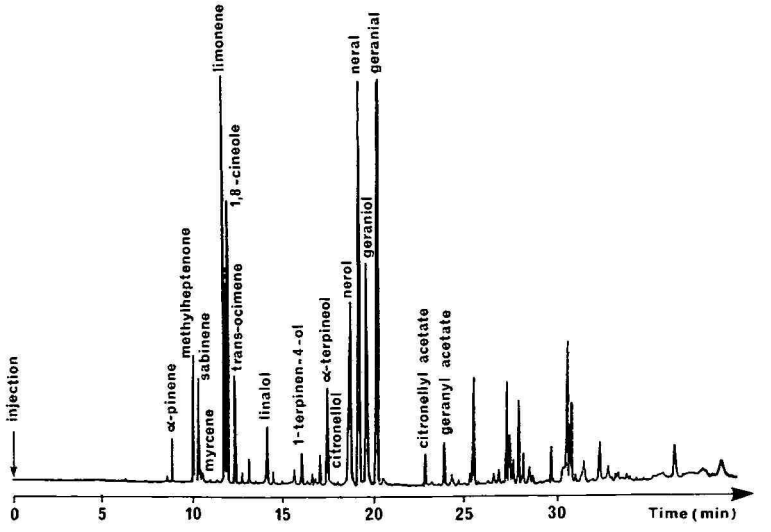

Fig. 5. GC resolution of a Vervain essential oil. Fused-silica capillary column: 25 m × 0.32 mm I.D. Stationary phase: DB 5 (J & W). The oven temperature was increased from 60 to 220°C at 4°C/min and held for 10 min at the upper limit. Detection: flame ionization.

Semipreparative separation

We selected a semipreparative column packed with the same packing material (Zorbax C_{18}, 7 μm). Each sample of essential oil was dissolved in a mixture of the eluent and tetrahydrofuran (THF) (50:50) at a concentration of 50 mg/100 ml. The mobile phase composition (acetonitrile–water) varies from 70:30 to 95:5 as shown in Fig. 3. This separation, into the main classes of terpenoids, is accomplished in about 20 min (Fig. 4) and allows five main fractions to be collected.

If monoterpene components of an essential oil can be analysed by GC–MS in

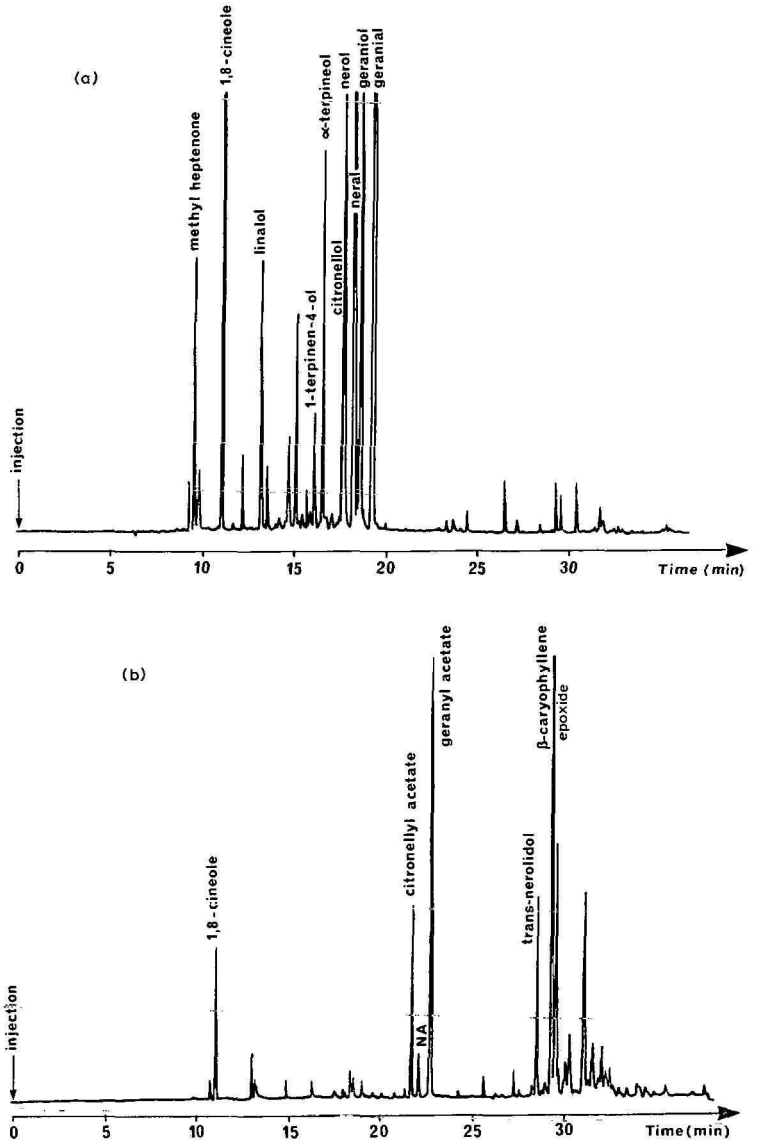

Fig. 6.

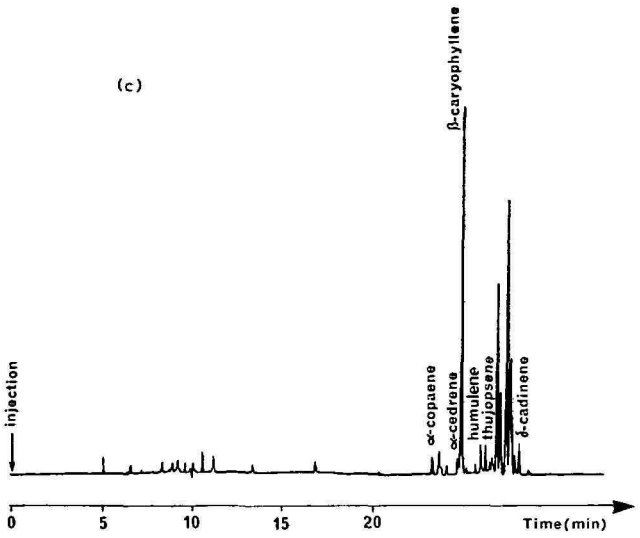

Fig. 6. GC resolution of HPLC fractions from the Vervain essential oil. For experimental conditions, see Fig. 5. Solutes: (a) fraction 1; (b) fraction 2; (c) fraction 5. NA = neryl acetate.

a single experiment, it is more convenient to perform an HPLC prefractionation for minor and thermosensitive components such as sesquiterpenoids.

The different HPLC fractions were collected and the terpenoids recovered by liquid–liquid extraction with diethyl ether–pentane (50:50). The organic layer was dried over anhydrous sodium sulphate and the solvent was removed at 30°C under vacuum with a rotary evaporator, to yield an oil which was analysed by fused-silica (DB 5) capillary GC. The characterization of the products was carried out by comparison of their mass spectra and retention data with those of authentic samples or with those present in our mass spectra library.

TABLE V

GC COMPOSITION OF VERVAIN ESSENTIAL OIL

Compound	*Content (%)*	*Compound*	*Content (%)*
α-Pinene	0.6	Geraniol	6.6
Methylheptenone	2.3	Geranial	19.9
Sabinene	1.8	Citronellyl acetate	0.6
Myrcene	0.4	Geranyl acetate	1.0
Limonene	13.5	α-Cedrene	0.2
1,8-Cineole	4.9	β-Caryophyllene	2.0
trans-Ocimene	1.7	Humulene	0.20
Linalol	1.2	Thujopsene	0.30
1-Terpinen-4-ol	0.6	Aromatic curcumene	2.4
α-Terpineol	2.1		
Citronellol and nerol	5.9	Nerolidol	0.7
Neral	14.4	β-Epoxycaryophyllene	2.1

TABLE VI

GC COMPOSITION OF HPLC FRACTIONS

Fraction no.	*Terpenoids*	*Content (%)*	*Fraction no.*	*Terpenoids*	*Content (%)*
1	1-Octen-3-ol	0.33	2	Neryl acetate	1.10
	Methylheptenone	1.48		Geranyl acetate	11.30
	3-Octanol	0.33		Citronellyl acetate	4.40
	1,8-Cineole	5.83		Nerolidol	4.50
	Linalol	1.56		β-Epoxycaryophyllene	7.50
	1-Terpinen-4-ol	1.13		1,8-Cineole	2.70
	α-Terpineol	2.47	4	Aromatic curcumene	74.0
	Citronellol	1.25	5	α-Cubebene	traces
	Nerol	3.72		α-Copaene	0.92
	Neral	28.22		α-Cedrene	0.95
	Geraniol	4.63		β-Caryophyllene	22.7
	Geranial	40.46		Humulene	2.15
				Thujopsene	2.65
				δ-Cadinene	2.4

GS–MS analysis of HPLC fractions

The chromatograms of a Vervain essential oil and HPLC fractions are shown in Figs. 5 and 6. The compounds identified in these mixtures are summarized in Tables V and VI. Fraction 1 comprises the most polar compounds, *i.e.*, monoterpene alcohols (3-octanol, 1-octen-3-ol), monoterpene oxide (1,8-cineole), monoterpene aldehydes (neral, geranial, citronellal) and aliphatic ketone (methylheptenone). In fraction 2 are present the medium polarity solutes such as monoterpene alcohol esters (neryl acetate, geranyl acetate and citronellyl acetate) and oxygenated sesquiterpenoids (nerolidol, β-epoxycaryophyllene). The apolar fractions 3, 4 and 5 contain respectively monoterpene hydrocarbons (α-pinene, sabinene, limonene, myrcene, α-terpinene, *trans*-ocimene), a sesquiterpene hydrocarbon of intermediate polarity, aromatic curcumene, and sesquiterpene hydrocarbons (α-copaene, α-cedrene, β-caryophyllene, humulene, thujopsene, δ-cadinene).

The comparison of the data in Tables V and VI demonstrates the advantages of the LC–GC–MS technique over direct GC–MS. The LC prefractionation step allows the concentration of minor compounds like sesquiterpene hydrocarbons. For instance, the humulene content in Vervain essential oil is about 0.2%, whereas its concentration is ten times greater in fraction 5. This enrichment gives a better precision and accuracy for GC and GC–MS experiments and allows identification of a greater number of terpenoids. In addition, LC prefractionation of essential oil, at room temperature, avoids the thermal degradations of sesquiterpenoids which occur in the traditional method, where monoterpene hydrocarbons and sesquiterpene hydrocarbons are separated by vacuum distillation of the *n*-hexane fraction.

CONCLUSION

Essential oil analysis by HPLC in a single experiment is difficult due to the complexity of the mixture (great number of compounds and large polarity range)

and the insufficient resolution for minor compounds. Semipreparative liquid chromatography and fraction analysis by GC–MS solves this problem. First, the essential oil is separated into several main fractions by semipreparative reversed-phase chromatography; these are subsequently analysed by GC–MS. In this way, a greater number of terpenoids can be resolved and identified.

REFERENCES

1 N. Ikekawa, *Methods Enzymol.*, 15 (1969) 200.
2 W. Bruhn, *Dragoco Report 21*, 6 (1974) 115.
3 S. Bitteur, *Analusis*, 12 (1984) 51.
4 R. O'Connors and L. A. Goldblatt, *Anal. Chem.*, 26 (1954) 1726.
5 Ph. Morin, M. Caude, H. Richard and R. Rosset, *Analusis*, 13 (1985) 196.
6 K. A. Kovar and D. Friess, *Arch. Pharm. (Weinheim Ger.)*, 313 (1980) 416.
7 T. G. McCloud and P. Heinstein, *J. Chromatogr.*, 174 (1979) 461.
8 D. Strack, P. Proksch and P. G. Gülz, *Z. Naturforsch.*, 35 (1980) 675.
9 D. Strack, P. Proksch and P. G. Gülz, *Z. Naturforsch.*, 35 (1980) 915.
10 B. Marchand, H. M. Behl and E. Rodriguez, *J. Chromatogr.*, 265 (1983) 97.
11 G. K. Trivedi, I. Kubo and T. Kubota, *J. Chromatogr.*, 179 (1979) 219.
12 A. Lobstein-Guth, F. Briançon-Scheid and R. Anton, *J. Chromatogr.*, 267 (1983) 431.
13 R. G. Enriquez, L. I. Escobar, M. L. Romero, M. A. Chávez and X. Lozoya, *J. Chromatogr.*, 258 (1983) 297.
14 G. J. Niemann and W. J. Baas, *J. Chromatogr. Sci.*, 16 (1978) 260.
15 T.-H. Yang, T. M. Zabriskie and C. D. Poulter, *J. Chromatogr.*, 312 (1984) 121.
16 K. H. Kubeczka, in P. Schreier (Editor), *Flavour 81 — Proceedings of the Third Weurman Symposium*, Walter de Gruyter, Berlin, New York, 1981, p. 345.
17 M. S. F. Ross, *J. Chromatogr.*, 118 (1976) 273.
18 M. Burnouf-Radosevich and N. E. Delfel, *J. Chromatogr.*, 292 (1984) 403.
19 J. P. Larmann, R. C. Williams and D. R. Baker, *Chromatographia*, 8 (1975) 92.
20 M. J. Pettei, F. G. Pilkiewicz and K. Nakanishi, *Tetrahedron Lett.*, (1977) 2083.
21 B. Marchand, H. M. Behl and E. Rodriguez, *J. Chromatogr.*, 265 (1983) 97.
22 E. C. Uebel, J. D. Warthen and M. Jacobson, *J. Liq. Chromatogr.*, 2 (1979) 875.
23 B. B. Jones, B. C. Clark, Jr. and G. A. Iacobucci, *J. Chromatogr.*, 178 (1979) 575.
24 B. B. Jones, B. C. Clark, Jr. and G. A. Iacobucci, *J. Chromatogr.*, 202 (1980) 127.
25 H. Sato, A. Kageyu, K. Miyashita and Y. Tanaka, *J. Chromatogr.*, 237 (1982) 178.
26 J. D. Warthen, *J. Liq. Chromatogr.*, 3 (1980) 279.
27 N. A. Bergman and B. Hall, *Acta Chem. Scand.*, 33 (1979) 148.
28 T. S. Chamblee, B. C. Clark, Jr., T. Radford and G. A. Iacobucci, *J. Chromatogr.*, 330 (1985) 141.
29 R. Kaiser and D. Lamparsky, *Helv. Chim. Acta*, 59 (1976) 1797.
30 J. Garnero, *Parfums, Cosmet., Aromes*, No. 13 (1977) 29.
31 M. C. Hennion, J. C. Thieblemont, R. Rosset, P. Scribe, J. C. Marty and A. Saliot, *J. Chromatogr.*, 280 (1983) 351.
32 R. J. Rekker, *The Hydrophobic Fragmental Constant*, Elsevier, Amsterdam, 1977.
33 H. G. Menet, P. C. Gareil and R. Rosset, *Anal. Chem.*, 56 (1984) 1770.
34 R. P. W. Scott and P. Kucera, *J. Chromatogr.*, 169 (1979) 51.

Journal of Chromatography, 363 (1986) 71–80
Elsevier Science Publishers B.V., Amsterdam — Printed in The Netherlands

CHROM. 18 645

FAST POLYMER LIQUID CHROMATOGRAPHY ISOLATION AND CHARACTERIZATION OF PLANT MYROSINASE, β-THIOGLUCOSIDE GLUCOHYDROLASE, ISOENZYMES

LONE BUCHWALDT
Danish Research Service for Plant and Soil Science, 2 Lottenborgvej, DK-2800 Lyngby (Denmark)
and
LONE MELCHIOR LARSEN, ANNETTE PLÖGER and HILMER SØRENSEN*
Chemistry Department, Royal Veterinary and Agricultural University, 40 Thorvaldsensvej, DK-1871 Frederiksberg C (Denmark)

SUMMARY

Rapid and high-yielding ion-exchange chromatographic and chromatofocusing methods using fast polymer liquid chromatography (FPLC) have been developed for plant myrosinase, β-thioglucoside glucohydrolase (EC 3.2.3.1), isoenzyme studies. The preparative FPLC methods showed a mean recovery of 85% for six myrosinase preparations from three different plant sources. FPLC chromatofocusing and analytical isoelectric focusing were used to demonstrate the presence of different mixtures of myrosinase isoenzymes in seeds of various crucifers. The stability of the isoenzymes was investigated. The proposed method of plant isoenzyme analysis is briefly discussed in relation to methods previously used for myrosinase isolation and characterization, and studies of glucosinolate catabolism.

INTRODUCTION

β-Thioglucoside glucohydrolase (EC 3.2.3.1) (myrosinases) occur in all glucosinolate-containing plants hitherto investigated[1]. Myrosinases catalyse the hydrolysis of glucosinolates (Fig. 1), thereby producing D-glucose and the unstable thiohydroxamate-O-sulphonates, which are further degraded to sulphate and various amounts of different products[1]. Only limited information on glucosinolate catabolism *in vivo*, including the possible role of myrosinases, is available[1,2]. It is, however, well established that both the intact glucosinolates and their degradation products are important quality factors for oilseed rape[3–5] and for other glucosinolate-containing plants used as food and feed[6]. Knowledge of myrosinases and glucosinolates is also important in relation to studies of the interactions between herbivores and glucosinolate-containing plants[7,8].

Myrosinases in crucifers are glycoproteins containing several thiol and disulphide groups, and they often exist as isoenzymes[9–15]. The reports concerning isoenzymes are not always in agreement with each other. Pihakaski and Pihakaski found

0021-9673/86/$03.50

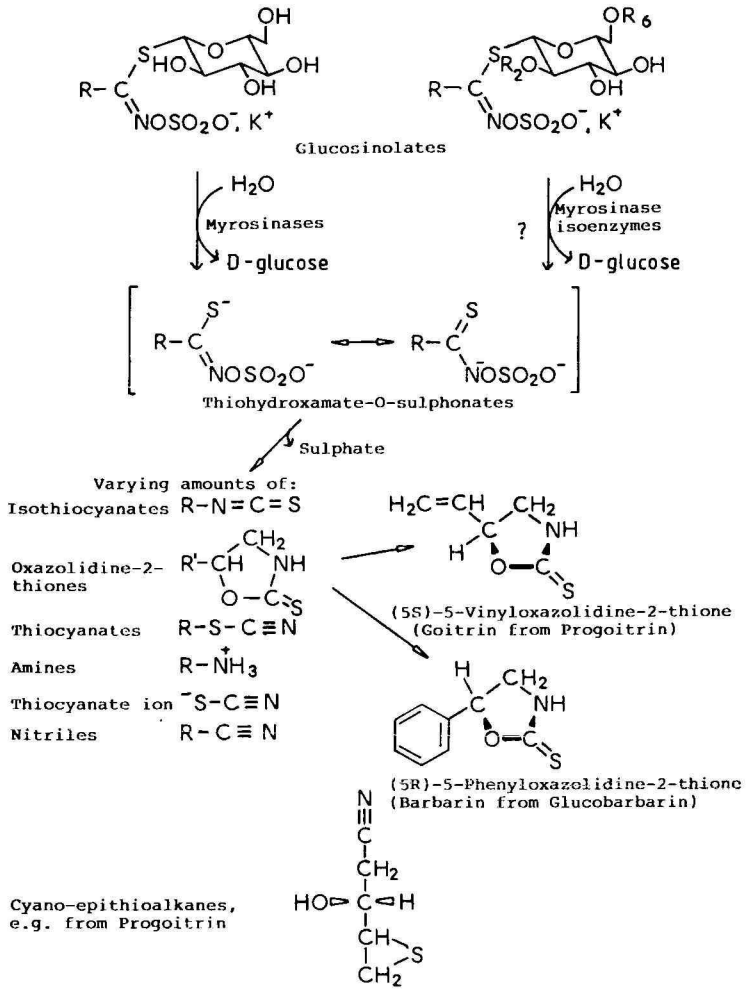

Fig. 1. Names and structures of degradation products of glucosinolates formed by myrosinase-catalysed hydrolysis: R = side-chain of glucosinolates; R_2 and/or R_6 = H or cinnamoyl derivatives. Glucosinolates are constituents of crucifers, but information on myrosinases attacking glucosinolates substituted with cinnamoyl derivatives is not yet available.

that the pattern of isoenzymes in *Sinapis alba* changed during germination[16], whereas Phelan and Vaughan found no differences in the isoenzyme pattern in seeds and seedlings of *S. alba*[17].

The isoenzyme pattern does not always seem to be stable. It was found to depend on the method of enzyme preparation[13], and the results should therefore be treated with caution. Some of the enzyme bands could originate from dissociation of enzyme aggregates or other alterations of the original enzyme molecule[13], or the enzyme could be composed of subunits that could associate and dissociate[13,15].

In seeds of *S. alba*, one glucosinolate, *p*-hydroxybenzylglucosinolate, constitutes *ca.* 95% of the total glucosinolate content, but as many as fourteen myrosinase

isoenzymes have been detected[17]. The reason for the presence of isoenzymes is not yet understood. It is, however, important to stress that most of the studies concerning myrosinase isoenzymes hitherto performed have been based on methods with low recoveries[9–21]. This is clearly a serious drawback with respect to quantitative behaviour and probably a cause of the inconsistencies in the literature[19–21].

This paper presents a new, rapid and high-yielding fast polymer liquid chromatographic (FPLC) technique for the isolation and characterization of plant myrosinase isoenzymes. The method is promising with respect to isoenzyme studies, *e.g.* in plant-breeding programmes or in clarification of the hitherto ambiguous results. It is the first report of a purification and stability study of the plant myrosinase isoenzymes by means of FPLC.

EXPERIMENTAL

Myrosinase assay

After mixing with enzyme solution, the decrease in A_{233} for a 33 μM sinigrin (allylglucosinolate) solution in McIlvaine buffer (pH 6.70) was measured (a modification of the method described by Schwimmer[22]). One unit (U) was defined as the amount of enzyme activity that hydrolysed 1 μmol of sinigrin per minute at 25°C and pH 6.70.

Protein determinations

The Coomassie brilliant blue method[23] was applied to crude extracts and ethanol powder preparations, using only 5 ml of reagent and bovine serum albumin as standard. For the fractions from FPLC, A_{280} and A_{260} were measured, and a correction for the content of nucleic acids was performed according to Warburg and Christian[24].

Spot test for myrosinase activity

This test was performed by mixing 50–100 μl of sinigrin solution (1 mg of sinigrin, 5 mg of barium chloride, 0.5 mg of ascorbic acid and 0.1 ml of acetic acid per millilitre of solution) and an equal volume of fractions from FPLC. The presence of myrosinase activity was visualized as a precipitate of barium sulphate.

Crude extracts

Seeds of *Brassica nigra* (L.) Koch, *B. napus* L. and *S. alba* L. were ground and extracted with water (45 ml/10 g meal) by use of an Ultra Turrax homogenizer (3 × 30 s, 2°C). Magnetic stirring (1 h, 5°C) yielded a suspension which, after centrifugation (14 000 *g*, 15 min, 4°C) and filtration through cheese-cloth, resulted in a crude extract.

Ethanol powder

Ethanol (96%, −15°C) was added dropwise to the crude extract (1:1). Centrifugation as above yielded a pellet, which was washed with ethanol (70%, 8 vols.). Centrifugation as above yielded a pellet, which was dissolved in water by stirring (50 ml, 10 min, 5°C). Centrifugation was performed again as above. The lyophilized supernatant was the ethanol powder.

Isolation of myrosinases by FPLC

Instrumentation. This consisted of Pharmacia gradient programmer GP-250, Pharmacia chromatography rack, Pharmacia single path monitor UV-1 (280 nm), fraction collector FRAC-100, Pharmacia two-channel recorder REC 482, two pharmacia high precision pumps P-500 and a valve V-7.

FPLC ion-exchange chromatography. A pre-packed mono Q HR 5/5 column (Pharmacia) equilibrated with buffer A (20 m*M* Tris, pH 7.50) was used. Elution gradient, 0–100% buffer B (20 m*M* Tris, 1 *M* sodium chloride, pH 7.50) in 10 min, followed by 100% B for 2 min; flow-rate, 1 ml/min; fraction size, 1 ml. To isolate myrosinase from *B. nigra*, the crude extract (500 μl) was applied for the first ion-exchange step, followed by re-chromatography of the obtained myrosinase-containing fraction (500 μl). To perform ion-exchange chromatography of ethanol powder preparations from the three species, ethanol powder (50 mg) was dissolved in buffer A (2.5 ml) and 1.3 ml were chromatographed in three consecutive runs.

FPLC chromatofocusing. A prepacked Mono P HR 5/20 column (Pharmacia) was used. It was equilibrated with buffer A (25 m*M* bis-Tris, pH 7.10). The column was eluted with 2 ml of buffer A, followed by 46 ml of buffer B [Polybuffer 74 (Pharmacia) diluted with water (1:9, pH 4.00)] and 2 ml of buffer A. The flow-rate and fraction size were as above. For the three species, 1 ml of the purest fraction from the ion-exchange step was applied to the column after changing the solvent to buffer A on a Sephadex G-25 column. The pH in the fractions was measured with a glass electrode (Radiometer). For *S. alba* myrosinase, re-chromatofocusing was performed on four fractions from the first separation.

Isoelectric focusing (IEF)

Agarose gel IEF. This was performed as described in the manufacturer's instructions (Pharmacia). Ampholine (LKB) pH 3.5–10 was used. A crude extract (20 μl) of *S. alba* was applied on paper (0.5 × 1 cm). Electrophoresis was carried out for 2.5 h, at 500 V, 15–20 mA, and 8°C. To determine the pH gradient, gel pieces (1 × 1 cm) were extracted with water (5 ml, 1 h, 20°C), and the pH in the solutions was measured. Myrosinase activity bands were developed as described for the spot test (a modification of the method by MacGibbon and Allison[10]). The gel was pressed and dried after washing with ethanol–acetic acid–water (35:10:55) (2 × 15 min).

Polyacrylamide gel IEF. LKB Ampholine PAG plates 1804-101, pH 3.5–9.5 were used as described in the manufacturer's instructions. Ethanol powder solution (50 μl) from the three species, as well as fractions from the ion-exchange and chromatofocusing steps, were applied by soaking paper strips in the solutions. Electrophoresis was carried out for 16 h, at 250 V, 4 mA, and 8°C. Gels were stained as above.

RESULTS

Fig. 2 shows chromatograms from the isolation of myrosinases from *B. nigra* crude extract by a two-step FPLC ion-exchange chromatography procedure, resulting in a 26-fold purification.

Yields and purifications from FPLC ion-exchange chromatography and chromatofocusing of myrosinase isoenzymes from ethanol powders of the three examined species are shown in Table I: the mean recovery is 85%.

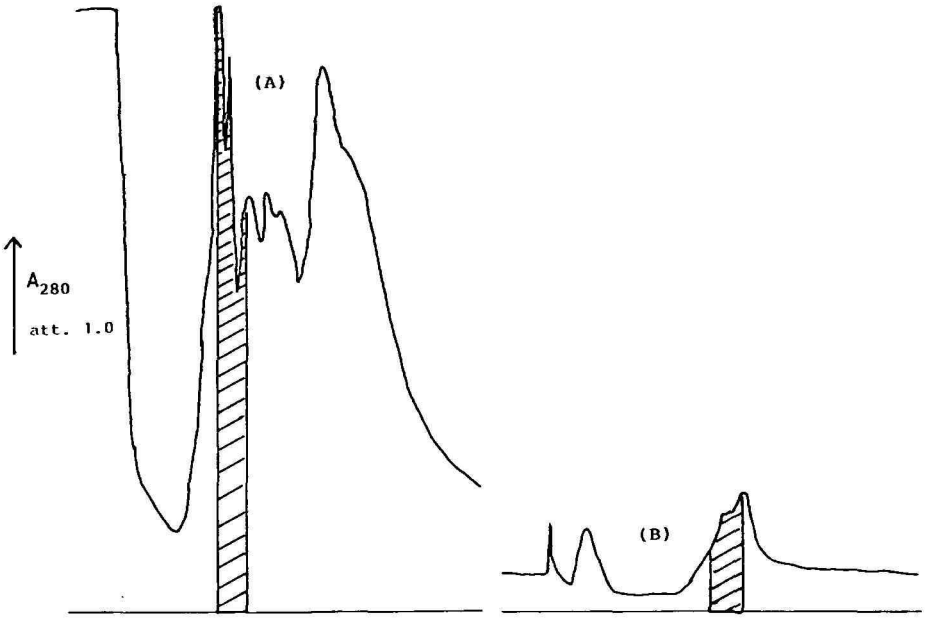

Fig. 2. FPLC ion-exchange chromatography of myrosinase crude extract from *B. nigra*: (A) first ion-exchange step; (B) re-chromatography of fraction 7.

FPLC chromatofocusing analysis of myrosinases from the examined species resulted in the following p*I* intervals for the enzymes: *B. nigra*, pH 5.14–5.33; *B. napus*, pH 5.61–5.90 and *S. alba*, pH 5.63–6.15. Fig. 3 shows an elution profile (pH) and the fractions containing myrosinase activity (three runs).

Results from the complete isolation procedure for myrosinase isoenzymes from seeds of *S. alba* appear in Table II, together with results from re-chromatofocusing of some of the fractions.

IEF investigations of the isoenzymes from *B. nigra*, *B. napus* and *S. alba* are shown in Figs. 4–6.

TABLE I

PURIFICATION OF MYROSINASE ISOENZYMES FROM SEEDS OF CRUCIFERS

Species	*FPLC ion-exchange chromatography of ethanol powder*		*FPLC chromatogocusing of ion-exchange fractions*	
	Recovery (%)	*Purification*	*Recovery (%)*	*Purification*
Brassica nigra	80	3.6× (Fr. 7)*	91	2.8×
Brassica napus	76	4.1× (Fr. 7)	71	2.5×
Sinapis alba	84	1.7× (Fr. 6)	114	5.3×

* Fr. 7 = fraction 7, etc.

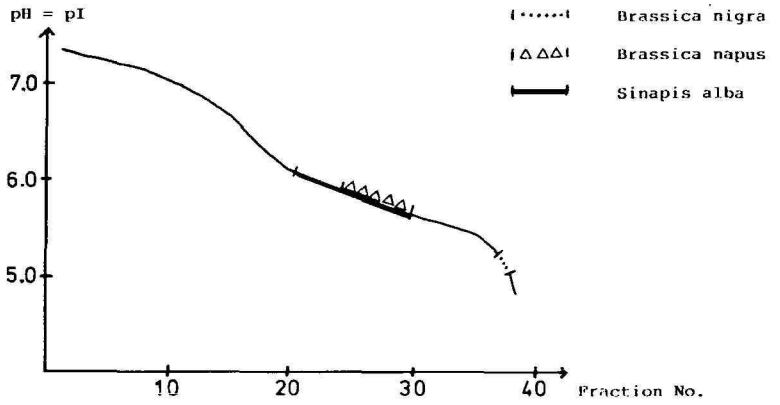

Fig. 3. Elution curve (pH) obtained by FPLC chromatofocusing of myrosinase isoenzymes from seeds of crucifers.

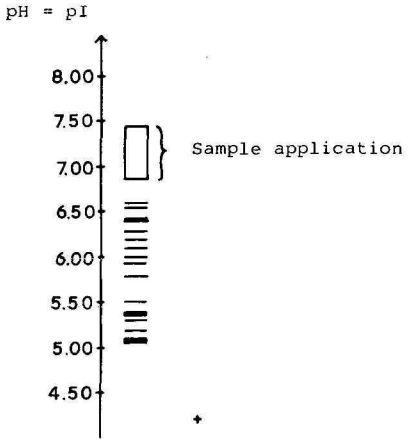

Fig. 4. Agarose IEF of crude extract from *S. alba*. The gel was stained for myrosinase activity.

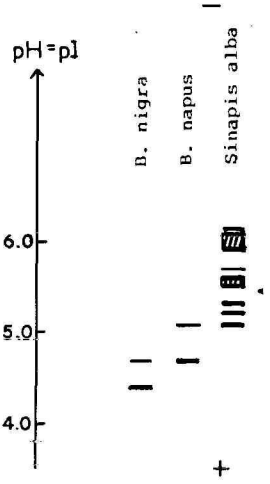

Fig. 5. Polyacrylamide IEF of ethanol-powder preparations. The gel was stained for myrosinase activity.

TABLE II

ISOLATION OF MYROSINASE ISOENZYMES IN *S. ALBA* BY FPLC

	Protein (mg/ml)	*Activity (U/ml)*	*Total activity (U)*	*Specific activity (U/mg protein)*	*Purification*	*pI*
Crude extract (200 ml)	28.1	0.3755	75.1	0.0134		
Ion-exchange chromatography						
Ethanol powder*	2.40	2.8493	3.7041	1.19	89×	
Fr. 2**	1.864	0.2549		0.14		
Fr. 3	0.836	0.2174		0.26		
Fr. 4	0.034	0.0319	3.1185	0.94		
Fr. 5	0.015	0.0041	(84%)	0.27		
Fr. 6	0.196	0.4047		2.06	154×	
Fr. 7	0.174	0.1265		0.73		
Chromatofocusing						
Fr. 6***	0.099	0.1537	0.1537	1.55		
Fr. 20	0.012	0.0032		0.27		6.15
Fr. 21	0.001	0.0083		8.30	619×	6.08
Fr. 22	0.021	0.0340		1.62	121×	6.03
Fr. 23	0.023	0.0184		0.80		5.97
Fr. 24	0.042	0.0286	0.1758	0.68		5.91
Fr. 25	0.019	0.0368	(114%)	1.94	145×	5.85
Fr. 26	0.010	0.0214		2.14	160×	5.80
Fr. 27	0.014	0.0189		1.35		5.74
Fr. 28	0.024	0.0037		0.15		5.68
Fr. 29	0.011	0.0025		0.23		5.63
Re-chromatofocusing						
Fr. 21 + 22, 0.5 ml						
see above		0.0313	0.0157			
Fr. 21, 1.0 ml		0.0042	0.0042			5.70
			(27%)			
Fr. 27 + 28, 0.5 ml						
see above		0.0140	0.0070			
Fr. 25, 1.0 ml		0.0023	0.0023			5.40
			(33%)			

* Ethanol powder (50 mg) was dissolved in 2.5 ml of buffer A, and 1.3 ml of this enzyme solution were chromatographed by three identical runs. Each fraction consisted of 1 ml.

** Fr. 2 = fraction 2, etc.

*** Fr. 6 was diluted by changing the buffer in a G-25 column before it was applied to the column. Each fraction consisted of 1.0 ml.

DISCUSSION

Some of the previously reported investigations on myrosinase isoenzymes using traditional methods of analysis suffered from low recoveries, which probably explain the inconsistent results[11,16–21].

No reports of the FPLC technique now used for myrosinase separation have appeared previously. As shown by the results in Fig. 2 and Tables I and II, excellent

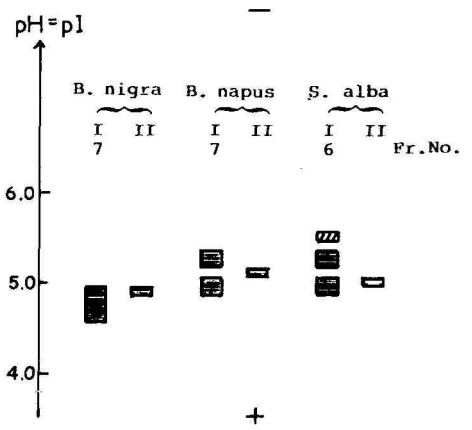

Fig. 6. Polyacrylamide IEF of the ion-exchange preparations used for chromatofocusing (I) and the purest preparation obtained by this purification (II). The gel was stained for myrosinase activity.

recovery and purification of myrosinase can be obtained by this FPLC technique. The high yields of the FPLC techniques almost certainly results from the rapidity of the methods, which ensures that the enzymes are exposed to potentially damaging conditions for only a very short time. Previously, the FPLC technique has successfully been used for isolation of other plant enzymes[25].

The myrosinase isoenzyme bands visualized in Fig. 4 indicate that myrosinase in *S. alba* crude extract consists of at least fourteen isoenzymes[17]. In the ethanol-powder preparation of the crude extract, this number is reduced, (Fig. 5), indicating that myrosinase preparations should be treated very carefully during isolation and characterization of the enzymes, especially when comparative studies of isoenzyme patterns are performed. This is in agreement with previously reported results[10,13,14].

Results from the chromatofocusing steps presented in Fig. 3 show that the three cruciferous species contain different myrosinase isoenzymes. The relative p*I* values for the isoenzymes are confirmed by the IEF results in Figs. 5 and 6. The p*I* values obtained in the chromatofocusing method differ from those obtained in the IEF experiments. This is caused by the differences between these two techniques, and only the relative positions of the isoenzymes should be compared. IEF of the ethanol-powder preparations (Fig. 5) shows that myrosinase isoenzymes from *B. nigra* are characterized by rather low pI values compared with myrosinase isoenzymes from *S. alba*. The isoenzymes from *B. napus* have p*I* values between those of the two other species. The same pattern is found in the IEF investigations of the ion-exchange preparations used for chromatofocusing (Fig. 6).

After ion-exchange chromatography, myrosinase activity is found in various amounts depending on the species in fractions 2–7; the majority containing the highest specific activity appear in fractions 6 and 7. The numbers of bands containing enzymatic activity by IEF before (Fig. 5) and after (Fig. 6) the FPLC ion-exchange chromatography step are similar, although the *S. alba* pattern spans less than one pH-unit after the step. This indicates that isoenzymes with higher p*I* values are not found in the later fractions of the ion-exchange step. The number of bands containing

enzymatic activity by IEF before and after the FPLC chromatofocusing step are not comparable in Fig. 6, because only the purest preparation of this step (containing one band) is shown. Other experiments (not shown) have shown that the myrosinase isoenzymes are well separated according to their p*I* values by chromatofocusing, the isoenzymes with the higher p*I* values being eluted first from the column.

In order to investigate the stability of the isoenzymes in fractions obtained from FPLC chromatofocusing, re-chromatofocusing was carried out on *S. alba* isoenzymes. The results show (Table II) that by re-chromatofocusing of the fractions (21 and 22) and fractions (27 and 28), the relative p*I* values are reproduced. The mean difference between the p*I* values of the two samples is 0.35 pH units in the first run compared with 0.30 pH unit in the re-chromatofocusings. The reproducibility shows the stable nature of the isoenzymes. If the enzymes in *S. alba* were subjected to a continuous turn-over, re-chromatofocusing of a fraction with a specific p*I* value would be expected to yield enzymes spread over a broad p*I* range.

The re-chromatofocusing and the IEF investigations indicate that myrosinases in *B. nigra*, *B. napus* and *S. alba* are composed of a mixture of isoenzymes with rather reproducible p*I* values. The three plant species each show a specific individual isoenzyme pattern.

The results presented here show that FPLC can be used successfully for a more detailed study of myrosinase isoenzymes. The rapidity and the high recovery imply that FPLC could be used to isolate the isoenzymes in a screening of myrosinases from different crucifers, for plant-breeding programmes, and for studies of glucosinolate catabolism and catalytical function–mechanism relationships of the different isoenzymes.

ACKNOWLEDGEMENTS

Support from the Danish Agricultural Research Council and from CEC is gratefully acknowledged.

REFERENCES

1 O. Olsen and H. Sørensen, *J. Am. Oil Chem. Soc.*, 58 (1981) 857.
2 L. M. Larsen, O. Olsen, L. H. Pedersen and H. Sørensen, *Phytochemistry*, 23 (1984) 895.
3 N. Bille, B. O. Eggum, I. Jacobsen, O. Olsen and H. Sørensen, *Z. Tierphysiol., Tierernähr. Futtermittelkd.*, 40 (1983) 148.
4 N. Bille, B. O. Eggum, I. Jacobsen, O. Olsen and H. Sørensen, *Z. Tierphysiol., Tierernähr. Futtermittelkd.*, 49 (1983) 195.
5 B. O. Eggum, O. Olsen and H. Sørensen, in H. Sørensen (Editor), *Advances in the Production and Utilization of Cruciferous Crops*, Martinus Nijhoff, Dordrecht, 1985, p. 50.
6 R. K. Heany and G. R. Fenwick, in H. Sørensen (Editor), *Advances in the Production and Utilization of Cruciferous Crops*, Martinus Nijhoff, Dordrecht, 1985, p. 40.
7 L. M. Larsen, J. K. Nielsen, A. Plöger and H. Sørensen, in H. Sørensen (Editor), *Advances in the Production and Utilization of Cruciferous Crops*, Martinus Nijhoff, Dordrecht, 1985, p. 230.
8 L. Buchwaldt, J. K. Nielsen and H. Sørensen, in H. Sørensen (Editor), *Advances in the Production and Utilization of Cruciferous Crops*, Martinus Nijhoff, Dordrecht, 1985, p. 260.
9 M. G. Ettlinger, G. P. Dateo, B. W. Harrison, T. J. Mabry and C. P. Thompson, *Proc. Natl. Acad. Sci. U.S.A.*, 47 (1961) 1875.
10 D. B. MacGibbon and R. M. Allison, *Phytochemistry*, 9 (1970) 541.
11 J. R. Vose, *Phytochemistry*, 11 (1972) 1649.

12 M. Ohtsuru and T. Hata, *Agric. Biol. Chem.*, 36 (1972) 2495.
13 H. M. Henderson and T. J. McEwen, *Phytochemistry*, 11 (1972) 3127.
14 R. Björkman and J.-C. Janson, *Biochim. Biophys. Acta*, 276 (1972) 508.
15 M. Ohtsuru and T. Hata, *Agric. Biol. Chem.*, 37 (1973) 1971.
16 K. Pihakaski and S. Pihakaski, *J. Exp. Bot.*, 29 (1978) 335.
17 J. R. Phelan and J. G. Vaughan, *J. Exp. Bot.*, 31 (1980) 1425.
18 B. Lönnerdal and J.-C. Janson, *Biochim. Biophys. Acta*, 315 (1973) 421.
19 M. Ohtsuru and H. Kawatani, *Agric. Biol. Chem.*, 43 (1979) 2249.
20 M. Ohtsuru and T. Hata, *Biochim. Biophys. Acta*, 567 (1979) 384.
21 A. P. Wilkinson, M. J. C. Rhodes and R. G. Fenwick, *J. Sci. Food Agric.*, 35 (1984) 543.
22 S. Schwimmer, *Acta Chem. Scand.*, 15 (1961) 535.
23 M. M. Bradford, *Anal. Biochem.*, 72 (1976) 248.
24 O. Warburg and W. Christian, *Biochem. Z.*, 310 (1942) 384.
25 S. Clausen, L. M. Larsen, A. Plöger and H. Sørensen, in H. Sørensen (Editor), *Advances in the Production and Utilization of Cruciferous Crops*, Martinus Nijhoff, Dordrecht, 1985, p. 138.

Journal of Chromatography, 363 (1986) 81–93
Elsevier Science Publishers B.V., Amsterdam — Printed in The Netherlands

CHROM. 18 661

PREPARATIVE SEPARATION OF RACEMIC TERTIARY PHOSPHINE OXIDES BY CHIRAL HIGH-PERFORMANCE LIQUID CHROMATOGRAPHY

A. TAMBUTE
Attaché au Service Technique de l'Armée, Centre d'Etudes du Bouchet, B.P. 3, Le Bouchet, 91710 Vert-le-Petit (France)
and
P. GAREIL*, M. CAUDE and R. ROSSET
Laboratoire de Chimie Analytique, École Supérieure de Physique et de Chimie Industrielles de la Ville de Paris, 10 Rue Vauquelin, 75231 Paris Cedex 05 (France)

SUMMARY

It is shown that preparative chromatography on a chiral stationary phase (CSP) may constitute a useful alternative to chemical methods for the separation of enantiomers of some tertiary phosphine oxides starting from racemic mixtures. Optimization of the mobile phase, carried out by addition of a third solvent (chloroform) to the classical binary mixture (hexane–alcohol), results in a higher selectivity per unit time. A column packed with 500 g of CSP prepared by bonding (*R*)-N-(3,5-dinitrobenzoyl)phenylglycine to an aminopropylsilica gel (7 μm) enabled the injection of 1 g of methyl(4-methoxy-1-naphthyl)phenylphosphine oxide in a single experiment. In this manner the two enantiomers were obtained with an optical purity greater than 99% and a good yield (96%).

INTRODUCTION

The preparation of enantiomers is usually achieved by fractional recrystallization of diastereoisomeric salts; another method is enantioselective synthesis. However, it is not always possible to use those techniques; for instance, the first method cannot be used in the case of compounds lacking reactive functional groups[1].

Pirkle and co-workers[2,3] recently showed that liquid chromatography on a preparative scale with a chiral stationary phase (CSP) is an interesting method for obtaining enantiomers in high optical purities. These authors described the resolution of a number of compounds belonging to various chemical classes and reported the preparation of enantiomers with optical purities higher than 99%. Quantities of $\geqslant 1$ g were obtained in a single experiment in favourable cases.

In a previous paper[4] we have shown that some tertiary phosphine oxides including an aromatic substituent derived from naphthalene were resolved on various CSPs, especially on that derived from (*R*)-phenylglycine using hexane–2-propanol as a classic mobile phase. In order to determine the absolute configuration of the dif-

0021-9673/86/$03.50

ferent enantiomers and possibly to specify the reaction mechanisms occurring during the liquid chromatographic resolution, we had to prepare enantiomers with a high optical purity.

In this work we describe the experiments done on the preparative separation of three tertiary phosphine oxides using 500 g of CSP derived from (*R*)-N-(3,5-dinitrobenzoyl)phenylglycine covalently bonded to an aminopropyl silica gel of fine particle diameter (7 μm):

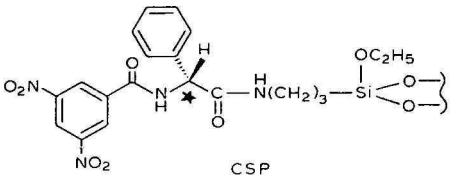

CSP

The mobile phase was chosen according to a previous analytical study[5] which revealed that a ternary mixture hexane–chloroform–ethanol exhibits a good selectivity within a short analysis time.

EXPERIMENTAL

Apparatus

Analytical chromatography was performed with a Model 1084 B liquid chromatograph (Hewlett-Packard, Waldbronn, F.R.G.) equipped with an automatic sampling system (79842 A) and a variable-wavelength detector (190–540 nm) (79875 A) or with a Model 8100 liquid chromatograph (Spectra-Physics, Santa Clara, CA, U.S.A.) equipped with a variable-wavelength detector (190–600 nm) (SP-8440) operating at 280 nm and a dual-channel computing integrator (SP 4200). The column temperature was 40°C.

Preparative chromatography was performed with a Modulprep apparatus (Jobin-Yvon, Longjumeau, France). The chiral stationary phase (500 g) was packed into the column (22 cm × 80 mm I.D.) by axial compression under 15 bar. UV detection was carried out at 325 nm with a variable-wavelength detector (195–370 nm) (Model SM-25, Jobin-Yvon). The preparative chromatograph was operated at room temperature. The eluent inlet pressure was about 9–10 bar, which gave a flow-rate of *ca.* 110 ml min^{-1}.

Melting points were measured on a Buchi-Tottli hot-stage apparatus and are given without correction. Optical rotations were measured on a Perkin-Elmer 141 micropolarimeter with thermostatted 1-dm quartz cells and using high purity solvents (usually from Merck). NMR spectra were recorded on a Brucker WP-200 (200 MHz) using tetramethylsilane (TMS) as an internal standard and [^{2}H]chloroform as a solvent. Chemical shifts (δ) values are given in ppm and coupling constants in Hz.

The compounds followed by "analysis" had elemental analyses consistent with their formulae within ± 0.30% (Service Central de Microanalyse du Centre National de Recherche Scientifique.

Materials

The solvents [*n*-hexane, ethanol, chloroform stabilized with 0.6% (w/w) etha-

nol] were analytical grade and were purchased from Prolabo (Paris, France). Classical chromatographic purifications were carried out on Merck silica gel 60; analytical thin-layer chromatography (TLC) was performed on Merck F 254 silica gel plates.

Synthesis of chiral stationary phase

The chiral moiety, (*R*)-N-(3,5-dinitrobenzoyl)phenylglycine, $[\alpha]_D^{25} = -86.9°$ [*C* = 0.92% (w/w); tetrahydrofuran, THF], m.p. 209–211°C, was prepared as described[6].

Solid (*R*)-N-(3,5-dinitrobenzoyl)phenylglycine (43 g, 124 mmol) and N-ethoxycarbonyl-2-ethoxy-1,2-dihydroquinoline (EEDQ) (39.4 g, 150 mmol) were successively added with swirling to 500 g of LiChrosorb NH_2 (7 μm), suspended in 2.5 l of dichloromethane. The reaction mixture turned dark as the reagents dissolved, and was periodically swirled over 2 h, then the supernatant was removed by suction. The solid was washed three times with portions of 500 ml of methanol. The last washing was done with 500 ml of diethyl ether. After drying under vacuum, 576 g of CSP were obtained with the following elemental analysis: 24.59% C, 3.47% H, 2.10% N, 24% Si, corresponding to 0.30 mmol of chiral sites per gram of support. This means that only 34% of the aminopropyl sites were bonded.

Synthesis of racemic phosphine oxide

Three racemic compounds (±)-I–III were studied (Table I), of which I and II have been described previously[4]. Compound III was prepared in a similar manner. Experiments showed that a good yield was obtained reproducibly when the methylphenylphosphonyl chloride was freshly prepared.

(±)-Methyl(4-methoxy-1-naphthyl)phenylphosphine oxide (III), m.p. 199–201°C (toluene), yield 62%. ^1H NMR ([^2H]chloroform): 2.12 (d, $J_{P-CH_3} = 13$, P–$\underline{CH}_3$), 4.02 (s, O–$\underline{CH}_3$), 6.84 (d, $J_{P-H3} = 1.7$, $\underline{H}^3$), 7.87 (d, $J_{P-H2} = 15$, $\underline{H}^2$), 7.71 (d, $J_{P-H9} = 12.1$, $\underline{H}^9$), 7.4–8.36 (m, 7H). Analysis (C, H, P): $C_{18}H_{17}O_2P$.

1-Bromo-4-methoxynaphthalene, used as an intermediate for the preparation of III, was prepared as follows.

TABLE I

PHOSPHINE OXIDES STUDIED

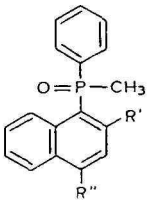

Phosphine oxide	*R'*	*R''*
I	H	H
II	OCH_3	H
III	H	OCH_3

1-Bromo-4-hydroxynaphthalene

To a solution of iodine (1390 g, 5.47 mol) in 3.2 l of acetic acid, was added, at 20°C, bromine (837 g, 5.24 mol) within 2 h, then the mixture was stirred at 50°C for 3 h and at room temperature for 16 h.

To a solution of 1-hydroxynaphthalene (750 g, 5.2 mol) in 2.4 l of acetic acid was added at 10–15°C for 4 h the solution prepared as above. Stirring was maintained for 16 h. The reaction mixture was added in 15 min to a solution of sodium bisulphite (857 g) in 28 l of water. After stirring for 0.5 h the mixture was neutralized by adding 8.6 kg of sodium bicarbonate (pH 5). The organic material was then extracted successively with 2 l of diisopropyl ether and with 500 ml (twice) of the same solvent. The diisopropyl ether fractions were pooled and then washed (twice) with 500 ml of water then brine. The insoluble part was discarded by filtration through Celite. After evaporation of the solvent, the crude product was dissolved in 600 ml of dichloromethane and then cooled. The resulting crystalline precipitate was collected by filtration, washed with 200 ml of heptane–dichloromethane (9:1) and dried under vacuum at room temperature. A 264-g amount (22%) of 1-bromo-4-hydroxynaphthalene was obtained, m.p. 122–123°C (lit.[7] 121–122°C). ^{1}H NMR([^{2}H]chloroform): 5.34 (s, OH).

1-Bromo-4-methoxynaphthalene

To a solution of 1-bromo-4-hydroxynaphthalene (33.45 g, 150 mmol) in 450 ml acetonitrile was added potassium carbonate (22.8 g, 165 mmol) and the resulting suspension was stirred for 1 h under nitrogen. Then methyl iodide (42.6 g, 300 mmol) was added and the mixture was heated under reflux for 3 h. The precipitate was removed by filtration and washed twice with 100 ml acetonitrile. The filtrate was then evaporated and the organic material extracted with 200 ml benzene, and washed successively with water (150 ml, four times) until neutral and with brine. After drying by filtration through an hydrophobic filter and stripping off the solvent 34.6 g of crude product were obtained. The compound was purified by chromatography on 1200 g of silica gel with hexane as eluent, and 25.2 g (70%) of 1-bromo-4-methoxynaphthalene as were obtained a pale yellow viscous oil and used directly for the preparation of the Grignard reagent. ^{1}H NMR([^{2}H]chloroform): 3.81 (s, $OC\underline{H}_3$).

RESULTS AND DISCUSSION

Analytical optimization

Recently we have shown[5] that the ternary mixture hexane–chloroform–alcohol, obtained by mixing two isoeluotropic binary mixtures hexane–alcohol and hexane–chloroform, always gives a higher selectivity per unit time than each isoeluotropic binary mixture. This interesting phenomenon is observed whatever the nature of the alcohol. Fig. 1 shows the results obtained with ethanol. A large decrease in the capacity factor is observed when the two isoeluotropic binary mixtures are mixed in about equal volumes. The selectivity increases linearly with increasing chloroform content. So a compromise between a short separation time and the highest possible selectivity led us to choose a ratio of 20:80 between the binary mixtures A (hexane–ethanol, 93:7) and B (hexane–chloroform, 60:40) corresponding to the following composition: hexane–chloroform–ethanol (66.6:32:1.4).

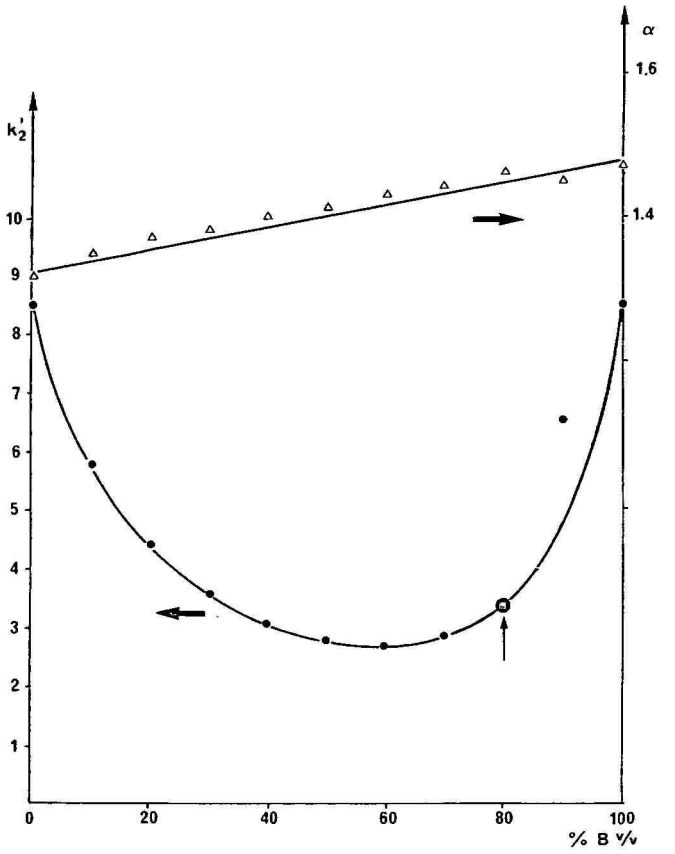

Fig. 1. Influence of the mobile phase composition on the capacity factor (●–●) and selectivity (△–△). The mobile phase is obtained by mixing binary mixture A (hexane–ethanol, 93:7) with binary mixture B (hexane–chloroform, 60:40) in different proportions. Solute: racemate (±)-methyl(4-methoxy-1-naphthyl)phenylphosphine oxide (III).

The chromatographic data are given in Table II for both analytical and preparative columns. The quantity injected on the preparative column is small compared to the amount of CSP and can be considered as an analytical one. The length of the stationary phase bed in the preparative column cannot be measured directly, but can be calculated from measurements of the dead volume, V_m, for the analytical and preparative columns. Assuming that the total porosities, ε, are not very different for the two columns ($\varepsilon = 0.77$ for the analytical one), one can derive a length of *ca* 22 cm for the preparative column. The only difference in operating conditions between the columns is the temperature. It is noted that the capacity factors of the less strongly retained isomers (isomers 1) are very close to each other on both columns, while those of the more strongly retained isomers (isomers 2) are higher on the preparative column. This behaviour is in agreement with a normal temperature dependence and results in a higher selectivity with the preparative column. The plate number is also higher for isomers 1 on both columns and is systematically higher on the analytical than on the preparative column. This can be explained by differences in the temper-

TABLE II

ANALYTICAL CHROMATOGRAPHIC DATA FOR THE OPTICAL ISOMER PAIRS STUDIED

Stationary phase: LiChrosorb NH_2 (7 μm) bonded with (*R*)-N-(3,5-dinitrobenzoyl)phenylglycine. Mobile phase: hexane–chloroform–ethanol (66.6:32.0:1.4). UV detection at 280 nm. Anal. = analytical column (25 cm × 0.46 cm I.D.) containing 2 g of CSP. Temperature: 40°C. Flow-rate: 2 ml min^{-1}. Dead volume: 3.2 ml. Injection: 10 μl of a 10 mg ml^{-1} solution (0.1 mg of the racemate III). Prep. = preparative column (22 cm × 8 cm I.D.) containing 500 g of CSP. Temperature: ambient. Flow-rate: 112 ml min^{-1}. Dead volume: 860 ml. Injection: 5 ml of a 2 mg ml^{-1} solution (10 mg of the racemate III).

Compound	*Capacity ratio, k'*		*Plate number, N*		*Selectivity*		*Resolution, R_s*	
	Anal.	*Prep.*	*Anal.*	*Prep.*	*Anal.*	*Prep.*	*Anal.*	*Prep.*
Naphthyl derivative (I)	3.3 4.3	3.3 4.9	4400 3800	1700 1300	1.30	1.48	3.0	2.4
2-Methoxynaphthyl derivative (II)	4.2 5.6	4.2 6.4	3700 3500	1400 1100	1.33	1.52	3.3	2.4
4-Methoxynaphthyl derivative (III)	5.5 8.0	5.6 9.4	4800 4100	1600 1100	1.45	1.68	4.5	3.0

ature, length and packing quality. In addition, the flow-rate (112 ml min^{-1}) on the preparative column might be a little too low. If we assume a diffusion constant in the mobile phase of about $2.6 \cdot 10^{-9}$ m^2 s^{-1} (ref. 8), the reduced velocity would be about 1.3, which indicates that there might be a slight band broadening due to axial diffusion.So, in spite of its higher selectivity, the preparative column produces a lower resolution than the analytical one, but the resolution remains quite satisfactory for preparative purposes.

For the sake of simplicity, results concerning only the (±)-methyl(4-methoxy-1-naphthyl)phenylphosphine oxide (III) will be presented and discussed.

Preparative chromatography

Fig. 2 shows three preparative chromatograms obtained from injections of three different amounts of the racemic compound III. One can see a strong decrease in the overall retention of each enantiomer, compared to the analytical chromatogram. The analytical retention volumes, V_R, and standard deviations, σ, for each isomer, calculated from the data in Table II, on the preparative column are V_{R_1} = 5676 ml, σ_1 = 142 ml and V_{R_2} = 8944 ml, σ_2 = 270 ml. For the three injections of Fig. 2, the injected volume, V_0, remains lower than σ_1. The injected concentration profile is "seen" by the column as a sharp impulse. There is no band broadening

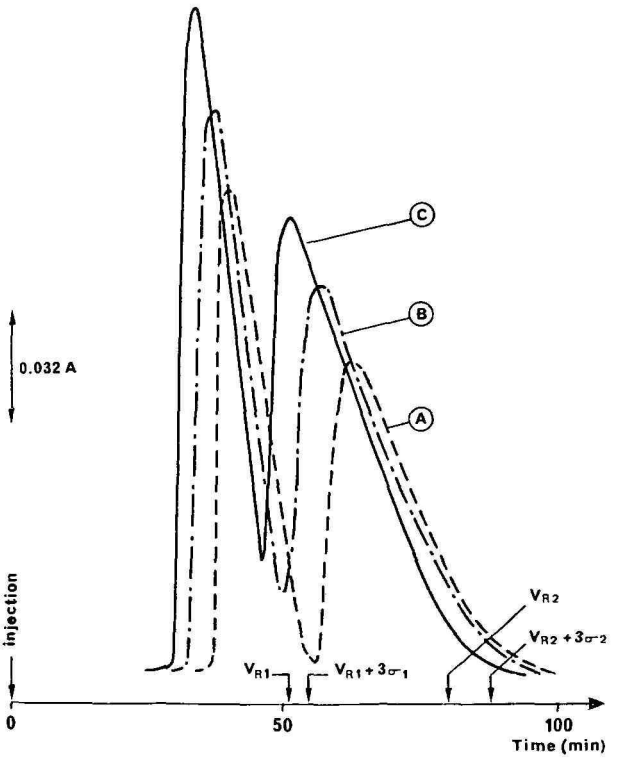

Fig. 2. Preparative chromatograms of the racemate III. Operating conditions as in Table II except injected amount: (A) 500 mg (10 ml of a 50 g l^{-1} solution in chloroform; (B) 750 mg (100 ml of a 7.5 g l^{-1} solution in the mobile phase) (C) 1 g (100 ml of a 10 g l^{-1} solution in the mobile phase). UV detection at 325 nm.

TABLE III

QUANTITATIVE ANALYSIS OF FRACTIONS RECOVERED DURING THE SEPARATION OF 1 g OF RACEMATE III (100 ml OF A 10 g l^{-1} SOLUTION IN THE MOBILE PHASE)

Preparative chromatogram: see Fig. 3. Operating conditions for analytical chromatography: see Table II, except injected volume 20 μl. Tr = cumulative recovery ratio; Ti = cumulative impurity ratio.

Fraction No.	*Volume (ml)*	*Total concentration · 10^3 (M)*	*Isomer 1 (%)*	*Isomer 2 (%)*	*Tr(1) (%)*	*Ti(1) (%)*	*Tr(2) (%)*	*Ti(2) (%)*
1	900	1.441	>99.9	<0.1	72.9	<0.1		
2	340	0.671	99.5	0.5	85.7	<0.1		
3	230	0.433	99.0	1.0	91.2	<0.2		
4	200	0.262	98.7	1.3	94.1	<0.2		
5	220	0.180	91.3	8.7	96.1	<0.4		
6	230	0.513	19.3	80.7	97.4	5.9	99.7	3.9
7	1120	0.724	5.1	94.9	99.7	49.2	94.4	2.7
8	1120	0.386	0.8	99.2			51.1	0.5
9	2350	0.205	0.3	99.7			27	0.3

arising from the injected volume, or no volume overload as it is sometimes referred to[9–11].

We also note from Fig. 2 that the elution profiles exhibit similar peak tails, resembling an envelope curve. These tails join the baseline at an elution volume of approximately $V_R + 3\sigma$. All these properties were described previously[11–12] and are in accord with a strongly non-linear behaviour of the preparative column. This behaviour, arising from a strongly non-linear solute distribution isotherm, is surprising in so far as the injected amount (500 mg to 1 g) lies in the range of 1–2 mg per g of stationary phase, within which the column behaviour is usually only slightly non-linear. It could be related to the fact that the silica gel support has undergone two consecutive bondings, with aminopropyl and (*R*)-N-(3,5-dinitrobenzoyl)phenylglycine moieties, which result in a low number of chiral sites and thereafter in a low stationary phase capacity. This explanation is supported by the elemental analysis data given in the Experimental.

Because of this strong non-linearity, the maximum injected amount leading to a total recovery of pure enantiomers is lower than expected according to a non-linear model for injection optimization[11]. It seems that the elution profiles begin to overlap on the chromatogram when the injected amount is 1 g (Fig. 2C). However it is often difficult to assess the actual purity of a compound from the on-line detection signal only. Fig. 3 shows the fractions collected manually during the separation and quantitatively analyzed on the analytical column. The results are given in Table III. The volumes, V_i, total racemate concentrations, C_i, and percentage enantiomeric compositions were determined for each fraction *i*. From these data one can calculate the cumulative recovery and impurity ratios[13] as follows: the recovery ratio of the first enantiomer eluted, obtained when the first *j* fractions are pooled, is

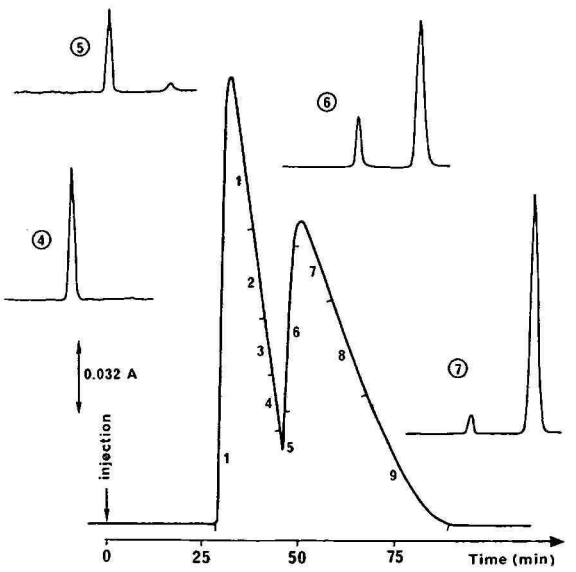

Fig. 3. Fraction collection during the preparative separation of 1 g of racemate III (100 ml of a 10 g l^{-1} solution in the mobile phase). Operating conditions: preparative chromatography, see Fig. 2; analytical chromatography, see Table III.

$$\mathrm{Tr}(1)_j = \frac{\sum_{i=1}^{j} \%(1)_i \cdot C_i V_i}{\frac{1}{2}\sum_{i=1}^{9} C_i V_i}$$

but, according to the mass balance, we have:

$$\frac{1}{2}\sum_{i=1}^{9} C_i V_i = 0.5\ \mathrm{g} = 1.779\ \mathrm{m}M$$

So, $\mathrm{Tr}(1)_j = [\sum_{i=1}^{j} \%(1)_i \cdot C_i V_i]/1.779$. The impurity ratio in these first j fractions is:

$$\mathrm{Ti}(1)_j = \frac{\sum_{i=1}^{j} \%(2)_i \cdot C_i V_i}{\sum_{i=1}^{j} \%(1)_i \cdot C_i V_i} = \frac{\sum_{i=1}^{j} \%(2)_i \cdot C_i V_i}{1.779\ \mathrm{Tr}(1)_j}$$

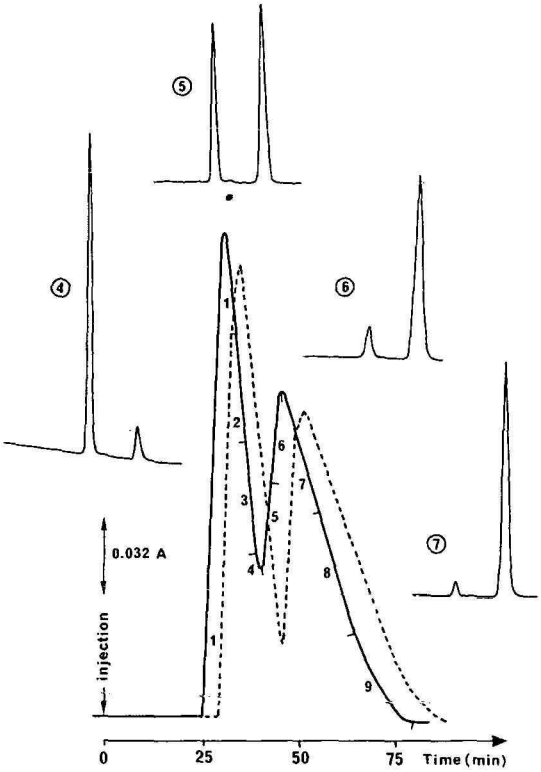

Fig. 4. Fraction collection during the preparative separation of 1 g of racemate III (10 ml of a 100 g l^{-1} solution in chloroform). Operating conditions: preparative chromatography, see Fig. 2 and Table II; analytical chromatography, see Table IV. The preparative chromatogram of Fig. 3 is shown as a dashed line.

The recovery and impurity ratios of the last isomer eluted, obtained when the last j fractions are pooled, are calculated in a similar manner (Table III). By pooling the first five fractions, about 96% of the first enantiomer eluted can be recovered with less than 0.5% impurity. Likewise, about 70–75% of the last enantiomer eluted can be recovered with less than 1% impurity, if fractions 9, 8 and a part of fraction 7 are pooled. Fraction 6 and the other part of fraction 7 should be discarded or recycled.

Fig. 4 allows one to compare two preparative chromatograms obtained by injection of the same amount, 1 g, but different concentration–volume (C_0, V_0) pairs. The dashed line corresponds to the chromatogram discussed above (V_0 = 100 ml, C_0 = 10 g l^{-1}; see Fig. 2). The full line was obtained from a ten-fold more concentrated racemic solution in chloroform. The effluent was fractionated as in the previous case and quantitative results from the analytical chromatography are given in Table IV. A decrease in the overall retention of both peaks and an apparently poorer resolution are observed. This is in agreement with the analytical chromatographic pattern for fractions 4–7 in Figs. 3 and 4, and indicates that the behaviour of the preparative column is, as expected, more non-linear with a more concentrated solution. However, if we calculate the cumulative recovery and impurity ratios (Table IV), we can see that about 92–93% of the first enantiomer eluted can be recovered with approximately 0.5% impurity, while 65–60% of the second enantiomer eluted is recovered with about 1% impurity. These figures are only slightly lower than those derived from Table III.

The optical purity of each fraction was also measured in order to confirm the purity attainable by preparative chromatography. The results are in good agreement with the values calculated from the difference between the percentages of each isomer (Table IV).

After each preparative chromatography the various fractions corresponding to an enantiomeric purity higher than 99% were pooled, evaporated and the final product was crystallized from benzene–diisopropyl ether (1:1). The following enantiomers were obtained. (*S*)-(+)-Methyl(1-naphthyl)phenylphosphine oxide, I-*S*(+), m.p. = 140–144°C, $[\alpha]_D^{22}$ = + 21°(*C* = 2, methanol); lit.[14], m.p. = 142°C, $[\alpha]_D^{22}$ = + 18.6° (*C* = 2, methanol). Enantiomer I-*R*(−) has m.p. = 143–145°C, $[\alpha]_D^{22}$ = −17.3° (*C* = 2, methanol). For the enantiomers corresponding to the racemic compounds II and III the absolute configurations are unknown. (+)-Methyl(2-methoxy-1-naphthyl)phenylphosphine oxide, II-(+), m.p. = 131–132°C, $[\alpha]_D^{22}$ = +124° (*C* = 2, methanol). II-(−), m.p. = 130–132°C, $[\alpha]_D^{22}$ = −120.5° (*C* = 2, methanol). (+)-Methyl(4-methoxy-1-naphthyl)phenylphosphine oxide III-(+), m.p. = 145–150°C, $[\alpha]_D^{22}$ = + 29° (*C* = 2, methanol); III-(−), m.p. = 149–151°C, $[\alpha]_D^{22}$ = − 25.3° (*C* = 2, methanol).

It must also be borne in mind that chloroform, in spite of its high solubilizing power with regard to the racemic mixture (300 g l^{-1} at room temperature), cannot be advocated as a sample solvent owing to its too high eluent strength: with chloroform as mobile phase, the capacity factors of both enantiomers are 3.2 and 4.1 and the selectivity falls to 1.29. The ternary mobile phase is preferred (solubility of racemic mixture 35 g l^{-1} at room temperature). However, small volumes of chloroform, as here, can be injected without any detrimental effect on the separation.

Finally, it can be concluded that the recovery and impurity ratios are very satisfactory for injections of about 1 g of racemic mixture. it seems possible to in-

TABLE IV

QUANTITATIVE ANALYSIS OF FRACTIONS RECOVERED DURING THE SEPARATION OF 1g OF RACEMATE III (10 ml OF A 100 g l^{-1} SOLUTION IN CHLOROFORM)

Preparative chromatogram: see Fig. 4. Analytical chromatography as in Table III.

Fraction No.	*Volume (ml)*	*Total concentration · 10^3 (M)*	*Isomer 1 (%)*	*Isomer 2 (%)*	*Tr(1) (%)*	*Ti(1) (%)*	*Tr(2) (%)*	*Ti(2) (%)*	*Optical purity (%)*	
									Calculated	*Measured*
1	780									
2	340	1.245	>99.9	<0.1	78.4	<0.1				
3	340	0.566	>99.9	<0.1	89.2	<0.1			100	100
4	225	0.427	89.3	10.7	94.0	0.7			78.6	73
5	225	0.480	38.7	61.3	96.4	4.5	99.4	6.0	22.6	23
6	240	0.941	11.8	88.2	97.9	12.1	95.7	3.8	76.4	74
7	1100	0.840	4.0	96.0	99.9	50.7	84.5	2.5	92	92
8	1100	0.327	0.1	99.9			34.6	<0.1	100	100
9	1400	0.183	<0.1	>99.9			14.4	<0.1		

crease the purified amount recovered per injection and thereafter the time yield by increasing the injected amount to 2 g, but at the slight expense of the recovery ratio. We also have shown that it is better to inject a rather diluted racemic solution in the mobile phase, in order to reduce the effects of the non-linear isotherm and to improve the preparative resolution. Based on the analytical data taken from Table II, the linear theory for injection volume optimization[11,15] predicts injections of up to 2000 ml. Unfortunately, the injection volume is presently limited to about 100 ml for technological reasons. The maximum pressure the apparatus can withstand imposes a severe compromise on the choices of column length, stationary phase particle size and mobile phase flow-rate.

ACKNOWLEDGEMENT

We are grateful to Arlette Begos (Centre d'Études du Bouchet) for technical assistance in the experimental part of this work.

REFERENCES

1 O. Korpium, R. A. Lewis, J. Chickos and K. Mislow,*J. Am. Chem. Soc.*, 90 (1968) 4842.
2 W. H. Pirkle, A. Tsipouras and T. J. Sowin, *J. Chromatogr.*, 319 (1985) 392.
3 W. H. Pirkle and J. M. Finn, *J. Org. Chem.*, 47 (1982) 4037.
4 P. Pescher, M. Caude, R. Rosset, A. Tambute and L. Oliveros, *Nouv. J. Chim.*, 9 (1985) 621.
5 P. Pescher, M. Caude, R. Rosset and A. Tambute, *J. Chromatogr.*, submitted for publication.
6 W. H. Pirkle and M. H. Hyun, *J. Org. Chem.*, 49 (1984) 3043.
7 W. Militzer, *J. Am. Chem. Soc.*, 60 (1937) 256.
8 R. Rosset, M. Caude and A. Jardy, *Manuel Pratique de Chromatographie en Phase Liquide*, Masson, Paris, 2nd ed., 1982.
9 B. Coq, G. Cretier and J. L. Rocca, *J. Chromatogr.*, 186 (1979) 457.
10 L. Personnaz and P. Gareil, *Sep. Sci. Technol.*, 16 (1981) 135.
11 P. Gareil and R. Rosset, *Analusis*, 10 (1982) 397.
12 P. Gareil, L. Personnaz, J. P. Feraud and M. Caude, *J. Chromatogr.*, 192 (1980) 53.
13 P. Gareil, C. Durieux and R. Rosset, *Sep. Sci. Technol.*, 18 (1983) 441.
14 R. Luckenbach, *Phosphorus*, 1 (1972) 228.
15 R. P. W. Scott and P. Kucera, *J. Chromatogr.*, 119 (1976) 467.

Journal of Chromatography, 363 (1986) 95–100
Elsevier Science Publishers B.V., Amsterdam — Printed in The Netherlands

CHROM. 18 542

THROMBIN PURIFICATION BY ONE-STEP PREPARATIVE AFFINITY CHROMATOGRAPHY ON MODIFIED POLYSTYRENES

A. M. FISCHER*
Laboratoire d'Hématologie, C.N.R.S. GRECO 130048, C.H.U. Necker-Enfants Malades, 156 rue de Vaugirard, 75015 Paris Cedex 15 (France)
X. J. YU
Laboratoire de Recherches sur les Macromolécules, C.N.R.S. UA 502 GRECO 130048, Université Paris-Nord, Avenue Jean-Baptiste Clément, 93430 Villetaneuse (France)
J. TAPON-BRETAUDIERE
Laboratoire d'Hématologie, C.N.R.S. GRECO 130048, C.H.U. Necker-Enfants Malades, 156 rue de Vaugirard, 75015 Paris Cedex 15 (France)
D. MULLER
Laboratoire de Recherches sur les Macromolécules, C.N.R.S. UA 502 GRECO 130048, Université Paris-Nord, Avenue Jean-Baptiste Clément, 93430 Villetaneuse (France)
A. BROS
Laboratoire d'Hématologie, C.N.R.S. GRECO 130048, C.H.U. Necker-Enfants Malades, 156 rue de Vaugirard, 75015 Paris Cedex 15 (France)
and
J. JOZEFONVICZ
Laboratoire de Recherches sur les Macromolécules, C.N.R.S. UA 502 GRECO 130048, Université Paris-Nord, Avenue Jean-Baptiste Clément, 93430 Villetaneuse (France)

SUMMARY

Insoluble polystyrenes substituted with sulphonate and L-arginyl methyl ester have been synthesized. Using their specific affinity for thrombin, we developed a simple one-step chromatographic procedure for thrombin purification. As a control, insoluble polystyrenes substituted only with sulphonate groups were tested. The results obtained confirmed the importance of the arginyl residues grafted onto these polymers to obtain an affinity matrix useful for purifying thrombin with a high specific activity and a good recovery.

INTRODUCTION

Thrombin interacts with its main physiological inhibitor, antithrombin III, by the formation of a complex using the seryl group of the enzyme active center and an arginyl site of the inhibitor[1]. Polystyrenes modified with L-arginyl methyl ester mimic the reactive site of the inhibitor and exhibit a specific affinity for thrombin[2], but the presence of sulphonate groups on the polymer lead also to a non-specific ionic interaction with the enzyme.

0021-9673/86/$03.50

In the present paper, we compare the behaviour of insoluble polystyrenes, modified either with L-arginyl methyl ester and sulphonate groups or only with sulphonate, groups, towards thrombin obtained by activation of prothrombin concentrate. A simple preparative purification method of thrombin by a one-step chromatographic procedure is described.

MATERIALS AND METHODS

Preparation of the resins

Polystyrenes grafted with sulphonate groups ($PSSO_3$) are obtained by total hydrolysis of chlorosulphonated polymers[3]. Part of the chlorosulphonated polymer is immediately substituted with L-arginyl methyl ester (PAOM) as previously described[4]. The chemical structures of PAOM and $PSSO_3$ resins, and their characteristics, are presented in Fig. 1. The resins are carefully crushed and the fine particles are eliminated by sedimentation. The mean size of the polymer beads are *ca.* 50 μm.

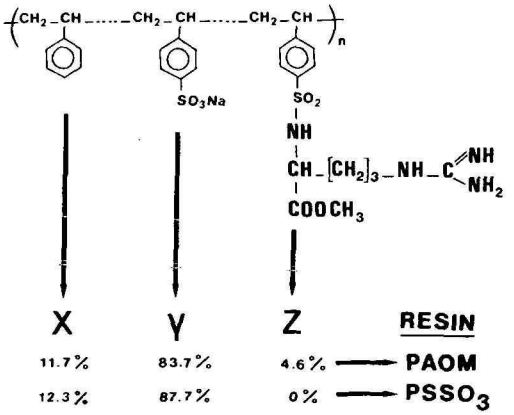

Fig. 1. Structure of PAOM and $PSSO_3$ resins.

Thrombin purification process

A column (200 × 10 mm I.D.) is packed with *ca.* 15 ml (corresponding to 4.5 g of dried resin) of a suspension of PAOM or $PSSO_3$ resin in 0.05 *M* Tris–HCl buffer and 0.1 *M* sodium chloride, pH 7.4. Commercial prothrombin complex concentrate is a partially purified human plasma fraction containing three coagulation factors: prothrombin (Factor II), Factor IX and Factor X. Prothrombin from prothrombin concentrate (batches 84 × 068 and 85 × 002, C.N.T.S., Paris, France) is activated in thrombin by the following procedure: at 37°C, human brain tissue factor, calcium chloride and bovine Factor V are added to the prothrombin solution according to Benamon *et al.*[5]. When the amount of generated thrombin reaches a steady level, the incubated mixture is centrifuged (20 000 *g*) at + 4°C for 3 h, and dialysed against 0.05 *M* Tris–HCl buffer and 0.1 *M* sodium chloride at pH 7.4.

Then, the mixture is applied onto the column, which had been pre-equilibrated with the dialysis buffer. Runs are performed at a flow-rate of 20 ml/h. After collection of the breakthrough, the column is extensively washed with the dialysis buffer until

the optical density at 280 nm comes down to 0.01; then, a linear gradient of sodium chloride from 0.1 to 2.5 *M* (40 ml in each chamber) buffered with 0.05 *M* Tris–HCl (pH 7.4) is applied to the column. The eluted fractions (2 ml) are collected and their optical density recorded at 280 nm using a LKB (Sweden) UV detector. The thrombin clotting activity of each fraction is measured on fibrinogen. The different fractions corresponding to the peaks of each chromatogram are pooled, concentrated and dialysed against 0.15 *M* sodium chloride and kept frozen at −80°C after characterization.

Characterization of the pooled fractions

Protein concentration is determined by the Lowry method[6]. Thrombin clotting activity is measured by addition of 0.1 ml of the eluent to 0.3 ml of a 0.2% human fibrinogen solution. Thrombin concentration is determined in NIH units by comparison to a standard curve. Electrophoresis in 7% polyacrylamide gels in sodium dodecyl sulphate (SDS) is carried out according to the method of Laemmli[7]. Highly purified human thrombin, 3000 NIH U/mg, provided by Dr. Boffa, C.N.T.S., Paris, France, is used as a control.

Presence of Factor IXa and Factor Xa is checked by the immunodiffusion method according to Ouchterlony[8], using rabbit anti-human Factor IX and Factor X antibodies (Stago, Asnières, France), which also react with activated Factor IX (factor IXa) and activated factor X (factor Xa). The rabbit anti-human prothrombin antibodies used (Behringwerke, Marburg, F.R.G.) react also with thrombin and prothrombin derivatives.

RESULTS AND DISCUSSION

Chromatography on PAOM resin

The elution diagram of activated prothrombin complex concentrate on PAOM resin is represented in Fig. 2. The breakthrough corresponds to peak 1 (P_1). Thrombin is eluted in one single peak (P_2) at 0.8 *M* sodium chloride ionic strength. This peak contains 69% of the amount of thrombin, tested by clotting activity, applied onto the column. The specific activity of thrombin recovered in the elution peak is 3000 U/mg (Table I). Electrophoresis on polyacrylamide gels reveals, in the eluted peak, one single band with the same mobility as the purified thrombin control (Fig. 3). No factor IXa or Xa, as possible contaminants, are detectable when checked by the immunodiffusion method (Fig. 4).

Chromatography on $PSSO_3$ resin

The elution diagram of activated prothrombin complex concentrate carried out on $PSSO_3$ resin is represented in Fig. 5. The breakthrough corresponds to peak 1 (P_1). Thrombin is eluted in one broad peak (P_3) at *ca.* 1.8 *M* sodium chloride ionic strength. The specific activity of thrombin is 915 NIH U/mg (Table I). No factor IXa or Xa are detectable when checked by the immunodiffusion method, but electrophoresis on polyacrylamide gels reveals the presence of thrombin and also of other contaminants (Fig. 6). The thrombin elution peak is preceded by a double peak (P_2) devoid of any thrombin activity, eluted within the gradient (Fig. 5).

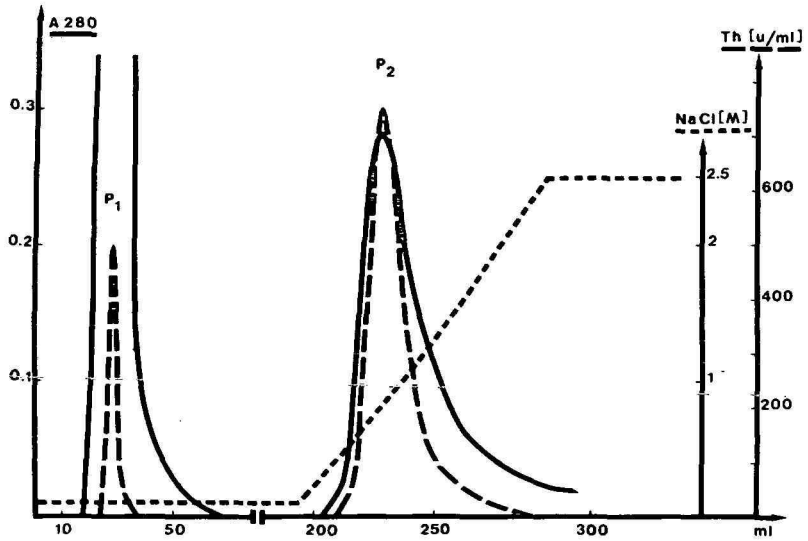

Fig. 2. Activated prothrombin complex chromatogram on PAOM resin. Peaks: P_1 = breakthrough; P_2 = eluted thrombin.

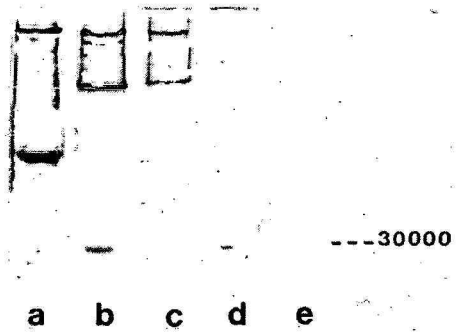

Fig. 3. SDS-polyacrylamide gel electrophoresis of the thrombin purification steps on PAOM resin. (a) Prothrombin complex concentrate; (b) activated prothrombin complex concentrate; (c) peak 1; (d) peak 2; (e) purified thrombin control.

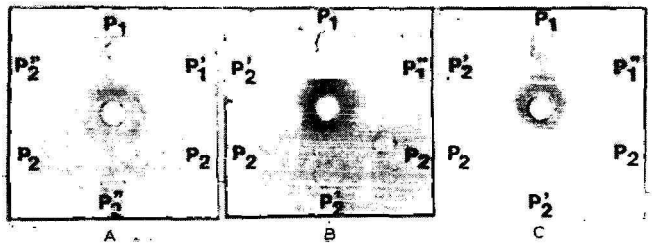

Fig. 4. Immunodiffusion of thrombin purification steps on PAOM resin. In the central well (A) specific anti-Factor II antiserum, (B) specific anti-Factor X antiserum, (C) specific anti-Factor IX antiserum. Peak 1 is tested at the following dilutions: (P_1) 1/1; (P_1') 1/5; (P_1'') 1/10. Peak 2 is tested at the following dilutions: (P_2) 1/1; (P_2') 1/2; (P_2'') 1/10.

TABLE I

THROMBIN PURIFICATION

	V (ml)	*Total thrombin (u)*	*Total proteins (Lowry) (mg)*	*Specific activity (thrombin u/mg)*	*Yield (%)*	*Purification*
PAOM						
Activated prothrombin concentrate	5.6	12000	102.5	117		
Peak 2	4.35*	8300	2.685	3091	69	26
$PSSO_3$						
Activated prothrombin concentrate	4	5000	50.2	99.6		
Peak 3	2.13*	1951	2.13	915	39	9

* After concentration.

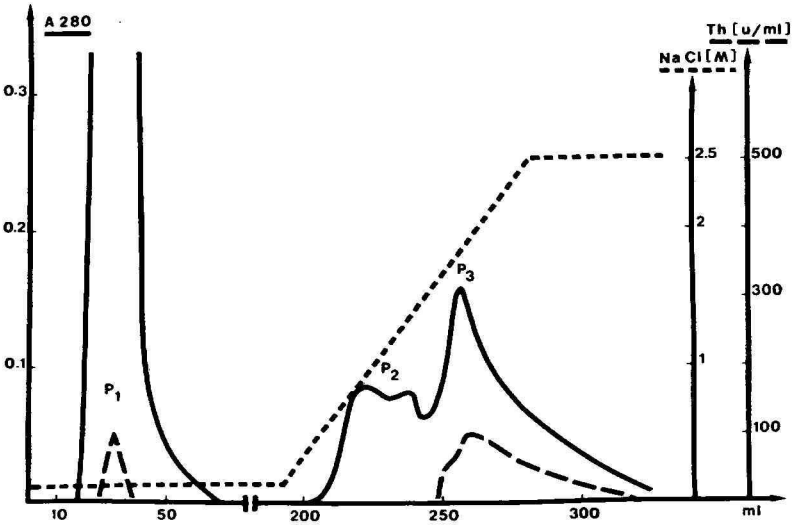

Fig. 5. Activated prothrombin complex chromatogram on $PSSO_3$ resin. Peaks: P_1 = breakthrough; P_2 = eluted peak without any clotting activity; P_3 = eluted thrombin.

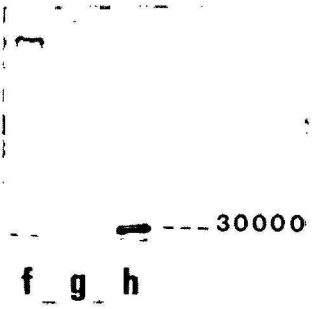

Fig. 6. SDS-polyacrylamide gel electrophoresis of the thrombin purification steps on $PSSO_3$ resin: (f) Peak 1; (g) peak 2; (h) peak 3.

Comparison of the two resins

Both $PSSO_3$ and PAOM resins exhibit a high affinity for thrombin, probably due to the presence of numerous negative charges. As a matter of fact, in most of the classical thrombin purification methods, ion-exchange chromatography is an important step, nevertheless preceded by other steps of fractionation[9].

When this type of chromatography is used as a one-step procedure, as in the case of $PSSO_3$ resin, thrombin is only roughly purified with a low specific activity (900 NIH U/mg), and numerous contaminants are detectable by polyacrylamide gel electrophoresis. By contrast, thrombin obtained after one chromatographic run on PAOM resin exhibits a high specific activity (3000 NIH U/mg), and the purity of the enzyme, as checked by polyacrylamide gel electrophoresis, is good. The yield of this purification procedure is remarkably high. The good performance of PAOM resin in thrombin purification must be due to the presence of arginyl groups, selectively interacting with thrombin. These results lead us to propose this insoluble resin as a useful simple tool for thrombin purification.

REFERENCES

1 R. D. Rosenberg and P. S. Damus, *J. Biol. Chem.*, 248 (1973) 6490.
2 C. Boisson, D. Gulino, J. Jozefonvicz, A. M. Fischer and J. Tapon-Bretaudiere, *Thromb. Res.*, 34 (1984) 269.
3 M. A. Petit and J. Jozefonvicz, *J. Appl. Polym. Sci.*, (1977) 2589.
4 X. J. Yu, A. M. Fischer, D. Muller, A. Bros, J. Tapon-Bretaudiere and J. Jozefonvicz, *J. Chromatogr.*, 376 (1986) 429.
5 D. Benamon-Djiane, F. Josso and J. P. Soulier, *Coagulation*, 1 (1968) 259.
6 O. H. Lowry, N. J. Rosebrough, A. I. Farr and R. J. Randall, *J. Biol. Chem.*, 193 (1951) 265.
7 U. K. Laemmli, *Nature (London)*, 227 (1984) 680.
8 O. Ouchterlony, in D. N. Weir (Editor), *Handbook of Experimental Immunology*, Blackwell Scientific Publications, Oxford, 1967, p. 655.
9 J. W. Fenton, M. J. Faso, A. B. Stackrow, D. L. Aronson, A. M. Young and J. S. Finlayson, *J. Biol. Chem.*, 252 (1977) 3587.

Journal of Chromatography, 363 (1986) 101–103
Elsevier Science Publishers B.V., Amsterdam — Printed in The Netherlands

CHROM. 18 551

Note

Isolation of factor IX concentrates for clinical use by ion-exchange chromatography and ammonium sulphate precipitation

D. STAMPE*, B. WIELAND and A. KÖHLE
German Red Cross Blood Bank, Ulm (F.R.G.)

Prothrombin complex factors are isolated usually by adsorbing on ion-exchangers[1,2]. The subsequent elution step provides solutions of moderate concentration, which, in addition, often have to be desalted[2,3]. However, further concentration by intermediate lyophilization[2–4] or alcohol precipitation[5] is expensive and time-consuming or detrimental[6]. We have therefore introduced ammonium sulphate as a concentrating agent.

EXPERIMENTAL

(A) Details of our standard procedure with DEAE-Sephadex as adsorbent are given in Scheme 1.

(B) In an alternative method, we used DEAE-cellulose 130 gr (Schleicher and Schüll). In this case, the prothrombin complex was eluted with buffers of lower ionic strength in columns of 100 × 21.5 cm I.D. (Pharmacia) or 50 × 18 cm I.D. (Amicon), respectively. Moreover, the first precipitation with ammonium sulphate was ommitted.

In both methods, heparin was added at the beginning and end of the process.

Assays (selected)

Activities of clotting factors II, VII, IX and X were determined by the one-stage method using the reagents of Merz and Dade. Tests for thrombogenicity and activated factors (Xa, thrombin) were performed as described by Kingdon[7] and with chromogenic substrate S 2222 (Kabi) or Chromozym TH (Boehringer, Mannheim, F.R.G.), respectively.

RESULTS

Purification of factor IX is *ca.* 220-fold and the yield is 45–55% with respect to the supernatant of cryoprecipitate. Final products are readily soluble, free of thrombogenicity or activated factors and contain 50–60 U of factors II, IX, X and *ca.* 16 mg/ml protein. Factor VII is poorly adsorbed under our experimental conditions. Most of its activity is found in the wash and first precipitate with ammonium sulphate. Procedure B yields less contaminating proteins than procedure A, as revealed by polyacrylamide gel electrophoresis. The concentrates can be heated in the

0021-9673/86/$03.50

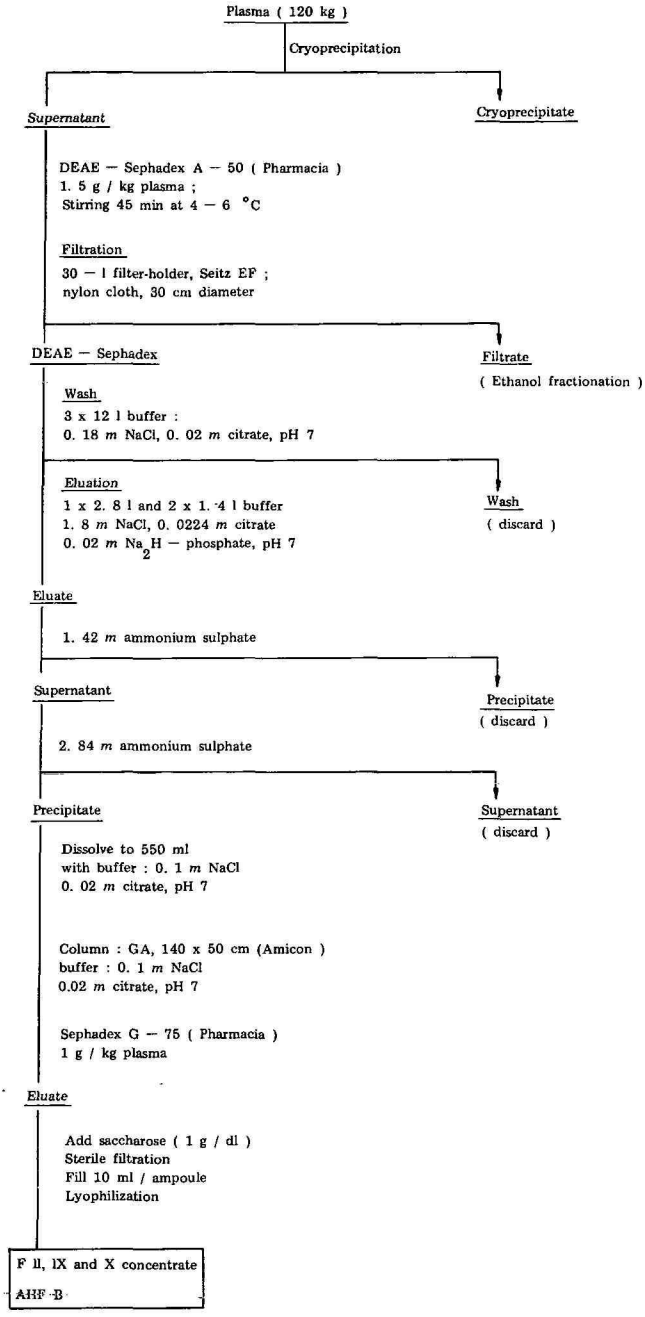
Plasma (120 kg)
Cryoprecipitation
Supernatant
Cryoprecipitate
DEAE — Sephadex A — 50 (Pharmacia)
1. 5 g / kg plasma ;
Stirring 45 min at 4 — 6 °C
Filtration
30 — l filter-holder, Seitz EF ;
nylon cloth, 30 cm diameter
DEAE — Sephadex
Filtrate
(Ethanol fractionation)
Wash
3 x 12 l buffer :
0. 18 m NaCl, 0. 02 m citrate, pH 7
Eluation
1 x 2. 8 l and 2 x 1. 4 l buffer
1. 8 m NaCl, 0. 0224 m citrate
0. 02 m Na2H — phosphate, pH 7
Wash
(discard)
Eluate
1. 42 m ammonium sulphate
Supernatant
Precipitate
(discard)
2. 84 m ammonium sulphate
Precipitate
Supernatant
(discard)
Dissolve to 550 ml
with buffer : 0. 1 m NaCl
0. 02 m citrate, pH 7
Column : GA, 140 x 50 cm (Amicon)
buffer : 0. 1 m NaCl
0.02 m citrate, pH 7
Sephadex G — 75 (Pharmacia)
1 g / kg plasma
Eluate
Add saccharose (1 g / dl)
Sterile filtration
Fill 10 ml / ampoule
Lyophilization
F II, IX and X concentrate
AHF-B

Scheme 1.

lyophilized state for up to 96 h at 70°C without perceptible changes in composition and activity.

DISCUSSION

Procedure A in particular is versatile and can be scaled up to larger volumes of plasma. Vessels of special design for the concentrating elution of DEAE-Sephadex[8] are not required. In the eluate, the ionic strength can be varied over a vast range. Thus, small elution volumes are possible. Precipitation by ammonium sulphate is, to some extent, insensitive to temperature and stabilizes proteins. Hence, precipitates can be stored and then combined for desalting in larger batches. Sephadex G-75 as a separation medium proved to be better than Sephadex G-25[9]. Respective gel bed heights of 18 and 21 cm allow short running times. The process is compatible with ethanol fractionation and other methods for the isolation of plasma proteins.

With method B and DEAE-cellulose as adsorbent we found pyrogen-like reactions in rabbits from time to time. This and the material's tendency to clog to the nylon gauze led us to use DEAE-Sephadex in routine preparations for clinical use,.

REFERENCES

1 G. W. R. Dike, E. Bidwell and C. R. Rizza, *Br. J. Haematol.*, 22 (1972) 469.
2 J. Heystek, H. G. J. Brummelhuis and H. W. Krijnen, *Vox Sang*, 25 (1973) 113.
3 S. Chandra and M. Wickerhauser, *Thromb. Res.*, 12 (1978), 571.
4 M. H. Coan, M. A. Fournel and M. M. Mozen, *Ann. N.Y. Acad. Sci.*, 370 (1981) 731.
5 J.P. Soulier,C. Blatrix and M. Steinbuch, *Presse Med.*, 72 (1964) 1223.
6 J. Heystek, G. M. Maier-van der Zande, H. G. J. Brummelhuis and H. W. Krijnen, *Vox Sang*, 29 (1975) 177.
7 H. S. Kingdon, R. L. Lundblad, J. J. Veltkamp and D. L. Aronson, *Thromb. Diath. Haemorrh.*, 33 (1975) 617.
8 H. G. J. Brummelhuis, in J. M. Curling (Editor), *Methods of Plasma Protein Fractionation*, Academic Press, London, 1980, p. 417.
9 H. Suomela, G. Myllylä and E. Raaska, *Vox Sang*, 33 (1977) 37.

Journal of Chromatography, 363 (1986) 105–110
Elsevier Science Publishers B.V., Amsterdam — Printed in The Netherlands

CHROM. 18 669

PREPARATIVE FRACTIONATION OF CARBOHYDRATE-RICH COMPONENTS PRESENT IN GERM-FREE RAT INTESTINAL MUCIN BY GEL FILTRATION

COMPARISON OF DYNOSPHERES® XP-3505 AND SEPHAROSE CL 4B

BERIT SMESTAD PAULSEN*, JENS KRISTIAN WOLD and SISSEL OTTERSEN
Department of Pharmacy, P.O. Box 1068 Blindern, 0316 Oslo 3 (Norway)
and
KARI SVANE MELLBYE and TORE BARLO
Dyno Particles A.S., P.O. Box 160, 2001 Lillestrøm (Norway)

SUMMARY

Fractionation of the carbohydrate-rich mucin present in the intestines of germ-free rats has been achieved on Dynospheres XP-3505. Comparison with Sepharose CL 4B shows that the separation on Dynospheres XP-3505 is better and quicker. The carbohydrate composition of the fractions show little difference from that of the crude material.

INTRODUCTION

The epithelial surface of the mammalian intestinal tract is protected by a flowing layer of mucus continuously produced by secretory cells of the intestinal mucosa. This layer is part of the barrier through which substances have to pass when absorbed from the intestinal tract. It also serves as a mechanical protective barrier and contributes to maintain a relatively constant pH and ion concentration in the environment of the tender microvilli[1]. The intestinal mucin secretions are degraded by the microflora of the digestive tract[2,3]. This fact complicates the isolation and the study of the native product. By the use of animals devoid of any microflora in the digestive tract, intestinal mucin can be isolated in a yield better than that obtained from conventional animals. Prior to structural studies of the carbohydrate moiety of this mucin, the product is digested with pronase.

The acidic part of the retentate after dialysis was precipitated as a cetyltrimethylammonium (CTAB) complex and further purified on a DEAE Sephadex A25 anion-exchange column. The fractions containing the major part of neutral sugars and sialic acid were subjected to partial separation on Sepharose 4B[1]. For more detailed studies on the carbohydrate moiety of the rat intestinal mucin further separation of the material is necessary, and the high-molecular-weight (HMW) fraction was rechromatographed on Dynospheres XP-3505 and Sepharose CL 4B in order to find a suitable separation medium for the actual material.

0021-9673/86/$03.50

EXPERIMENTAL

The starting material was prepared as described earlier[1]. Gel filtration was performed on two different columns:

(i) Sepharose CL 4B, (Pharmacia, Uppsala, Sweden) 37 × 1 cm I.D. The column was eluted with 0.1 *M* ammonium hydrogen carbonate at a flow-rate of 0.3 ml/min, controlled by a Pharmacia P-1 pump. Fractions of 1.2 ml were collected using a LKB Redirac 2112 fraction collector. The carbohydrate profile was determined by the method of Dubois *et al.*[4] and the protein profile by the Lowry[5] method. The results are presented in Fig. 1.

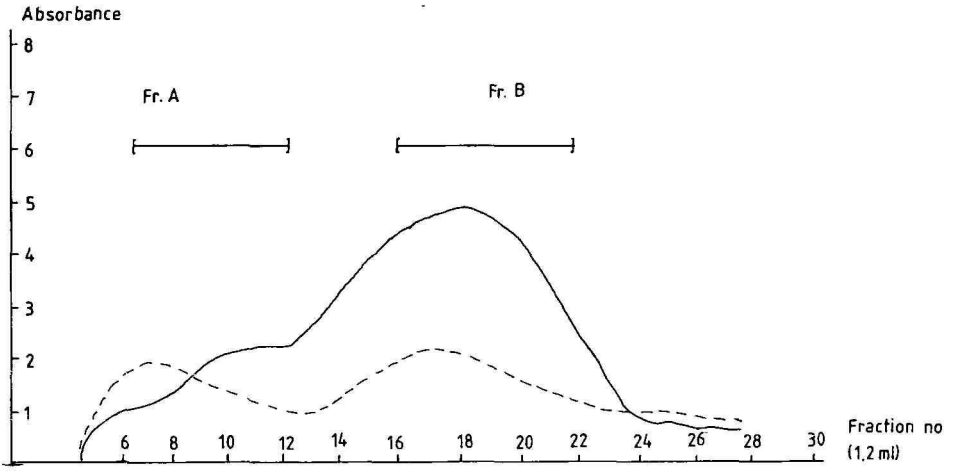

Fig. 1. Gel filtration on Sepharose CL 4B of HMW fraction from the rat intestinal mucus prepared as described in the text. Fractions A and B were rechromatographed on Dynospheres XP-3505. The continuous line is the carbohydrate[4] profile, and the dashed line is the protein profile[5]. Flow-rate, 0.3 ml/min; eluent, 0.1 *M* ammonium hydrogen carbonate.

(ii) Dynospheres XP-3505, (Dyno, Lillestrøm, Norway) 44 × 1 cm I.D. The column was eluted with 10 m*M* ammonium hydrogen carbonate at a flow-rate of 2 ml/min. The column was coupled to a LKB 2150 HPLC pump, and the eluent was monitored by an Optilab 5902 refractometer. The column was also coupled to a Waters HPLC system (510 pump, 481 UV detector, 840 data system) and OD 280 was monitored throughout the elution of the column (Fig. 2).

Characteristics of Dynospheres XP-3505

The pressure–flow curve is linear over a wide range, *i.e.* a flow of 2000 ml/cm^2 × *h* gives a pressure of 30 bar. The medium is stable in water, 1 *M* hydrochloric acid, 0.1 *M* sodium hydroxide, 24% ethanol and 8 *M* urea.

Dextrans T 2000, T 250, T 70 and T 40 were chromatographed on the Dynospheres XP-3505 column. Dextran T 2000 was eluted with the void volume (6.7 ml); the other dextrans were eluted as indicated by arrows on Fig. 2.

Fractions A and B (Fig. 1) and fractions 1 and 2 (Fig. 2) were, after dialysis

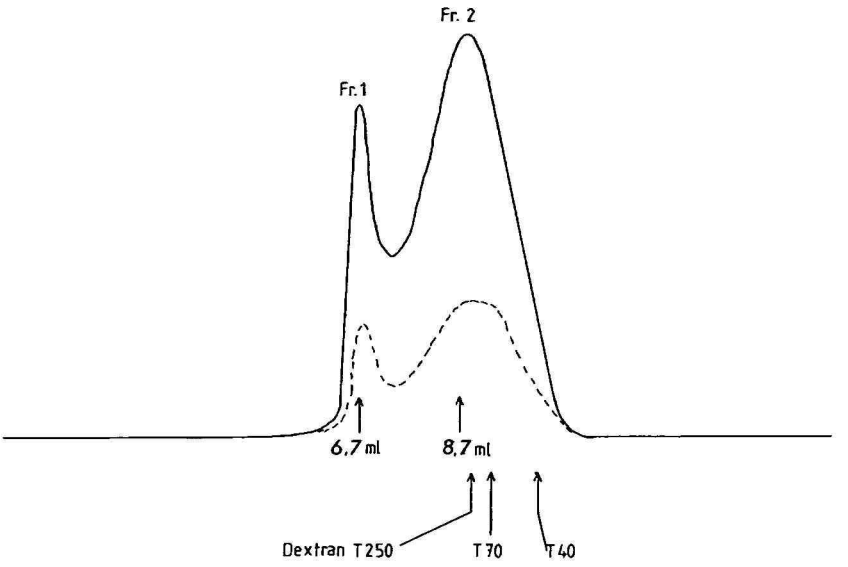

Fig. 2. Gel filtration on Dynospheres XP-3505 of HMW fraction from the rat intestinal mucus prepared as described in the text. Fraction 1 and 2 were rechromatographed on Dynospheres XP-3505. The continuous line is from refractive index detection, and the dashed line is the optical density at 280 nm. Flow-rate, 2 ml/min; eluent, 10 m*M* ammonium hydrogen carbonate.

(cut of 12.000) and freeze drying, rechromatographed on the Dynospheres XP-3505 column with conditions as described above. The results are presented in Figs. 3 and 4. The carbohydrate composition of the starting material and fractions A, B, 1 and 2 were determined by gas chromatography (GC) of the TMS derivatives of the methylglycosides[6] of the sugars present in the samples. GC was performed on DB-5 fused-silica column, (25 m × 0.25 mm I.D.), with the following programme: injection temperature 140°C followed by an increase of 1°C/min to 170°C, then an increase of 6°C/min to 250°C. The method does to separate glycolyl and acetylneuraminic acid (sialic acids). The carbohydrate composition is presented in Table I.

RESULTS AND DISCUSSION

The object of this work was to find a suitable medium for preparation of pure mucin present in the rat intestinal mucus. Chromatography of the HMW fraction on the Sepharose CL 4B column and on the Dynospheres XP-3505 column was performed, and the results are presented in Fig. 1 and 2, respectively. The separation of compounds present in the HMW fraction of the rat intestinal mucus appears from these results to be achieved better on the Dynospheres XP-3505 column than on the Sepharose CL 4B column.

A comparison of fraction A (Fig. 1) and fraction 1 (Fig. 2), when rechromatographed on Dynospheres XP-3505, demonstrates that A contains a substantial part of B, whereas 1 is almost devoid of 2. Fraction B and fraction 2 appear to constitute the same portion of HMW.

TABLE I

CARBOHYDRATE COMPOSITION OF THE VARIOUS FRACTIONS OBTAINED FROM THE RAT INTESTINAL MUCUS

Expressed as percentages of the total carbohydrate present.

	Fucose	*Mannose*	*Galactose*	*Glucose*	*N-Acetylglucosamine*	*N-Acetylgalactosamine*	*Sialic acid*
Starting material	6.7	1.1	23.6	1.8	17.5	25.6	23.6
Fraction 1, Dynospheres	8.2	0.8	22.8	–	20.7	28.4	19.1
Fraction A Sepharose	8.1	0.4	23.2	–	17.7	28.2	21.3
Fraction 2, Dynospheres	9.5	1.3	22.2	–	19.9	25.9	21.2
Fraction B Sepharose	12.1	1.2	22.3	–	15.1	25.1	24.3

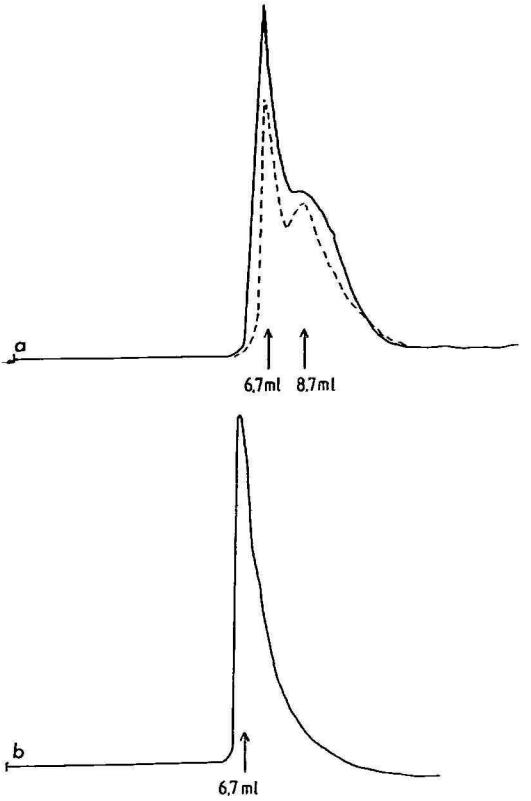

Fig. 3. (a) Gel filtration of fraction A (Fig. 1) on Dynospheres XP-3505. (b) Gel filtration of fraction 1 (Fig. 2) on Dynospheres XP-3505. Conditions as given for Fig. 2.

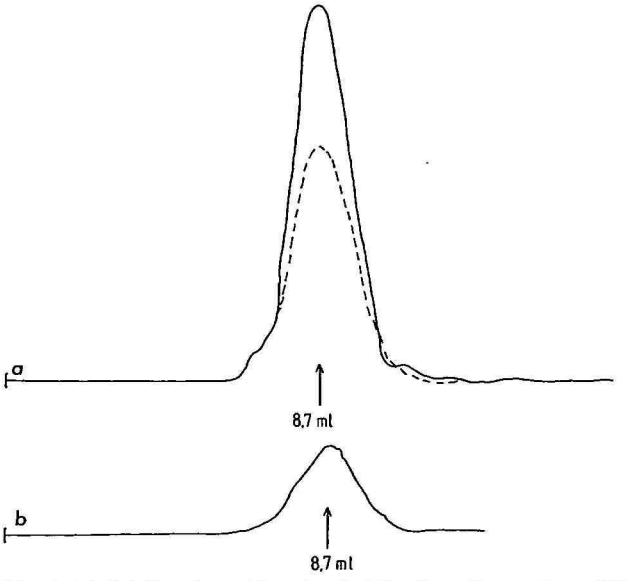

Fig. 4. (a) Gel filtration of fraction B (Fig. 1) on Dynospheres XP-3505. (b) Gel filtration of fraction 2 (Fig. 2) on Dynospheres XP-3505. Conditions as given for Fig. 2.

Fraction 1, being identical with the first peak of fraction A, is eluted with the void volume, whereas fraction 2, identical with fraction B, appears to have a molecular weight of 280 000 with reference to dextrans.

The carbohydrate compositions of the HMW fraction and subfractions obtained by separation on Sepharose CL 4B and Dynospheres XP-3505 show little difference (Table I), which is in accord with results obtained from previous separation studies on the rat intestinal mucus[1].

CONCLUSION

Our results show that Dynospheres XP-3505 is a more suitable gel filtration medium for separation of components present in rat intestinal mucion than Sepharose CL 4B. The Dynospheres XP-3505 column can be eluted at a higher flow-rate (at least 6 times) than the Sepharose CL 4B column, and gives better separation.

Large-scale gel filtration on Dynospheres XP-3505 will be time-saving compared with gel filtration media based on other matrices.

REFERENCES

1 J. K. Wold, T. Midtvedt and R. W. Jeanloz, *Acta Chem. Scand.*, B28 (1974) 277.
2 G. Lindstedt, S. Lindstedt and B. E. Gustafsson, *J. Exp. Med.*, 121 (1965) 201.
3 L. C. Hoskins and N. Zamchek, *Gastroenterology*, 54 (1968) 210.
4 M. Dubois, K. A. Gilles, J. K. Hamilton, P. A. Rebers and F. Smith, *Anal. Chem.*, 28 (1956) 350.
5 O. H. Lowry, N. J. Rosebrough, A. L. Farr and R. J. Randall, *J. Biol. Chem.*, 193 (1951) 265.
6 R. E. Chambers and J. R. Clamp, *Biochem. J.*, 125 (1971) 1009.

END OF SYMPOSIUM PAPERS

PUBLICATION SCHEDULE FOR 1986

Journal of Chromatography (incorporating *Chromatographic Reviews*) and *Journal of Chromatography, Biomedical Applications*

MONTH	J 1986	F	M	A	M	J	J	A	S	O	N	D	The publication schedule for further issues will be published later
Journal of Chromatography	351/1 351/2 351/3	352 353 354	355/1 355/2 356/1	356/2 356/3 357/1	357/2 357/3 358/1 358/2 359	360/1 360/2 361	362/1 362/2 362/3	363/1 363/2	364 365 366				
Chromatographic Reviews					373/1								
Bibliography Section		372/1		372/2		372/3		372/4		372/5		372/6	
Biomedical Applications	374/1 374/2	375/1	375/2	376 377	378/1	378/2 379	380/1	380/2 381/1	381/2	382	383/1	383/2	

INFORMATION FOR AUTHORS

(Detailed *Instructions to Authors* were published in Vol. 329, No. 3, pp. 449–452. A free reprint can be obtained by application to the publisher.)

Types of Contributions. The following types of papers are published in the *Journal of Chromatography* and the section on *Biomedical Applications:* Regular research papers (Full-length papers), Short communications and Notes. Short communications are preliminary announcements of important new developments and will, whenever possible, be published with maximum speed. Notes are usually descriptions of short investigations and reflect the same quality of research as Full-length papers, but should preferably not exceed four printed pages. For review articles, see page 2 of cover under Submission of Papers.

Submission. Every paper must be accompanied by a letter from the senior author, stating that he is submitting the paper for publication in the *Journal of Chromatography.* Please do not send a letter signed by the director of the institute or the professor unless he is one of the authors.

Manuscripts. Manuscripts should be typed in double spacing on consecutively numbered pages of uniform size. The manuscript should be preceded by a sheet of manuscript paper carrying the title of the paper and the name and full postal address of the person to whom the proofs are to be sent. Authors of papers in French or German are requested to supply an English translation of the title of the paper. As a rule, papers should be divided into sections, headed by a caption (*e.g.,* Summary, Introduction, Experimental, Results, Discussion, etc.). All illustrations, photographs, tables, etc., should be on separate sheets.

Introduction. Every paper must have a concise introduction mentioning what has been done before on the topic described, and stating clearly what is new in the paper now submitted.

Summary. Full-length papers and Review articles should have a summary of 50–100 words which clearly and briefly indicates what is new, different and significant. In the case of French or German articles an additional summary in English, headed by an English translation of the title, should also be provided. (Short communications and Notes are published without a summary.)

Illustrations. The figures should be submitted in a form suitable for reproduction, drawn in Indian ink on drawing or tracing paper. Each illustration should have a legend, all the *legends* being typed (with double spacing) together on a *separate sheet.* If structures are given in the text, the original drawings should be supplied. Coloured illustrations are reproduced at the author's expense, the cost being determined by the number of pages and by the number of colours needed. The written permission of the author and publisher must be obtained for the use of any figure already published. Its source must be indicated in the legend.

References. References should be numbered in the order in which they are cited in the text, and listed in numerical sequence on a separate sheet at the end of the article. Please check a recent issue for the layout of the reference list. Abbreviations for the titles of journals should follow the system used by *Chemical Abstracts.* Articles not yet published should be given as "in press", "submitted for publication", "in preparation" or "personal communication".

Dispatch. Before sending the manuscript to the Editor please check that the envelope contains three copies of the paper complete with references, legends and figures. One of the sets of figures must be the originals suitable for direct reproduction. Please also ensure that permission to publish has been obtained from your institute.

Proofs. One set of proofs will be sent to the author to be carefully checked for printer's errors. Corrections must be restricted to instances in which the proof is at variance with the manuscript. "Extra corrections" will be inserted at the author's expense.

Reprints. Fifty reprints of Full-length papers, Short communications and Notes will be supplied free of charge. Additional reprints can be ordered by the authors. An order form containing price quotations will be sent to the authors together with the proofs of their article.

Advertisements. Advertisement rates are available from the publisher on request. The Editors of the journal accept no responsibility for the contents of the advertisements.

HPLC columns for optical resolution

CHIRALPAK
CHIRALCEL

Daicel Chemical Industries, Ltd. has developed excellent chiral columns for the separation of optical isomers. "CHIRALPAK" or "CHIRALCEL" in combination with High Performance Liquid Chromatography has proven to be a highly successful technique for separation of optical isomers and for the determination of enantiomeric purity of compounds. Now a wide variety of optically pure compounds are readily available without laborious resolution techniques!

CHIRALCEL OA

Eluent: hexane-2-propanol (9/1)
Flow rate: 0.5ml/min.
Detection: UV 210nm

CHIRALCEL OB

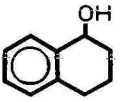

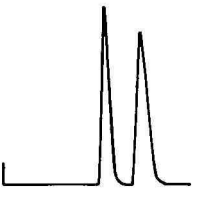

Eluent: hexane-2-propanol (9/1)
Flow rate: 0.5ml/min.
Detection: UV 210nm

CHIRALCEL OB

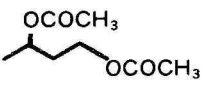

Eluent: hexane-2-propanol (9/1)
Flow rate: 0.5ml/min.
Detection: UV 210nm

CHIRALCEL OC

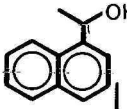

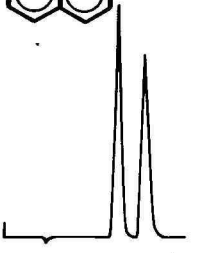

Eluent: hexane-2-propanol (9/1)
Flow rate: 0.5ml/min.
Detection: UV 254nm

For more details about HPLC columns, please contact:

DAICEL CHEMICAL INDUSTRIES, LTD.

Tokyo
8-1, Kasumigaseki 3-chome,
Chiyoda-ku, Tokyo 100, Japan
Phone: 03 (507) 3173, 3178
Telex 222-4632 DAICEL J

DAICEL (Europa) GmbH
Königsallee 92a,
4000 Düsseldorf 1, F.R. Germany
Phone: (0211) 134158
Telex. (41) 8588042 DCEL D

New York
Pan-Am Bldg., 200 Park Avenue,
New York, N.Y. 10166-0130, U.S.A.
Phone (212) 878-6765, 6766
Telex. (23) 236154 DCC UR

DAICEL (U.S.A.), INC.
611 west 6th Street, Room 2152
Los Angeles California 90017, U.S.A.
Phone: (213) 629-3656
Telex: 215515 DCIL UR